

Dissertation zur Erlangung des Doktorgrades
der Fakultät für Chemie und Pharmazie
der Ludwig-Maximilians-Universität München

Modulation of NF- κ B signaling by measles virus P gene products



Kerstin Monika Schuhmann

aus

Lauf an der Pegnitz, Deutschland

2012

Erklärung

Diese Dissertation wurde im Sinne von §7 der Promotionsordnung vom 28. November 2011 von Herrn Prof. Conzelmann betreut und von Herrn Prof. Hopfner vor der Fakultät für Chemie und Pharmazie vertreten.

Eidesstattliche Versicherung

Diese Dissertation wurde eigenständig und ohne unerlaubte Hilfe erarbeitet.

München, den 09.08.2012

.....

(Unterschrift des Autors)

Dissertation eingereicht am:	09.08.2012
Erstgutachter:	Prof. Dr. Karl-Peter Hopfner
Zweitgutachter:	Prof. Dr. Karl-Klaus Conzelmann
Tag der mündlichen Prüfung:	09.10.2012

This thesis has been prepared in the laboratory of Prof. Karl-Klaus Conzelmann at the Max von Pettenkofer-Institute and Gene Center of the Ludwig-Maximilians-University Munich.

Parts of this thesis were published in Journal of Virology in 2011:

Schuhmann, K.M., C.K. Pfaller, and K.K. Conzelmann. 2011. The measles virus V protein binds to p65 (RelA) to suppress NF-kappaB activity. *J Virol.* 85:3162-3171.

Acknowledgment – Danksagung

Ein unglaublich interessanter und anspruchsvoller Lebensabschnitt geht mit dem Fertigstellen dieser Arbeit zu Ende. Hiermit möchte ich allen danken, die mich während dieser Zeit unterstützt haben.

In erster Linie bei **Prof. Dr. Conzelmann**, der mir die Möglichkeit gegeben hat meine Doktorarbeit in seinem Arbeitskreis anzufertigen. Er war immer mit einem offenen Ohr und vor allem mit viel Verständnis für uns da. Vielen Dank dafür.

Des Weiteren möchte ich mich bei **Prof. Dr. Hopfner** bedanken, der sich dazu bereiterklärt hat die Arbeit von seitens der Fakultät für Chemie und Pharmazie zu betreuen, sowie bei den weiteren Mitgliedern der Promotionskommission, **Prof. Dr. Förstemann, Prof. Dr. Martin, Dr. Fürst und Prof. Dr. Gaul** für Ihre Mühen.

Ein ganz besonderer Dank gilt meinen Arbeitskollegen:

Alex für seine Hilfe bei komplexen Klonierungen; **Anika** für Ihre vielen ausführlichen Geschichten und dass sie auf jeder Tagung Ihr Bett mit mir geteilt hat; **Christian** für die Etablierung des Masern Rescue Systems; **Konstantin** für die vielen fachlichen Diskussionen; **Lisa** für die Einführung in alle Laborgepflogenheiten am Anfang meiner Doktorarbeit; **Martina** für Ihre allmontägliche Begleitung ins Grako; **Max** und **Tobias** für Ihr tägliches Entertainment; **Moni** für die Zeit die wir auch außerhalb der Arbeit verbrachten und verbringen; **Nadin** für ihre grenzenlose Hilfsbereitschaft; **Vanessa** für ihre lebensfrohe Art und Ihre unvergleichliche Freundschaft. Und allen zusammen für die unvergleichlich entspannte, aber dennoch produktive Arbeitsatmosphäre im Labor.

Insbesondere möchte ich mich an dieser offiziellen Stelle bei meinen **Eltern** und **Schwestern** für ihre Unterstützung, ihr Verständnis und ihren Zuspruch in jedem Lebensabschnitt bedanken.

Zuletzt, aber mit besonderem Nachdruck, möchte ich mich bei **Markus** bedanken, der durch seine unkomplizierte und lebensfrohe Art vieles erleichtert hat.

Table of Contents

Summary.....	ix
1 Introduction.....	1
1.1 Measles virus – a representative of the virus family <i>Paramyxoviridae</i>	1
1.1.1 The measles virus virion – composition of the viral particle.....	1
1.1.2 The viral life cycle.....	4
Viral entry	4
Replication cycle.....	5
Viral exit	5
1.1.3 Measles virus infection <i>in vivo</i>	6
Infection route of MV	6
MV-induced immunosuppression and life-long immunity.....	7
1.2 The transcription factor family NF-κB – an important player during an antimicrobial immune response.....	8
1.2.1 The NF- κ B family and its inhibitors	8
1.2.2 NF- κ B activation: Two distinct pathways	10
The classical NF- κ B signaling pathway	11
The alternative NF- κ B pathway.....	12
1.3 The innate immune response during MV infection	13
1.3.1 Activation of the innate immune system by RNA viruses	13
Toll-like receptor signaling.....	13
RIG-I-like receptor signaling.....	15

1.3.2	Strategies of measles virus to evade innate immune responses – it’s all about the P gene products	18
1.4	Objective of the study	19
2	Material and Methods.....	20
2.1	Material.....	20
2.1.1	Chemicals.....	20
2.1.2	Enzymes and recombinant proteins	20
2.1.3	Commercial kits	21
2.1.4	Additional reagents.....	22
2.1.5	Antibodies.....	23
2.1.6	Buffers and solutions	25
2.1.7	Bacteria and cell lines.....	29
2.1.8	Oligonucleotides	30
2.1.9	Plasmids.....	34
2.1.10	Viruses	40
2.1.11	Equipment	41
2.2	Methods.....	43
2.2.1	Molecular biological methods	43
	Polymerase chain reaction (PCR)	43
	Enzymatic manipulation of DNA	45
	Agarose gel electrophoresis	46
	Extraction of DNA from agarose gels	47
	Transformation of competent bacteria.....	47
	Cultivation and storage of bacteria.....	47
	Plasmid preparation on analytical scale (Miniprep)	48

Plasmid preparation on preparative scale (Midiprep)	48
RNA isolation and reverse transcription (RT) PCR	49
Quantitative real-time RT-PCR.....	50
2.2.2 Cell biological methods	51
Cell culture	51
Thawing and freezing of eukaryotic cells	52
Transfection	52
2.2.3 Biochemical and protein biochemical methods	53
SDS polyacrylamide gel electrophoresis (SDS-PAGE).....	53
Western blot analysis and immunodetection	53
Immunoprecipitation (IP)	54
Immunofluorescence microscopy.....	55
Luciferase assay.....	56
2.2.4 Virological methods	57
Generation of recombinant MV from cDNA (virus rescue).....	57
Virus titration	58
Generation of virus stocks	58
Virus growth curve	58
3 Results	59
3.1 Measles virus P gene products suppress NF-κB activation upon TNFR stimulation	59
3.2 NF-κB signaling via PRRs can be suppressed by MV P gene products.....	61
3.3 MV V inhibits NF-κB signaling downstream of the IKK complex.....	62
3.4 MV V specifically binds the NF-κB subunit p65	64
3.5 RHD of p65 is sufficient for interaction with MV V.....	66

3.6	Binding of MV V to p65 is mediated via both N- and C-terminal domains of the RHD of p65	67
3.7	Binding of MV V to p65 does not compete with binding of p50 or I κ B α to p65	69
3.8	MV V prevents nuclear translocation of p65	70
3.9	Nuclear translocation of p65 upon TNF α treatment in the presence of MV P and C	71
3.10	MV V does not directly bind to the NLS of p65 or interfere with importin α 5 binding to p65	73
3.11	The CTD of MV V is required and sufficient for p65 binding and suppression of p65/p50-mediated NF- κ B activity	75
3.12	Mutational analysis of MV V	76
3.13	The V protein of the measles wild type isolate D5 inhibits NF- κ B activity and binds to p65.....	79
3.14	CDV V and NiV V act like MV V and suppress classical NF- κ B activity	81
3.15	The Rel homology domain of p65 is also bound by CDV V and NiV V.....	84
3.16	Binding of P gene products to other NF- κ B subunits.....	85
3.17	Inhibition of the alternative NF- κ B pathway	87
3.18	Generation and characterization of recombinant viruses MV-vac2, MV-MCS, MV-VKO, MV-VKO+V.....	88
3.19	NF- κ B activation upon infection with MV-MCS, MV-VKO, MV-VKO+V	91
4	Discussion	93
4.1	Inhibition of NF- κ B by MV P and C	94
4.2	Inhibitory mechanism of MV V.....	95
4.3	MV V binds a variety of cellular proteins but with specificity	99
4.4	Interactions of V with cellular molecules are often conserved among paramyxoviruses	100

4.5	p65 shares binding sites at the C-terminal domain of V with MDA5 and IRF7	101
4.6	Relevance of the P gene products for the alternative pathway	102
4.7	Role of the V protein during MV infection	104
4.8	Future prospects	106
5	References	107
6	List of abbreviations	119
7	List of figures	123

Summary

Nuclear factor- κ B (NF- κ B) transcription factors are involved in controlling numerous cellular processes, including inflammation, innate and adaptive immunity, and cell survival. In this study I show that the immunosuppressive measles virus (MV, *Morbillivirus* genus, *Paramyxoviridae*) has evolved multiple functions to interfere with NF- κ B signaling in epithelial cells. The MV P, V, and C proteins, also involved in preventing host cell interferon responses, were found to individually suppress NF- κ B-dependent reporter gene expression upon triggering of classical NF- κ B pathways, including TNF receptor-, RIG-I-like receptor-, or Toll-like receptor-signaling. The MV V protein showed the strongest suppression of classical NF- κ B activity, while the inhibitory capacities of P or C were less pronounced. Reporter gene assays involving overexpression either of the IKK complex, which phosphorylates the inhibitor of κ B to liberate NF- κ B dimers, or the NF- κ B dimer p65/p50 itself, indicate that MV V targets canonical NF- κ B signaling downstream of the IKK complex. Accordingly, co-immunoprecipitation (CoIP) experiments revealed that the V protein of MV, but not the P or the C protein, binds to the Rel-homology domain (RHD) of the NF- κ B subunit p65. Both domains of the RHD of p65, responsible either for DNA binding or I κ B α and p50 binding, were shown to be involved in the interaction with MV V. I κ B α and p50, which are associated to p65 in non-stimulated cells, were not bound by any of the P gene products in CoIP experiments. Further CoIP experiments from cells co-expressing all NF- κ B complex members, p65, p50, and I κ B α , together with MV V simultaneously, suggest that binding of p50, I κ B α and MV V to p65 are independent of each other and that MV V does not influence the composition of the NF- κ B complex. However, the presence of V abolished nuclear accumulation of p65 upon TNF α stimulation as observed by confocal microscopy. Inhibition of TNF α -mediated nuclear accumulation was also observed in some cells expressing MV P, but all MV C-expressing cells showed nuclear p65 upon TNF α stimulation indicating that the C protein acts in the nucleus to suppress canonical NF- κ B activity. Retention of p65 in the cytoplasm by the V protein is

neither due to direct binding of MV V to the nuclear localization signal (NLS) of p65 as revealed by CoIP experiments involving p65 mutants deficient in their NLS nor do MV V and importin α 5 compete for p65 binding. Notably, the short C-terminal domain of the V protein (V_{CTD}), which is also involved in binding STAT2, IRF7, and MDA5, was sufficient for the interaction and for preventing reporter gene activity. As revealed by mutational analysis of the V_{CTD} , binding of p65 and also of IRF7 to MV V involves at least two independent sites located at loop1 and 2 of V_{CTD} . The C-terminal domain of V was found to be completely identical in the Schwarz MV vaccine strain, which was used during this study, and a wild type MV isolate. Consequently, the capacity to suppress NF- κ B activity and the ability to bind to p65 were also equal. Interestingly, the V_{CTD} is also highly conserved among different paramyxoviruses. As revealed by reporter gene assays and CoIP experiments the V proteins of canine distemper virus and Nipah virus exhibit the same NF- κ B inhibitory potency and binding affinity to the RHD of p65 as MV V. In contrast, the parainfluenza virus type 5 V protein did not bind to p65 and therefore cannot interfere with NF- κ B activation. Besides inhibition of the classical NF- κ B pathway, interference of MV P gene products with the alternative NF- κ B signaling was investigated as well. CoIP experiments suggested binding of RelB specifically to MV V, as already observed for p65. In contrast, p100, the precursor of p52, showed no interaction with any of the MV proteins similar to p50, whereas p52 was found to interact with both MV P and V.

The effect of MV V on NF- κ B activity was also investigated in the viral context. Therefore different recombinant viruses were generated, including the parental virus, a virus with a knock out of the V protein, and a virus in which the knock out was rescued by expression of the V protein from an inserted ORF. As illustrated by growth curves and Western blotting of the viral proteins, the V knock out virus exhibited the same growth kinetics on Vero and A549 cells as the viruses expressing the V protein. NF- κ B-dependent reporter gene assays and quantitative real-time RT-PCR on NF- κ B-dependent genes upon infection did not reveal a major impact of the presence of V on NF- κ B activation in epithelial cells to a certain time point. This indicates that the P and C proteins can substitute for the inhibitory effects of the V protein in these cells.

1 Introduction

1.1 Measles virus – a representative of the virus family *Paramyxoviridae*

Measles virus (MV) is a non-segmented, negative-sense RNA virus and belongs therefore to the order of *Mononegvirales*. It is further grouped into the family of *Paramyxoviridae*, which consists of two subfamilies the *Paramyxovirinae* and the *Pneumovirinae*. MV is part of the *Morbillivirus* genus in the *Paramyxovirinae* subfamily along with respiroviruses, rubulaviruses, henipaviruses, and avulaviruses (Fig. 3-14A).

1.1.1 The measles virus virion – composition of the viral particle

MV is a pleomorphic, enveloped virus with a wide range of diameters between 180 nm and 1 μm (Lund et al., 1984; Nakai and Imagawa, 1969). However, most of the virions appear to have a spherical shape with an average diameter between 100 and 300 nm (Rima and Duprex, 2011) (Fig. 1-1A). The lipid bilayer envelope derived from the host cell encloses the negative sense, single stranded RNA genome, which comprises 15,894 nucleotides and contains six genes, separated from each other by trinucleotide intergenic sequences. These six genes in the order 3'-N-P-M-F-H-L-5' encode eight proteins due to leaky scanning of cellular ribosomes and RNA editing by the viral polymerase complex (Fig. 1-1B). The transcription units are flanked by a leader (Le) region at the 3'-terminus encoding a short RNA of 56 nucleotides and a 40 nucleotide long trailer (Tr) region at the 5'-terminus. Six of the viral proteins are components of the virion. The 58kDa nucleocapsid (N) protein encapsidates the viral genome to protect it from cellular RNAses forming the ribonucleo-protein complex (RNP), which is the basic unit of infectivity (Fig. 1-1A). Each N protein associates with exactly six nucleotides of the genome. This may explain why MV strictly follows the "rule of six",

which states that the genome must consist of a multiple of six nucleotides to get properly packaged and to replicate efficiently (Kolakofsky et al., 2005). The viral RNA-dependent RNA polymerase (vRdRp) is composed of the large (L) protein and the phosphoprotein (P), with L bearing the enzymatic activity and P serving as non-catalytic co-factor. The P (54 kDa) and the L (247 kDa) protein associate with the RNP, which is additionally coated with the 38 kDa matrix (M) protein (Liljeroos et al., 2011), mediating virus assembly and budding (Cathomen et al., 1998; Iwasaki et al., 2009). The viral hemagglutinin (H) and fusion (F) glycoproteins surround the virion and are responsible for viral entry and exit. The type 2 membrane protein H (69 kDa) builds a dimer or a dimer of dimers (Hashiguchi et al., 2007) and mediates attachment of the virion to the cell by recognition of the cellular receptors, whereas the integral type 1 membrane protein F (60 kDa) forms trimers that require proteolytic cleavage to be able to fuse cell membranes (Zhu et al., 2003).

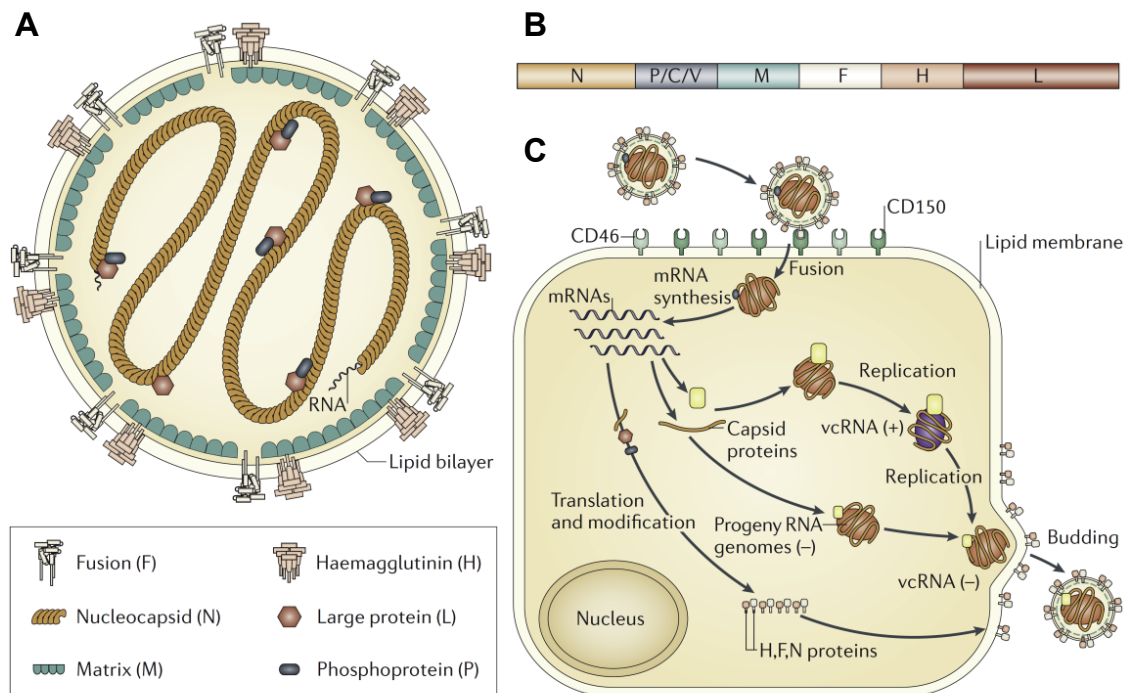


Figure 1-1 Measles virus – the basics

(A) Schematic representation of a MV virion. The negative strand RNA genome is enclosed by the N protein building the ribonucleoprotein (RNP) complex, which is associated with the viral polymerase composed of the large protein (L) and the phosphoprotein (P). The matrix (M) protein links the RNP to the viral glycoproteins, the fusion (F) and the hemagglutinin (H) protein, located on the cellular plasma membrane. (B) The MV genome comprises six genes. The P gene allows expression of three different proteins. (C) Schematic overview of the MV life cycle. The whole replication cycle takes place in the cytoplasm. Upon binding to the cognate cellular receptor, fusion of viral and cellular membranes is initiated mediating entry of MV. Transcription and replication take place subsequently and the newly synthesized RNP is transported to the plasma membrane, where assembly and budding takes place. Adapted from (Moss and Griffin, 2006).

The two non-structural proteins, V and C, are additionally expressed from the P gene (Fig. 1-2). Co-transcriptional RNA editing allows expression of the 32 kDa V protein. In this process, the viral polymerase stutters at a defined editing site and inserts an additional non-templated guanosine (G) into the transcript of the P gene between nucleotide 748/749 that leads to the V mRNA and a frameshift of the open reading frame (ORF) at that position (Cattaneo et al., 1989). Thus, the translated V protein has a 231 aa long N-terminal domain identical to the P protein (PV_{NTD}), but a unique cysteine-rich C-terminal domain (V_{CTD}) of 68 aa.

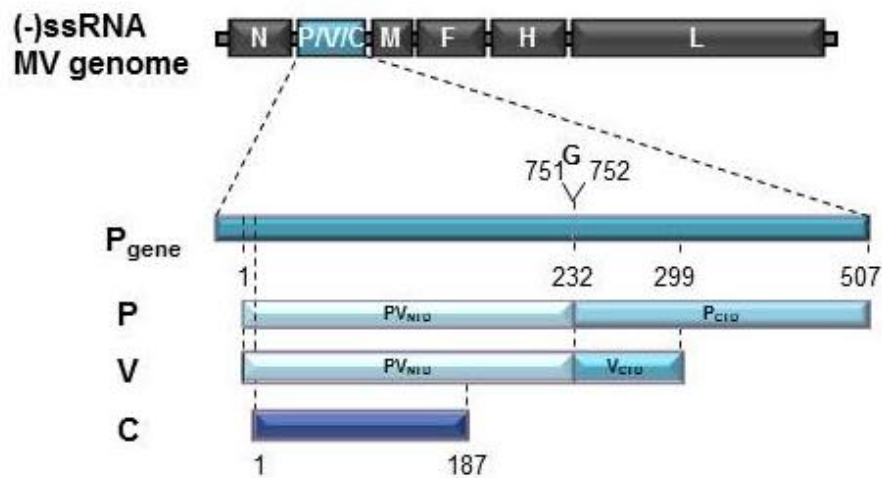


Figure 1-2 Measles virus P gene products

In addition to the P protein, the nonstructural proteins V and C are expressed due to insertion of an additional guanosine (G) between nucleotides 751 and 752 of the mRNA by RNA editing (MV V) or translation of an alternative ORF initiating 19 nucleotides downstream of the P/V start codon (MV C). Adapted from (Schuhmann et al., 2011).

The V_{CTD} was shown to incorporate two zinc atoms forming zinc finger motifs that are highly conserved among paramyxoviruses (Liston and Briedis, 1994). All members of the *Paramyxovirinae* subfamily are able to edit their P gene mRNA, however, the number of inserted G residues varies (Goodbourn and Randall, 2009). Expression of the C protein is achieved through leaky scanning of ribosomes and the use of an alternative translation initiation site on the P and V mRNAs downstream of the P/V start codon. This results in translation of an alternative ORF and the expression of the 21 kDa C protein (Bellini et al., 1985). Neither C nor V is essential for MV replication (Radecke and Billeter, 1996; Schneider et al., 1997), however, all P gene products were shown to be key players of MV evading the immune system (Rima and Duprex, 2011).

1.1.2 The viral life cycle

Viral entry

In order to enter a cell the MV virion attaches to the cell surface via the H protein that binds to the cellular entry receptors (Fig. 1-1C). Three different receptors were identified so far: Signaling lymphocytic activation molecule (SLAM), also known as CD150, is thought to be the primary MV receptor in terms of MV pathogenesis (Tatsuo et al., 2000). SLAM is a costimulatory molecule expressed on activated T-cells, B-cells, macrophages, mature dendritic cells (DCs), platelets, and thymocytes explaining the highly lymphotropic nature of MV (Sidorenko and Clark, 2003). Recently, the so far elusive epithelial entry receptor, which was already known to exist (Ludlow et al., 2010; Tahara et al., 2008; Takeda et al., 2007), was identified. Two independent studies characterized nectin-4, or poliovirus receptor-like protein 4 (PVRL4), as the MV entry receptor found on epithelial cells (Muhlebach et al., 2011; Noyce et al., 2011). Nectin-4 is expressed within adherens junctions, complexes that provide strong mechanical attachment between epithelial cells. The first identified, but least pathologically relevant receptor is CD46 or membrane cofactor protein (MCP) (Dorig et al., 1993; Naniche et al., 1993). Although expressed on nearly all nucleated human cells, CD46 can only be utilized by cell culture adapted vaccine viruses *in vitro* (Yanagi et al., 2009). However, there is recent evidence that vaccine viruses do not use CD46 *in vivo* (Kato et al., 2012).

Upon binding of the H protein to the cellular receptor, major conformational changes in the mature F protein are triggered, followed by insertion of the fusion peptide into the target membrane and ultimately in formation of a fusion pore, leading to the release of the RNP into the cytoplasm (Plempner et al., 2011).

Replication cycle

Once the RNP is released into the cytoplasm of the cell, viral gene expression and replication are set up (Fig. 1-1C). Therefore, the vRdRp transcribes the viral genes into mRNAs, which were shown to be 5'-capped and 3'-polyadenylated (Hall and Meulen, 1977; Yoshikawa et al., 1986). In contrast, the transcribed leader RNA is uncapped exhibiting 5' triphosphates. At every gene border, the viral polymerase either dissociates from the genome or reinitiates transcription of the next gene. This results in an mRNA gradient since genes closer to the 3'-end of the genome are transcribed to a higher extent than more distal genes (Cattaneo et al., 1987). The mRNAs are translated into proteins by the cellular translation machinery. At a certain point of infection, the vRdRp switches from the transcription to replication mode. This occurs probably when enough N protein is synthesized to encapsidate immediately the antigenomic RNA which serves as template for generation of new genomes. The emerging genome is cotranscriptionally packaged by N proteins generating new RNPs.

Viral exit

Both viral glycoproteins F and H are translated as transmembrane proteins and transported to the cell plasma membrane. The M protein mediates the interaction of the newly synthesized RNPs with the regions of the plasma membrane where the glycoproteins have been inserted to support assembly (Iwasaki et al., 2009). Finally, the virus is able to bud from the plasma membrane (Fig. 1-1C).

Incorporation of the glycoproteins into the cellular membrane, can lead to fusion with uninfected cells, mediated by binding of H to receptors on neighboring cells activating the fusion function of F. This leads to the formation of multinucleated giant cells also known as syncytia, a hallmark of MV infected cells (Bunting, 1950). Syncytia formation and cell to cell spread is the main spreading strategy of MV.

1.1.3 Measles virus infection *in vivo*

The measles virus is highly infectious to humans and causes measles, a disease that is still an important cause of child morbidity and mortality in many parts of the world, even though a safe and effective vaccine is available (Griffin et al., 2012). In 2010, there were around 140,000 measles deaths globally, with 95 % of them occurring in low-income countries with weak health infrastructures. The “MEASLES INITIATIVE” launched in 2001 helped to increase the vaccination rate among one-year old children from 72% in 2000 to 85% in 2010, which resulted in a 74% drop in measles deaths between 2000 and 2010 worldwide (WHO, 2012). The clinical symptoms of the disease like fever, rash, and conjunctivitis are just the signs of the adaptive immune responses against infection and not responsible for any deaths. However, MV infection induces several week of immunosuppression resulting in increased susceptibility to secondary infections that are the main causes of measles induced death (Griffin, 2010). Rare but serious complications of measles affect the central nervous system. 0.1% of the patients develop measles encephalitis within two weeks of the onset of the rash (Moss and Griffin, 2012). Another CNS complication that occurs months to years after acute infection is subacute sclerosing panencephalitis (SSPE) which is caused by a persistent measles virus infection. It is found in about one in 10,000–100,000 patients and most often occurs in people infected with measles virus before two years of age. Fortunately, measles vaccination programmes reduced the incidence of SSPE dramatically (Campbell et al., 2007).

Infection route of MV

Measles virus spreads among individuals via the respiratory route. Virus-containing droplets produced by sneezing or coughing enter the respiratory tract. Different to what was assumed in the past, initial infection with MV does not occur in epithelial cells of the upper respiratory tract, as revealed by infection studies with macaques (de Swart et al., 2007; Leonard et al., 2008) . Instead, the infection is rather initiated in the lower respiratory tract, where alveolar macrophages and DCs are infected transporting

MV to local lymphoid tissue (Ferreira et al., 2010; Lemon et al., 2011). The close spatial proximity to SLAM-positive T- and B- cells in this tissue amplifies the infection and promotes dissemination throughout the body. Infection of epithelial cells might come into play during the late phase of infection, when infected lymphocytes carry virus to the basal side of the respiratory epithelium infecting respiratory epithelial cells probably via nectin-4. Later on, the virus is released from these cells at the apical domain facilitating the viral transmission back into the airways. The proposed role of epithelial cells during virus exit is supported by a study in which a virus blind for the epithelial receptor remained virulent in rhesus macaques, but could not be released into the airways (Leonard et al., 2008).

MV-induced immunosuppression and life-long immunity

The MV-induced immune suppression comprises several phenomena concerning the adaptive immune response, like lymphopenia, predominance of Type 2 cytokine responses, and suppression of lymphocyte proliferation (Griffin, 2010). However, the underlying mechanisms are not well understood. The loss of lymphocytes (lymphopenia) might be due to increased susceptibility of the cells to apoptosis (Fugier-Vivier et al., 1997; Okada et al., 2000). Increased levels of Th2 cytokines such as interleukin-4 (IL-4), IL-10 and IL-13 produced by regulatory and CD4⁺ T-cells during MV infection (Griffin and Ward, 1993) leads on the one hand to an environment favoring B-cell maturation to establish the humoral memory important for life-long immunity against MV infection, on the other hand, macrophage activation is depressed and therefore induction of type 1 responses required for combating new pathogens is hampered (Griffin, 2010). Furthermore, MV F and H glycoproteins were shown to directly suppress proliferation of peripheral blood mononuclear cells (PBMCs), like lymphocytes, monocytes or a macrophages due to interaction with an unidentified molecule of the cell surface of PBMCs (Schlender et al., 1996). Considered together, these findings constitute the 'immunological paradox' of measles virus infections: On the one hand most individuals successfully clear an infection and establish life-long immunity against MV, on the other hand they suffer from several weeks of immune suppression (Beckford et al., 1985).

1.2 The transcription factor family NF- κ B – an important player during an antimicrobial immune response

The nuclear factor- κ B (NF- κ B) was discovered in 1986 as a regulator of expression of the κ light chain gene in B cells (Sen and Baltimore, 1986). Since then, extensive research was done on the NF- κ B family of transcription factors and revealed the involvement of NF- κ B in numerous fundamental cellular processes. Besides its crucial role in cell survival, differentiation, and proliferation, NF- κ B plays its most important part in the regulation of the immune system (Hayden and Ghosh, 2012). Thus, it controls not only the development and homeostasis of immune cells and lymphoid organs but is also an indispensable regulator during an immune response (Hayden et al., 2006). Activation of pattern recognition receptors (PRRs) such as Toll-like receptors (TLRs) and RIG-I-like receptors (RLRs) results in NF- κ B-regulated expression of a large variety of cytokines and antimicrobial effector molecules that propagate and elaborate the initial recognition event of an invading pathogen (Dev et al., 2011). Besides this fundamental role in the innate immune system, NF- κ B is activated upon T-cell and B-cell receptor (TCR and BCR) engagement controlling the adaptive immune response as well (Ghosh et al., 1998). Accordingly, it is obvious that NF- κ B is a key player during the host response to infection and is therefore a common target of microbial pathogens.

1.2.1 The NF- κ B family and its inhibitors

The mammalian NF- κ B family comprises five members: p65 (RelA), RelB, c-Rel, p50 (NF- κ B1), and p52 (NF- κ B2). The p50 and p52 proteins are generated by proteolytic processing of the precursor proteins p105 and p100, respectively. The NF- κ B subunits exist as homo- or heterodimers in the cell. All family members share a structurally conserved N-terminal region of about 300 amino acids, named the Rel homology domain (RHD). The RHD, which contains a nuclear localization signal (NLS), is critical for binding to cognate DNA-sequences termed κ B motifs, homo/heterodimerization, and interaction with specific inhibitory proteins (Ghosh et al., 2012). Only p65, RelB, and

c-Rel possess a C-terminal transactivation domain (TAD), which is essential to initiate transcription. In contrast to Rel proteins, p50 and p52 lack the TAD (Fig. 1-3). However, p50 and p52 form either heterodimers with the Rel proteins to positively regulate transcription or homodimers to function as repressors by competing with TAD-containing dimers for binding to κ B sites (Hayden and Ghosh, 2012). The main activated form of NF- κ B is a heterodimer of p65 associated with the p50 subunit.

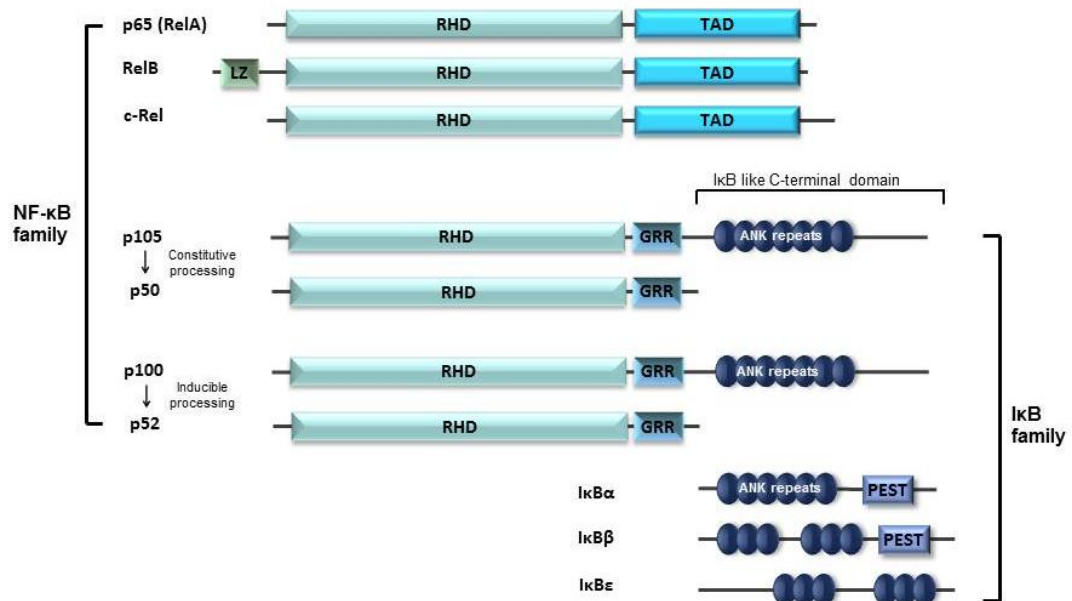


Figure 1-3 The mammalian NF- κ B family and its inhibitors

In mammalian cells five NF- κ B family members exist, p65 (RelA), RelB, c-Rel, p105/p50 and p100/p52. p50 and p52 are derived from longer precursor proteins p105 and p100, respectively. While p105 is constitutively processed, p100 needs a specific stimulus to induce processing. All NF- κ B family members contain an N-terminal Rel-homology domain (RHD), but only p65, RelB, and c-Rel comprise a C-terminal transactivation domain (TAD). RelB contains additionally a leucine zipper (LZ) at the N-terminus. The inhibitor of NF- κ B (I κ B) family consists of I κ B α , I κ B β , and I κ B ϵ and contain ankyrin repeat motifs (ANK) in their C-termini. Due to the presence of ANK repeats, the C-terminal domains of the precursors p100 and p105 are called I κ B-like domains. According to (Ghosh et al., 2012).

A hallmark of the NF- κ B pathway is its regulation by inhibitor of κ B (I κ B) proteins. In unstimulated cells, NF- κ B dimers are retained in the cytoplasm by these regulatory proteins, which include I κ B α , I κ B β and I κ B ϵ . They are characterized by the presence of multiple ankyrin repeats at their C-terminus. These 33-amino acid motifs mediate protein-protein interactions with the RHD of NF- κ B dimers. Thereby I κ B proteins mask the NLS within the NF- κ B dimers and sequester them in the cytosol in a transcriptionally inactive state (Hinz et al., 2012). The ankyrin repeats are also present in the C-terminal domains of the p100 and p105 precursors, which also function as I κ Bs (Fig. 1-3).

1.2.2 NF- κ B activation: Two distinct pathways

Two major pathways for activation of NF- κ B are described, the classical (canonical) and alternative (non-canonical) pathway (Fig. 1-4) (Oeckinghaus et al., 2011). Although a wide range of diverse receptors stimulate the classical NF- κ B signaling, only a selected set of receptors within the TNF receptor superfamily appears to initiate the alternative pathway.

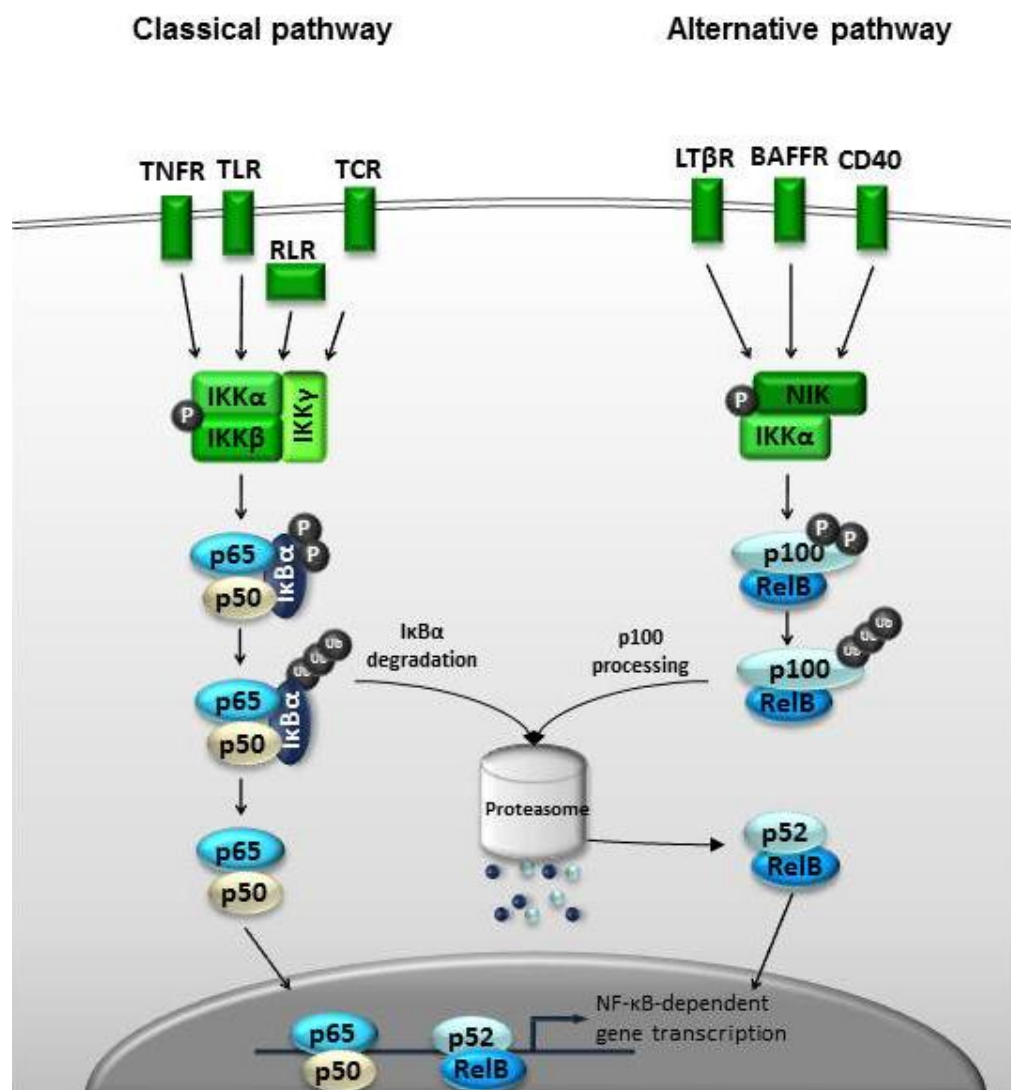


Figure 1-4 Two different NF- κ B signaling pathways

The classical pathway is activated by a variety of inflammatory signals. Activation of this pathway depends on the IKK complex which phosphorylates I κ B α to induce its degradation allowing NF- κ B dimers to enter the nucleus. The alternative pathway is activated by triggering of the receptors for lymphotoxin- β and BAFF or CD40. This pathway requires NF- κ B-inducing kinase (NIK) and IKK α which induce processing of p52 from p100, resulting in activation of the p52/RelB heterodimer.

The classical NF- κ B signaling pathway

The classical pathway is induced by pro-inflammatory cytokines, such as tumor-necrosis factor α (TNF α) and interleukin-1 (IL-1), by triggering innate immune receptors like TLRs and RLRs, as well as by antigen-receptor engagement (BCR and TCR). Signaling in the classical pathways generally occurs through the recruitment of adaptor proteins to the receptors resulting in signaling platforms crucial for the recruitment and activation of the central mediator of these pathways, namely the I κ B kinase (IKK) complex. The 700-900 kDa IKK complex contains two catalytical subunits, IKK α and IKK β , as well as a regulatory subunit IKK γ (NEMO (NF- κ B essential modulator)) (Liu et al., 2012). It has been shown that IKK α and IKK β form heterodimers *in vivo* and interact with the regulatory subunit NEMO through their C-terminal NEMO-binding-domain (NBD). The NBD peptide on its own was shown to inhibit the interaction between IKK γ and IKK α /IKK β in a dominant negative manner and blocks activation of NF- κ B. (May et al., 2000; May et al., 2002). Both IKK α and IKK β contribute to the activation of classical signaling pathways, although in many cases IKK β is sufficient as catalytical subunit. However, the regulatory subunit of the IKK complex, IKK γ is essential to activate these pathways (Solt and May, 2008). Upon activation, the IKK complex phosphorylates I κ B-proteins at specific serine residues, for example serines 32 and 36 of I κ B α . Subsequently, the phosphorylated I κ B α is ubiquitinated at lysines 21 and 22, which targets it for its degradation by the 26S proteasome. The NF- κ B dimers are released and translocate to the nucleus where they bind to specific DNA sequences, called κ B sites with the consensus sequence GGGRNNYYCC (N - any base, R - purine, Y - pyrimidine), to activate transcription of target genes (Hayden and Ghosh, 2012).

The alternative NF- κ B pathway

The alternative pathway responds to signals of a selected set of receptors within the TNF superfamily such as lymphotoxin- β receptor (LT β R), B-cell activating factor receptor (BAFFR) and CD40 (Sun, 2011). In unstimulated cells, a protein complex of TRAF2, TRAF3 and cIAP mediates constitutive proteasomal degradation of one of the central kinases of alternative signaling namely the NF- κ B-inducing kinase (NIK). Upon receptor ligation, the complex is recruited to the receptor leading to a switch from NIK- towards TRAF3-ubiquitin-dependent degradation. This allows NIK accumulation (Liao et al., 2004; Qing et al., 2005) which then binds and phosphorylates IKK α . In contrast to classical NF- κ B signaling, the alternative pathway depends strictly on IKK α and is independent of IKK β and IKK γ (Senftleben et al., 2001). Activated IKK α then cooperates with NIK in phosphorylation of C-terminal serine residues of the NF- κ B precursor p100. This results in p100 ubiquitination and proteasomal processing generating p52, eliminating the I κ B-like function of p100 at its C-terminus. Therefore, the p52/RelB dimer is no longer sequestered in the cytosol and can translocate to the nucleus where it initiates expression of a variety of genes responsible for the functional cellular outputs of the alternative pathway, like development of secondary immune organs, presentation of self-antigens by thymic epithelial cells, or isotype switching of peripheral B cells. However, the precise identity of the target genes still remains elusive (Razani et al., 2011).

Besides its crucial role in the signaling cascade of the alternative pathway NIK also exhibits the capacity to activate the IKK complex, the gatekeeper of the classical pathway, through phosphorylation of IKK α (Ramakrishnan et al., 2004; Zarnegar et al., 2008). As a result, nearly all receptors initiating the alternative pathway also activate p65/p50 dimers which are part of the classical NF- κ B signaling pathway. This leads to a cross talk between the classical and the alternative NF- κ B pathway (Oeckinghaus et al., 2011).

1.3 The innate immune response during MV infection

1.3.1 Activation of the innate immune system by RNA viruses

The first line of host defense against an invading pathogen is the innate immune system. Activation of innate immune cells rapidly generates an anti-microbial environment to defend pathogens in a general way. The sensors of the cells to recognize signs of infection are the PRRs which are triggered by microbial components known as pathogen associated molecular patterns (PAMPs). Among the array of PRRs, TLRs and RLRs are the primary receptors in controlling infections by RNA viruses. Triggering of these receptors induces a series of signaling cascades and leads to activation of multiple transcription factors, such as NF- κ B and interferon regulatory factors (IRFs), resulting in the expression of proinflammatory cytokines and type I and III interferons (IFNs), which are potent antiviral effector proteins.

Toll-like receptor signaling

The Toll receptor was originally identified in *Drosophila* and shown later on to be essential for the defense against infections by fungi (Hashimoto et al., 1988; Lemaitre et al., 1996). Subsequently, a human homolog was identified and to date ten members of Toll-like receptors are known in humans. TLRs contain leucine-rich repeats required for pathogen recognition and Toll/interleukin-1 receptor (TIR) domains responsible for initiation of downstream signaling (Takeda and Akira, 2004).

Each TLR is able to detect distinct molecular patterns of microorganisms. While TLR1, 2, 4, 5, 6, and 11 bind mainly protein components of bacteria and parasites on plasma membranes, TLR3, 7, 8, and 9, which are found in the endosomal membrane, are the main sensors for viruses recognizing the nucleic acids that are internalized during an infection via endocytosis (Kumar et al., 2011). TLR3, which is expressed in various cell types, recognizes dsRNA, whereas TLR7 and 8 are restricted to immune cells and sense

Triggering of TLR signaling by the appropriate ligand causes the recruitment of adaptor proteins to the cytoplasmic TIR domain. Nearly all TLRs utilize myeloid differentiation primary response gene 88 (MyD88) as adaptor. Only TLR3 does not recruit MyD88, but TIR-domain-containing adapter-inducing interferon- β (TRIF) (Yamamoto et al., 2004) (Fig. 1-5).

Upon recruitment to the TLRs, MyD88 binds a subset of Interleukin-1 receptor-associated kinases (IRAKs) such as IRAK4, IRAK1 and IRAK2. Subsequently, IRAK kinases dissociate from MyD88 and interact with TRAF6, which ubiquitinates itself and activates the formation of a complex of transforming growth factor β -activated kinase 1 (TAK1), TAK1-binding protein 1 (TAB1), TAB2 and TAB3. The TAK1 complex then activates the IKK complex leading to NF- κ B activation as described in chapter 1.2.2 (Takeuchi and Akira, 2010). Simultaneously, it stimulates the mitogen-activated protein kinase (MAPK) pathway to facilitate activation of the transcription factor AP-1 (activator protein-1) (Fig. 1-5). In plasmacytoid dendritic cells (pDC), TLR7, 8, and 9 additionally activate IRF7 by a TRAF3-dependent mechanism resulting in the expression of type I IFNs (Honda et al., 2005).

In contrast, the TRIF-dependent TLR signaling activates IRF3 in addition to NF- κ B and AP-1. Upon recruitment of TRIF to TLR3, it associates with TRAF6 and TRAF3. Subsequently, TRAF6 stimulates in cooperation with receptor-interacting protein 1 (RIP1) the TAK1 complex, which leads to activation of MAPK and NF- κ B, whereas TRAF3 mediates TBK1/IKKi dependent phosphorylation of IRF3 and consequently expression of type I IFN genes (Fig. 1-5) (Hacker et al., 2006). TLR4 triggers the MyD88-dependent as well as the TRIF-dependent pathway (Takeuchi and Akira, 2010).

RIG-I-like receptor signaling

The RNA helicase RIG-I (retinoic acid-inducible gene I) was initially identified as a cytoplasmic PRRs for viral RNAs (Yoneyama et al., 2004) followed closely by the characterization of the other two RLR family members MDA5 (melanoma-differentiation-associated gene 5) and LGP2 (laboratory of genetics and physiology 2) (Yoneyama et al., 2005). The RLRs RIG-I and MDA5 are composed of two caspase

activation and recruitment domains (CARDs) at their N-terminus, a central DExD/H-box helicase domain, and a C-terminal regulatory domain (Ireton and Gale, 2011). The helicase domain of RIG-I and MDA5 is responsible to bind viral RNAs and exerts ATPase activity, whereas the CARDs mediate downstream signaling. As LGP2 lacks the CARD domains it has rather regulatory functions.

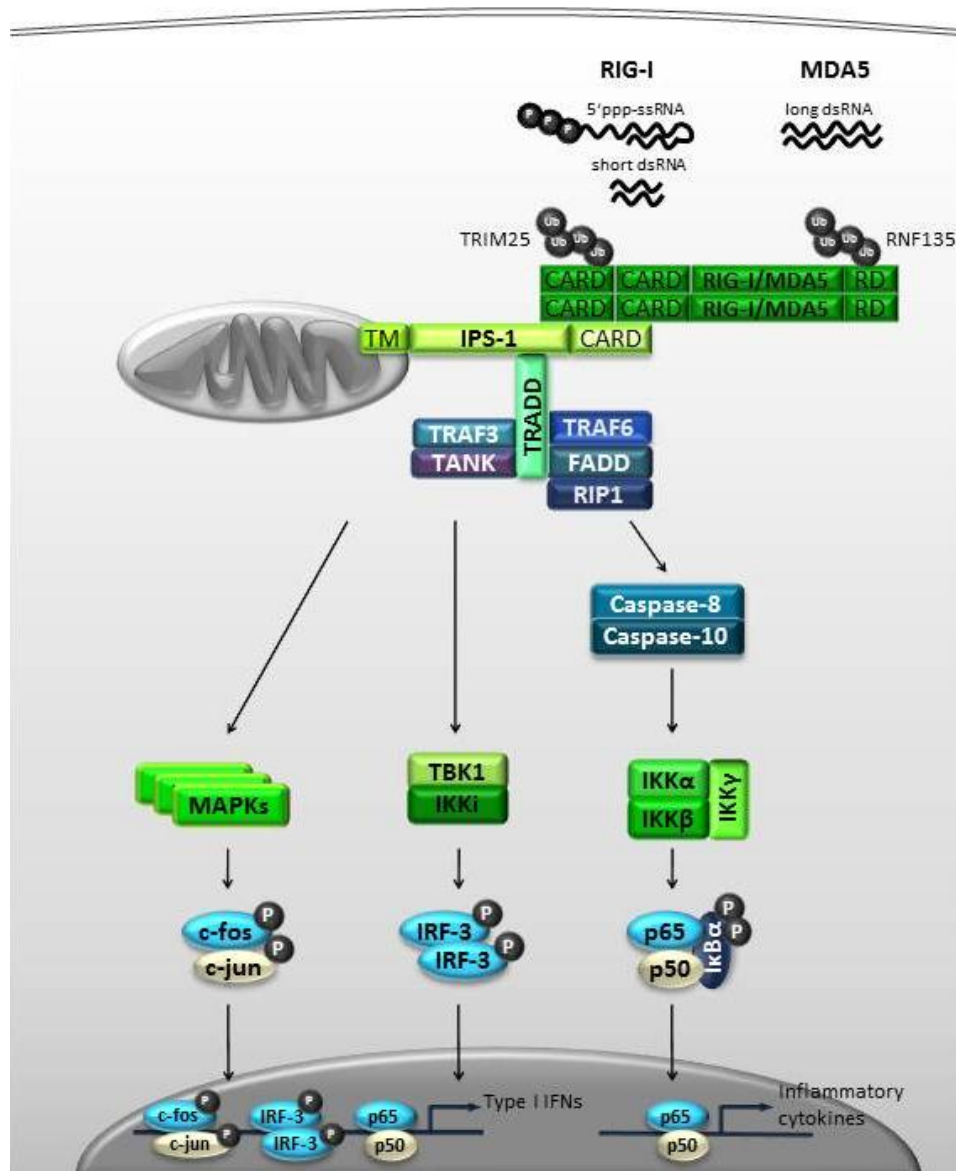


Figure 1-6 RLR signaling pathways

The RIG-I-like receptor (RLR) signaling pathway can be activated via RIG-I or MDA5, which bind RNA with a 5' triphosphate (5'ppp-RNA) and short double-strand RNA (dsRNAs) or long dsRNAs, respectively. Upon ligand binding RLRs dimerize and bind to IPS-1, which is located in the mitochondrial membrane activating kinases and subsequently transcription factors to initiate expression of inflammatory cytokines or type I interferons (IFNs).

With the exception of pDCs, RIG-I and MDA5 are the primary sensors in nearly all cell types for RNA virus infections. However, they were shown to recognize different RNA viruses (Kato et al., 2006; Loo et al., 2008). The virus specificity of RIG-I and MDA5 is determined by the RNA species they detect. RIG-I is activated by uncapped 5'-triphosphate (5'-ppp) RNA (Hornung et al., 2006; Pichlmair et al., 2006), but for recognition of short dsRNA 5'-ppp it might be dispensable (Hausmann et al., 2008; Kato et al., 2008). The distinct natural ligand of MDA5 remains still elusive, however, MDA5 is thought to bind to long, stable dsRNA structures (Kato et al., 2008; Pichlmair et al., 2009). RIG-I detects both negative and positive strand RNA viruses among them Sendai virus (SeV), rabies virus (RV), or Hepatitis C virus (HCV), while MDA5 has been shown to detect picornaviruses such as encephalomyocarditis virus (EMCV) (Gitlin et al., 2006; Kato et al., 2006). Interestingly, MV and other negative strand RNA viruses were shown to be recognized by both RIG-I and MDA5 (Berghall et al., 2006; Ikegame et al., 2010). Under steady-state conditions the best characterized receptor RIG-I is present in a closed, inactive conformation shielding the CARDs. Upon triggering, an ATP-dependent conformational change occurs enabling the helicase domain to bind RNA. Subsequently, RIG-I dimerizes and the CARDs are released and accessible for further signaling (Cui et al., 2008). The initial recognition by RIG-I is also tightly controlled by ubiquitination events. K63-linked ubiquitination by TRIM25 and RNF135 have been found to be required for activation, whereas K48-linked ubiquitination by RNF125 leads to downregulation of RIG-I-mediated signaling (Arimoto et al., 2007; Gack et al., 2007; Oshiumi et al., 2010). Upon activation, RIG-I and MDA5 interact with interferon-beta promoter stimulator 1 (IPS-1) through homophilic interactions between CARD domains (Kawai et al., 2005). IPS-1, also known as MAVS, Cardif, or VISA, is located at the outer mitochondrial membrane, which was shown to be important for downstream signaling (Meylan et al., 2005; Seth et al., 2005; Xu et al., 2005). Once RIG-I or MDA5 interact with IPS-1, a complex is recruited to IPS-1 including TRAF6, TNF receptor type 1-associated DEATH domain (TRADD), Fas-associated death domain (FADD) and RIP1, mediating activation of the IKK complex through cleavage of caspase-8/-10 to activate NF- κ B. Activated IPS-1 also associates with TRAF3, followed by activation of TBK1 and IKKi to activate IRF3 and IRF7 analogous to TRIF-dependent IRF activation (Kumar et al., 2011) (Fig. 1-6).

1.3.2 Strategies of measles virus to evade innate immune responses – it's all about the P gene products

Since MV replication activates innate immune responses (Rima and Duprex, 2011), mainly through triggering of RIG-I and MDA5 or TLR3, it has developed several strategies to circumvent the full range of innate immune responses and the accompanied establishment of an anti-viral environment. MV was shown to interfere with innate immune responses at different stages. Its most upstream target is MDA5. The MV V protein binds to the helicase domain of MDA5 but not RIG-I, thereby blocking its activation by dsRNA and consequently inhibiting MDA5-mediated IFN expression (Andrejeva et al., 2004; Childs et al., 2007). Recently, it was shown that the V protein also binds to LGP2 probably mediating a complex between RIG-I and LGP2, which renders RIG-I unable to respond to RIG-I-specific PAMPs (Childs et al., 2012). Both interactions are mediated through the C-terminal domain of V and are conserved among paramyxovirus V proteins. Furthermore, V proteins of a subset of paramyxoviruses, including MV V, were reported to inhibit IRF3 activation, eventually through binding to IRF3 (Irie et al., 2012). The most downstream inhibition of PRR-induced IFN expression, is probably controlled by the C protein, which was shown to act in the nucleus to evade IFN expression by yet unidentified mechanisms (Sparrer et al., 2012). In MV infected pDCs, TLR7 and 9 signaling was shown to be suppressed (Schlender et al., 2005). Again the V protein is responsible for the inhibition of IFN induction through MyD88-dependent TLR signaling acting as a decoy substrate for IKK α (Pfaller, 2009).

Besides inhibition of IFN expression, MV proteins also inhibit IFN-signaling, which involves activation of the janus kinases (JAK) and the transcription factors signal transducers and activators of transcription (STAT) 1 and 2 upon IFN receptor (IFNR) triggering. MV P and V bind through their common N-terminus to STAT1, inhibiting its phosphorylation upon stimulation with type I IFN and subsequently the expression of IFN-stimulated genes (ISGs), which are important anti-viral effectors (Devaux et al., 2007; Ohno et al., 2004). Furthermore, MV V binds to the kinase domain of JAK1, an

additional mechanism to prevent phosphorylation of STAT1 (Caignard et al., 2007). MV V binds STAT2 as well, but with its C-terminal domain thus blocking the nuclear translocation of STAT2 presenting a further mechanism to inhibit ISG expression (Ramachandran et al., 2008). The C protein was found to inhibit IFN signaling as well, but by a so far unknown mechanism (Shaffer et al., 2003). Recently, a role for the MV N protein in IFN signaling inhibition was suggested (Takayama et al., 2012).

In summary, MV has evolved multiple and powerful strategies to counteract IRF3/7-dependent IFN induction and STAT-dependent IFN signaling mainly mediated by the P-gene products (Goodbourn and Randall, 2009).

1.4 Objective of the study

While numerous recent studies on paramyxovirus innate immune antagonistic activities have shed light on how control of IRF3/7 and STAT is achieved, their potential to interfere with NF- κ B is less well studied. However, activation of the NF- κ B pathway is of critical importance during an immune response and thus it is likely that MV modulates this pathway. Therefore, I wanted to assess the capacity of the MV proteins to interfere with NF- κ B signaling and to understand the underlying mechanism of the presumed inhibition. For this purpose different biochemical and virological assays were performed in cultured cells either transiently expressing MV proteins or infected with MV.

2 Material and Methods

2.1 Material

2.1.1 Chemicals

All chemicals were purchased from the following companies: BD, Biorad, Fluka, Invitrogen, Merck, Roth, Sigma-Aldrich, Serva, VWR Prolab.

2.1.2 Enzymes and recombinant proteins

All restriction enzymes and the appropriate buffers were purchased from New England Biolabs. All additional enzymes were purchased with the appropriate buffers from the listed companies.

DNA polymerase	Manufacturer
<i>Pfu</i> DNA Polymerase	Fermentas
<i>Phusion</i> ® <i>High Fidelity</i> DNA Polymerase	NEB
<i>Taq</i> DNA Polymerase	Biomaster
DNase/RNase	Manufacturer
<i>TURBO</i> DNase Deoxyribonuclease I, RNase free	Fermentas
<i>RNase A</i>	Macherey&Nagel
Reverse Transcriptase	Manufacturer
<i>Transcriptor</i> Reverse Transcriptase	Roche
RNase inhibitor	Manufacturer
<i>SUPERase-In</i>	Ambion

Ligase	Manufacturer
T4 DNA Ligase	New England Biolabs
Phosphatase	Manufacturer
Calf Intestine Alkaline Phosphatase (CIAP)	New England Biolabs
Protease Inhibitor	Manufacturer
<i>Complete ULTRA</i> Protease Inhibitor Cocktail Tablets	Roche
Recombinant Protein	Manufacturer
Human TNF α	Biomol

2.1.3 Commercial kits

Plasmid purification	Manufacturer
<i>Nucleobond</i> [®] <i>Xtra</i> Midi	Macherey&Nagel
Cloning	Manufacturer
<i>QIAquick</i> [®] Gel Extraction Kit	Qiagen
<i>QIAEX</i> [®] II Gel Extraction Kit	Qiagen
<i>QIAquick</i> [®] Nucleotide Removal Kit	Qiagen
<i>QIAquick</i> [®] PCR Purification Kit	Qiagen
Luciferase reporter gene assay	Manufacturer
<i>Dual Luciferase</i> [®] Reporter Assay System	Promega
RNA isolation	Manufacturer
<i>RNeasy</i> [®] Mini Kit	Qiagen
Real time PCR	Manufacturer
<i>Quantitect SYBR</i> [®] <i>Green</i> PCR Kit	Qiagen
Transfection	Manufacturer
<i>ProFectin</i> [®] Mammalian Transfection System-CaPO ₄	Promega

2.1.4 Additional reagents

Additional reagents	Manufacturer
1 kb DNA Ladder	New England Biolabs
0,25 % Trypsin-EDTA	Gibco
Anti-Flag® M2-Agarose	Sigma-Aldrich
Anti-HA Affinity Matrix; (clone 3F10)	Roche
dNTP Set	Bioline
Immobilon-P blotting membrane (PVDF)	Millipore
Lipofectamine™ 2000	Invitrogen
Oligo(dT)12-18 Primer	Invitrogen
PCR Marker	New England Biolabs
Precision Plus Protein Standards	Biorad
Protein A-Sepharose	GE Healthcare
Vectashield® Mounting Medium for Fluorescence	Vector Laboratories
Versene	Gibco
Whatman Blotting Paper	Machery-Nagel
<i>Western Lightning® Plus ECL</i> Chemiluminescence Substrate	Perkin Elmer

2.1.5 Antibodies

Primary antibodies (antigen)	Host	Manufacturer	Dilution	
			WB	IF
Anti-c-Rel	rabbit	Cell Signaling #4727	1:1000	-
Anti-Flag M2	mouse	Sigma-Aldrich	-	1:200
Anti-Flag M2	rabbit	Sigma-Aldrich	1:10000	-
Anti-HA (3F10)	rat	Roche	1:1000	-
Anti-IkBa (L35A5)	mouse	Cell Signaling #4814	1:1000	-
Anti-MV N (2D7)	mouse	Abcam ab9882	1:500	-
Anti-MV N	mouse	Millipore MAB8906	1:500	-
Anti-MV N-FITC	mouse	Millipore MAB8906F	-	1:2000
Anti-MV P (37069) (aa 2-15)	rabbit	D.Gerlier (Chen et al., 2003)	1:10000	-
Anti-MV V _{CTD} (WBA/10/2) (aa 286-299)	rabbit	Metabion; custom-made	1:5000	-
Anti-MV C (1240) (aa 176-186)	rabbit	R. Cattaneo	1:2500	-
Anti-MV C (FEA/10/1) (aa 176-186)	rabbit	Metabion; custom-made	1:2500	-
Anti-p65	rabbit	Santa Cruz sc-109	1:1000	1:200
Anti-p65 (C22B4)	rabbit	Cell Signaling #4764	1:1000	-
Anti-p65-CT	rabbit	Millipore #06-418	1:1000	-
Anti-p100/p52	rabbit	Cell Signaling #4882	1:1000	-
Anti-p105/50	rabbit	Cell Signaling #3035	1:1000	-
Anti-RelB (H-200)	rabbit	Santa Cruz sc-28689	1:1000	-
Anti-RelB (C1E4)	rabbit	Cell Signaling #4922	1:1000	-
Anti-RV P (P160-5)	rabbit	S. Finke	1:50000	-

Secondary antibodies (antigen)	Host	Manufacturer	Dilution	
			WB	IF
Anti-mouse HRP	goat	Jackson ImmunoResearch Laboratories	1:20000	-
Anti-rabbit HRP	goat	Jackson ImmunoResearch Laboratories	1:20000	-
Anti-rat HRP	goat	Jackson ImmunoResearch Laboratories	1:5000	-
Anti-human HRP	goat	Jackson ImmunoResearch Laboratories	1:20000	-
Anti-mouse tetramethylrhodamine	goat	MoBiTec	-	1:1000
Anti-rabbit Alexa Fluor 488	goat	MoBiTec	-	1:1000

2.1.6 Buffers and solutions

All solutions and buffers were made in double distilled water (ddH₂O). If solutions had to be autoclaved it is indicated. Unless indicated otherwise, all solutions were stored at room temperature. LB medium and LB plates were supplemented with the appropriate antibiotics: ampicillin (100 µg/ml), or kanamycin (25 µg/ml).

Mini Preparation	
Flexi I	100 mM Tris-HCl pH 7.5 10 mM EDTA 200 µg/ml RNase Stored at 4°C
Flexi II	200 mM NaOH 1 % (w/v) SDS
Flexi III	3 M potassium acetate 2 M acetic acid, pH 5.75

Agarose gel electrophoresis	
10x TAE	2 M Tris-HCl, pH 7.8 0.25 M Sodium acetate x 3 H ₂ O 0.25 M EDTA
1x TAE + EtBr	200 ml 10x TAE 150 µl Ethidium bromide solution 1% Add ddH ₂ O to 2 l
OG loading buffer	50 % (v/v) 10x TAE 15 % (w/v) Ficoll 400 0.125 % (w/v) Orange G
10x TE	100 mM Tris-HCl, pH 7.5 10 mM EDTA

Blue juice	0.125 % (w/v) Bromphenol blue 0.125 % (w/v) Xylenecyanol 0.125 % (w/v) Orange G 15 % (w/v) Ficoll 400 50 % (v/v) 10x TAE Store at -20°C
1 kb marker	380 µl 1x TE 100 µl Blue juice 20 µl 1 kb DNA ladder (New England Biolabs) Store at 4°C/-20°C
PCR marker	167 µl Gel loading dye blue (6x) 733 µl H ₂ O 100 µl PCR Marker (New England Biolabs) Store at 4°C/-20°C

SDS-PAGE	
Jagow gel buffer	3 M Tris-HCl, pH 8.45 0.3 % (w/v) SDS
Jagow anode buffer	200 mM Tris-HCl, pH 8.9
Jagow cathode buffer	100 mM Tris-HCl, pH 8.25 100 mM Tricine 0,1 % (w/v) SDS
Protein lysis buffer	62.5 mM Tris-HCl, pH 6.8 2 % (w/v) SDS 10 % (w/v) glycerol 6 M Urea 5 % (v/v) β-mercaptoethanol 0.01 % (w/v) Bromphenol blue 0.01 % (w/v) Phenol red Store at -20°C

Stacking gel 4%	3.5 ml Jagow gel buffer 1.4 ml acrylamide 29:1 Rotiphorese Gel 40 18 µl TEMED 116 µl APS (10 %) 9 ml H ₂ O
Separating gel 10%	12 ml Jagow gel buffer 9 ml acrylamide 29:1 Rotiphorese Gel 40 2 ml glycerol 17 µl TEMED 175 µl APS (10%) 12.9 ml H ₂ O

Western blotting	
10x Semi dry buffer	480 mM Tris-HCl pH 8.6 390 mM Glycine 0.05 % (w/v) SDS
1x Semi dry buffer	100 ml 10x Semi dry buffer 180 ml Methanol abs. 720 ml H ₂ O
1x PBS	1.37 M NaCl 27 mM KCl 12 mM KH ₂ PO ₄ 65 mM Na ₂ HPO ₄ ·2H ₂ O (pH 7.4)
PBS-Tween	1x PBS 0.05 % Tween 20

Co-Immunoprecipitation	
Standard Co-IP buffer	50 mM Tris-HCl pH 7.5 150 mM NaCl 2 mM EDTA 1 mM Na ₃ VO ₄ 0.5 % (v/v) NP-40 Store at 4°C Add 1 Complete Protease Inhibitor Tablet per 50 ml before use
Sepharose A Co-IP Buffer	Buffer A: 100 mM Tris pH 8.0 Buffer B: 10 mM Tris pH 7.4 Store at 4°C
PBS 5mM EDTA	1x PBS 5mM EDTA

Immunofluorescence	
3 % PFA/PBS	1x PBS 3 % (w/v) paraformaldehyde
80 % Acetone	800 ml acetone p.a. Add ddH ₂ O to 1l
50mM NH₄Cl/PBS	1x PBS 50mM NH ₄ Cl
PBS/0.5 % Triton X-100	1x PBS 0.5 % (v/v) Triton X-100
PBS/2,5 %milk/0.1 % Triton X-100	1x PBS 0.1 % (v/v) Triton X-100 2.5 % (w/v) milk powder
PBS/0.1 % Triton X-100	1x PBS 0.1 % (v/v) Triton X-100

Bacteria growth media	
LB	85 mM NaCl 0.5 % (w/v) Bacto yeast extract 1 % (w/v) Bactotryptone 1 mM MgSO ₄ Autoclaved and stored at 4 °C
LB ++	1x LB 20 mM MgSO ₄ 10 mM KCl
LB plates	1 l LB medium 15 g Agar

2.1.7 Bacteria and cell lines

The *E.coli* strain XL1 Blue (Stratagene) was used for amplification of plasmids.

Cell line	Description
HEK-293T (ATCC-CRL-11268)	HEK-293 was established from a human primary embryonic kidney transformed by adenovirus type V (Graham et al., 1977). The cell line HEK-293T is a derivative, which constitutively expresses the simian virus 40 (SV40) large T antigen.
HEp-2 (ATCC-CCL-23)	The HEp-2 cell line was initiated from tumors that had been produced in irradiated-cortisonized weanling rats after injection with epidermoid carcinoma tissue from the larynx of a 56-year-old male (Toolan, 1954).
A549 (ATCC-CCL-185)	The A549 cell line was developed from culturing of cancerous lung tissue in the explanted tumor of 58-year-old Caucasian male (Giard et al., 1973). A549 cells are human alveolar basal epithelial cells.
293-3-46	Derived from the human embryonic kidney 293 cell line. The cells constitutively express T7 RNA polymerase together with MV nucleocapsid protein and phosphoprotein (Radecke et al., 1995)
Vero-hSLAM	This cell line is a derivative of Vero cells which constitutively expresses the human SLAM receptor (Ono et al., 2001).
Vero (ATCC- CCL-81)	The Vero cell line was established from the kidney of a normal adult African green monkey (Yasumura, 1963).

2.1.8 Oligonucleotides

Primers were purchased from Metabion.

Primers for cloning:

#	Primer name	Sequence (5'-3')
11	NBD-Peptide forw	ATA GAA TTC CTA GAC TGG AGC TGG TTA CTC GAG ATA
12	NBD-Peptide rev	TAT CTC GAG TAA CCA GCT CCA GTC TAG GAA TTC TAT
17	p65 EcoRV forw	ATA GCC ACC GAT ATC ATG GAC GAA CTG TTC CCC
34	p65 XhoI rev	TAT CTC GAG TTA GGA GCT GAT CTG ACT
39	p50 HindIII forw	ATA AAG CTT GCC ACC ATG GCA GAA GAT GAT
40	flag p50 HindIII forw	ATA AAG CTT GCC ACC ATG GAC TAC AAA GAC GAT GAC GAT AAA GCA GAA GAT GAT CCA
41	p50 XhoI rev	ATA CTC GAG TTA AAC TTT CCC AAA GAG GTT
43	p65 HindIII forw	ATA AAG CTT GCC ACC ATG GAC GAA CTG TTC CCC
44	p65 flag XhoI rev	ATA CTC GAG CTA TTT ATC GTC ATC GTC TTT GTA GTC GGA GCT GAT CTG ACT CAG
45	p65 1-309 XhoI rev	ATA CTC GAG TTA GAA GGT CTC ATA TGT
46	p65 1-309 flag XhoI rev	ATA CTC GAG TTA TTT ATC GTC ATC GTC TTT GTA GTC GAA GGT CTC ATA TGT
47	p65 310-551 HindIII forw	ATA AAG CTT GCC ACC ATG AAG AGC ATC ATG AAG
48	p65 310-551 flag XhoI rev	TAT CTC GAG TTA TTT ATC GTC ATC GTC TTT GTA GTC GGA GCT GAT CTG ACT
49	p65 310-551 XhoI rev	TAT CTC GAG TTA GGA GCT GAT CTG ACT
50	flag-PIV5-V EcoRI forw	ATA GAA TTC GCC ACC ATG GAC TAC AAA GAC GAT GAC GAT AAA GAT CCC ACT GAT CTG
51	p50 RHD 1-399 XhoI rev	ATA CTC CAG TTA CTT CTG ACG TTT CCT
52	MV-V E235A forw	CCA TTA AAA AGG GGC ACA GAC GCG CGA TTA GCC TCA TTT GGA ACG G

53	MV-V E235A rev	CCG TTC CAA ATG AGG CTA ATC GCG CGT CTG TGC CCC TTT TTA ATG G
54	MV-V R233A forw	CAC CCA TTA AAA AGG GGC ACG CAC GCG AGA TTA GCC TCA TTT GGA ACG G
55	MV-V R233A rev	CCG TTC CAA ATG AGG CTA ATC TCG CGT GCG TGC CCC TTT TTA ATG GGT G
56	MV-V R233A,E235A forw	CAC CCA TTA AAA AGG GGC ACG CAC GCG CGA TTA GCC TCA TTT GGA ACG G
58	p65 1-300 XhoI rev	ATA CTC GAG TTA CTC CTC AAT CCG GTG
59	p65 NLS- 301AAA forw	GAT CGT CAC CGG ATT GAG GAG GCA GCT GCA AGG ACA TAT GAG ACC TTC AAG AGC
60	p65 NLS- 301AAA rev	GCT CTT GAA GGT CTC ATA TGT CCT TGC AGC TGC CTC CTC AAT CCG GTG ACG ATC
62	Nipah V XhoI rev	TAT CTC GAG TTA ACC GCA GTG GAA GCA
67	flag Nipah V HindIII forw	ATA AAG CTT GCC ACC ATG GAC TAC AAA GAC GAT GAC GAT AAA GAT AAA TTG GAA CTA
70	flag-p65 HindIII forw	ATA AAG CTT GCC ACC ATG GAC TAC AAA GAC GAT GAC GAT AAA GAC GAA CTG TTC CCC
71	flag-p65 180 XhoI rev	ATA CTC GAG TTA AGA AAG GAC AGG CGG
72	p65 181 HindIII forw	ATA AAG CTT GCC ACC ATG CAT CCC ATC TTT GAC
73	HA-importin a3 NheI forw	ATA GCT AGC GCC ACC ATG TAT CCT TAT GAC GTG CCT GAC TAT GCC AGC CTG GGA GGA CCT GCG GAC AAC GAG AAA CTG
74	importin a3 NotI rev	ATA GCG GCC GCC TAA AAC TGG AAC CCT TC
75	HA-importin a4 NheI forw	ATA GCT AGC GCC ACC ATG TAT CCT TAT GAC GTG CCT GAC TAT GCC AGC CTG GGA GGA CCT GCC GAG AAC C CC AGC TTG GAG
76	importin a4 NotI rev	ATA GCG GCC GCT TAA AAA TTA AAT TCT TT
77	HA-importin a 5 NheI forw	ATA GCT AGC GCC ACC ATG TAT CCT TAT GAC GTG CCT GAC TAT GCC AGC CTG GGA GGA CCT ACC ACC CCA GGA AAA GAG
78	importin a5 NotI rev	ATA GCG GCC GCT CAA AGC TGG AAA CCT TCC AT
79	flag-CDV PV _{NTD} HindIII forw	ATA AAG CTT GCC ACC ATG GAC TAC AAA GAC GAT GAC GAT AAA GCA GAG GAG CAG GCC TAT

81	CDV-V XhoI rev	ATA CTC GAG TCA TTT GAG GTC TTG GGA
115	c-Rel HindIII forw	ATA AAG CTT GCC ACC ATG GCC TCC GGT GCG TAT
116	c-Rel XhoI rev	TAT CTC GAG TTA TAC TTG AAA AAA TTC
118	MV VdC dloop1 BsmBI forw 3'	ATA CGT CTC CTG GAT GCA ACC CAA TGT GCT CG
119	MV VdC dloop2 BsmBI reverse 5'	ATA CGT CTC CTC CAC CGC ACA TTG GGT TGC ACC A
120	MV VdC dloop2 BsmBI forw 3'	ATA CGT CTC CTG GAA CCT GCG GGG AAT GTC CC
121	MV VdC dloop2 BsmBI forw 3'	ATA CGT CTC CTG GAT GCA CCT GCG GGG AAT GTC CC
124	MV PdeltaV mut fwd	TAG GGC CAG CAC TTC CGG GAC ACC CAT TAA GAA GGG CAC AGA CGC GAG ATT AGC CTC ATT
125	MV PdeltaV mut rev	AAT GAG GCT AAT CTC GCG TCT GTG CCC TTC TTA ATG GGT GTC CCG GAA GTG CTG GCC CTA
126	MV VdC dloop1 BsmBI reverse 5'	ATA CGTCTC C TCC ACC GTG CCC CTT TTT AAT GGG
129	flag p100/p52 HindIII forw	ATA AAG CTT GCC ACC ATG GAC TAC AAA GAC GAT GAC GAT AAA GAG AGT TGC TAC AAC CCA
131	p52 BamHI rev	TAT GGA TCC TCA CCT CCT CCA GCT CCT
CP 50	MV V NotI rev	ATA TGC GGC CGC TTA TTC TGG GAT CTC
CP 127	PIV5 V XhoI rev	TAT CTC GAG TTA AGT ATC TCG TTC
CP 201	V SnaBI+5nt fwd	ATA TAC GTA CCA CCA TGG CAG AAG AGC AGG CA

Primers for quantitative real-time RT-PCR

Primer name	Sequence (5'-3')	Annealing Temperature
GAPDH for	TGG TAT CGT GGA AGG ACT CA	53 °C
GAPDH rev	CCA GTA GAG GCA GGG ATG AT	53 °C
IFN β forw	TCC AAA TTG CTC TCC TGT TG	47°C
IFN β rev	GCA GTA TTC AAG CCT CCC AT	47°C
IL-6 forw	TAGTCCTTCCTACCCCAATTCC	53 °C
IL-6 rev	TTGGTCCTTAGCCACTCCTTC	53 °C
MV-N forw	TCA GAA CAA GTT CAG TGC AG	48°C
MV-N rev	CTT ACC ATC TCT TGC CCT AA	48°C
RANTES forw	GAGCTTCTGAGGCGCTGCT	53 °C
RANTES rev	TCTAGAGGCATGCTGACTTC	53 °C

2.1.9 Plasmids

Plasmids commercially available

Plasmid name	Vector	Description	Provider
Flag-c-Rel	pcDNA	Expression plasmid for the human NF- κ B subunit c-Rel with N-terminal flag-tag	Addgene #27253
Flag-RelB	pReceiver	Expression plasmid for the human NF- κ B subunit RelB with N-terminal flag-tag	GeneCopoeia #EX-G0029-M11
p100	pCMV4	Expression plasmid for the human NF- κ B subunit p100	Addgene #23287
p50	pCMV4	Expression plasmid for the human NF- κ B subunit p50	Addgene #21965
p52	pCMV4	Expression plasmid for the human NF- κ B subunit p52	Addgene #23289
p65	pCMV4	Expression plasmid for the human NF- κ B subunit p65/RelA	Addgene #21966
pCR3	pCR3	Eukaryotic expression vector; CMV promoter controlled	Invitrogen
pRL-CMV	pRL-CMV	<i>Renilla</i> luciferase; CMV promoter controlled	Promega
RelB	pCMV-SPORT6	Expression plasmid for the human NF- κ B subunit RelB	Open Biosystems #1010-7507797

Plasmids kindly provided

Plasmid name	Vector	Description	Provider
Flag-ΔRIG-I	pEFBos	Expression plasmid for human RIG-I CARD domain (aa 1-284) with N-terminal flag-tag	A.Krug
Flag-IKKα	pRK7	Expression plasmid for human IKK α with N-terminal flag-tag	K. Ruckdeschel
Flag-IPS1	pCMV	Expression plasmid for human IPS1 with N-terminal flag-tag	S.Akira
Flag-TRIF	pRK7	Expression plasmid for human TRIF with N-terminal flag-tag	K. Ruckdeschel
IKKβ-flag	pRK7	Expression plasmid for human IKK β with C-terminal flag-tag	K. Ruckdeschel
Myc-MyD88	pRK7	Expression plasmid for human IKK β with N-terminal myc-tag	K. Ruckdeschel
p55A2-luc	pBL	<i>Firefly</i> luciferase controlled by NF- κ B binding sites (Yoneyama et al., 1996)	T.Fujita

Plasmids generated in this laboratory:

Unless otherwise indicated all ORFs were cloned into the pCR3 vector.

Plasmid name	Description	Generated by
Flag-MV C	Expression plasmid for measles virus C protein of the Schwarz strain with N-terminal flag-tag	C.Pfaller
Flag-MV P	Expression plasmid for measles virus P protein of the Schwarz strain with mutations avoiding the expression of the C protein and N-terminal flag-tag	C.Pfaller
Flag-MV V	Expression plasmid for measles virus V protein of the Schwarz strain with mutations avoiding the expression of the C protein and N-terminal flag-tag	C.Pfaller
Flag-IKKγ	Expression plasmid for human IKK γ /NEMO with N-terminal flag-tag in pCAGGS vector	M. Rieder

Ig	pCR3 vector with Ig-tag sequence upstream of MCS	K. Brzózka
Ig-MV C	Expression plasmid for measles virus C protein of the Schwarz strain	C.Pfaller
Ig-MV P	Expression plasmid for measles virus P protein of the Schwarz strain with mutations avoiding the expression of the C protein and N-terminal Ig-tag	C.Pfaller
Ig-MV P_{CTD}	Expression plasmid for the C-terminal domain (aa 233-507) of measles virus P protein of the Schwarz strain and N-terminal Ig-tag	C.Pfaller
Ig-MV PV_{NTD}	Expression plasmid for the common N-terminal domain (aa 1-232) of measles virus P and V protein of the Schwarz strain with mutations avoiding the expression of the C protein and N-terminal Ig-tag	C.Pfaller
Ig-MV V	Expression plasmid for measles virus V protein of the Schwarz strain with mutations avoiding the expression of the C protein and N-terminal Ig-tag	C.Pfaller
Ig-MV V_{CTD}	Expression plasmid for the C-terminal domain (aa 233-299) of measles virus V protein of the Schwarz strain and N-terminal Ig-tag	C.Pfaller
MV C	Expression plasmid for measles virus C protein of the Schwarz strain	S.Moghim
MV P	Expression plasmid for measles virus P protein of the Schwarz strain with mutations avoiding the expression of the C protein	C.Pfaller
MV V	Expression plasmid for measles virus V protein of the Schwarz strain with mutations avoiding the expression of	C.Pfaller
MV V_{dIRF7}	Expression plasmid for measles virus V protein of the Schwarz strain with point mutation 259AAAA avoiding IRF7 binding	C. Pfaller
MV V_{wt}	Expression plasmid for wild type measles virus V protein of the D5 genotype with mutations avoiding the expression of the C protein	C.Pfaller
RV P	Expression plasmid for rabies virus P protein	K. Brzózka

Plasmids generated during this thesis:

Unless indicated otherwise all ORFs were cloned into the pCR3 vector.

Plasmid name	Description	Template (provider)	Primers
c-Rel	Expression plasmid for the human NF- κ B subunit c-Rel	pCDNA-flag-c-Rel	115; 116
flag-CDV V	Expression plasmid for canine distemper virus V protein with mutations avoiding the expression of the C protein and N-terminal flag-tag	pCG-CDV V Δ C (V. von Messling)	79; 81
flag-NiV V	Expression plasmid for nipah virus V protein with mutations avoiding the expression of the C protein and N-terminal flag-tag	pGexGp2-NiV V Δ C (K.P. Hopfner)	62; 67
flag-p50	Expression plasmid for the human NF- κ B subunit p50 with N-terminal flag-tag	pCMV4-p50	40; 41
flag-p50 RHD	Expression plasmid for the REL homology domain (aa 1-366) of human p50 with N-terminal flag-tag	pCMV4-p50	40; 51
flag-p52	Expression plasmid for the human NF- κ B subunit p52 with N-terminal flag-tag	pCMV4-p52	129; 131
flag-p65	Expression plasmid for the human NF- κ B subunit p65/RelA with N-terminal flag-tag in pCDNA3.1 vector	pCMV4-p65	17; 34
flag-p65 NTD	Expression plasmid for the N-terminal domain of human p65 RHD (aa 1-180) with N-terminal flag-tag	pCR3-p65	70; 71
flag-PIV5 V	Expression plasmid for Para-influenza virus type 5 V protein and N-terminal flag-tag	pCR3-PIV5 V (C.Pfaller)	50;CP 127
HA-importin α3	Expression plasmid for human importin α 3 with N-terminal HA-tag	pCMVTNT-T7-importin α 3 (Addgene #26680)	73; 74

HA-importin α4	Expression plasmid for human importin α 4 with N-terminal HA-tag	pCMVTNT-T7-importin α 4 (Addgene #26679)	75; 76
HA-importin α5	Expression plasmid for human importin α 5 with N-terminal HA-tag	pCMVTNT-T7-importin α 5 (Addgene #26677)	77; 78
Ig-NBD	Expression plasmid for Nemo binding domain of IKK α (aa738-743) with N-terminal Ig-tag (May et al., 2000)	Annealing of primers	11; 12
MV V_{dMDA5 (1)}	Expression plasmid for measles virus V protein of the Schwarz strain with point mutation R233A avoiding MDA5 binding	pCR3-MV V	54; 55
MV V_{dMDA5 (2)}	Expression plasmid for measles virus V protein of the Schwarz strain with point mutation E235A avoiding MDA5 binding	pCR3-MV V	52; 53
MV V_{dMDA5 (1/2)}	Expression plasmid for measles virus V protein of the Schwarz strain with point mutations R233A E235A avoiding MDA5 binding	pCR3-MV V	56; 57
MV V_{Δloop1}	Expression plasmid for measles virus V protein of the Schwarz strain with deletion of aa 233-250 therefore insertion of two Glycins	pCR3-MV V	126; 118
MV V_{Δloop1}	Expression plasmid for measles virus V protein of the Schwarz strain with deletion of aa 256-266 therefore insertion of two Glycins	pCR3-MV V	119; 121
p50	Expression plasmid for the human NF- κ B subunit p50	pCMV4-p50	39; 41
p65	Expression plasmid for the human NF- κ B subunit p65/RelA	pCMV4-p65	43; 49
p65-flag	Expression plasmid for the human NF- κ B subunit p65/RelA with C-terminal flag-tag	pCMV4-p65	43; 44
p65 1-300	Expression plasmid for the REL homology domain of human p65 lacking the NLS (aa 1-300)	pCMV4-p65	43; 58

p65 TA-flag	Expression plasmid for transactivation domain (aa 310-551) of human p65 with C-terminal flag-tag	pCMV4-p65	47; 48
p65 CTD-flag	Expression plasmid for the C-terminal domain of human p65 RHD (aa 181-309) with C-terminal flag-tag	pCR3-p65	72; 46
p65 NLS-	(K301A,R302A,K303A)	pCR3-p65	59; 60
p65 RHD	Expression plasmid for the REL homology domain (aa 1-309) of human p65	pCMV4-p65	43; 45
p65 RHD-flag	Expression plasmid for the REL homology domain (aa 1-309) of human p65 with C-terminal flag-tag	pCMV4-p65	43; 46
RelB	Expression plasmid for the human NF- κ B subunit RelB	Digestion of pCMVSPORT6-RelB with EcoRI; NotI	none

Full length plasmid	Origin/Cloning strategy
pBS-HHRz-MVvac2-HdRz(sc)	C. Pfaller
pBS-HHRz-MVvac2-ATU-MCS-HdRz(sc)	C. Pfaller
pBS-HHRz-MVvac2-VKO-ATU-MCS-HdRz(sc)	Site directed mutagenesis of the editing site within the P gene (Schneider et al., 1997) within the helper plasmid pSK-NotI-ATU-SacII. Used primers: 124 + 125. Insertion into pBS-HHRz-MVvac2-ATU-MCS-HdRz(sc) with NotI + SacII.
pBS-HHRz-MVvac2-VKO-ATU-MCS-VdCdW- HdRz(sc)	Insertion of the V ORF with mutated editing site and mutation in the start codon of the C ORF into pBS-HHRz-MVvac2-VKO-ATU-MCS-HdRz(sc) using primers CP 201, CP 50 and restriction enzymes SnaBI and NotI.

2.1.10 Viruses

Virus	Description
MVvac2	Recombinant measles virus generated from the full-length cDNA plasmid pBS-HHRz-MVvac2-HdRz(sc). The virus has equivalent nucleotide sequence to Moraten and Schwartz vaccine strains (GeneBank accession numbers AF266287 and AF266291) (del Valle et al., 2007). The Moraten and Schwartz vaccines share an identical sequence in spite of a nominally different origin.
MVvac2 MCS	The full length cDNA plasmid pBS-HHRz-MVvac2-ATU-MCS-HdRz(sc) was used for rescue of the recombinant measles virus. It is a derivative of MVvac2 generated by insertion of a multiple cloning site between the P and the M gene flanked by the 5'-UTR and the 3'-UTR of the P gene.
MVvac2 VKO MCS	Recombinant measles virus generated from the full length plasmid pBS-HHRz-MVvac2-VKO-ATU-MCS-HdRz(sc). The virus is a derivative of MVvac2 MCS generated by a point mutation within the V editing site to destroy V mRNA production (Radecke and Billeter, 1997; Schneider et al., 1997). The introduced point mutation is silent for the P and C protein.
MVvac2 VKO MCS V	The full length cDNA plasmid pBS-HHRz-MVvac2-VKO-ATU-MCS-VdCdW-HdRz(sc) was used for rescue of the recombinant measles virus. It was generated by insertion of the V ORF with mutated editing site into the MCS of pBS-HHRz-MVvac2-ATU-MCS-VKO-HdRz(sc). Thus the expression of the V protein is restored in the recombinant virus MVvac2 VKO MCS V.

2.1.11 Equipment

Instrument	Manufacturer
Agarose vertical gel electrophoresis apparatus	Peqlab
Bacteria culture incubator <i>ISF-1-W</i>	Kühner
Centrifuges: Centrifuge <i>5417C</i> Centrifuge <i>5804R</i> Centrifuge <i>Evolution RC</i> <i>Biofuge pico</i> <i>Varifuge 3.0R</i>	Eppendorf Eppendorf Sorvall Heraeus Heraeus
Cell culture incubator	Sanyo
Chemiluminescence developing system <i>Fusion FX7</i>	Vilber-Lourmat
Gel Doc system	BioRAD
Freezers: -20°C -80°C <i>II Shin</i>	Liebherr Nunc
Laminar Flow <i>Sterileguard ClassII TypeA/B3</i>	Baker Company
LightCycler <i>2.0</i>	Roche
Luminometer <i>Centro LB 960</i>	Berthold
Magnetic stirrer/heater	VELP Scientifica
Mixer <i>5432</i>	Eppendorf
Microscopes: Laser scanning microscope <i>LSM 510 Meta</i> Light microscope <i>TMS</i> UV-Light microscope <i>IX71</i>	Carl Zeiss Nikon Olympus
Neubauer improved cell-counting chamber	Marienfeld
PH-meter	VWR International

<i>PIPETBOY acu</i>	IBS
Pipettes (2/2,5/10/20/200/1000µl)	Eppendorf; Gilson
Polyacrylamid gel electrophoresis system	Peqlab
Power supply <i>Power Pack P25</i>	Biometra
Roller mixer <i>SRT2</i>	Stuart
Semi-Dry blotting system	Peqlab
Shaker <i>Swip SM25</i>	Edmund Bühler
Spectrophotometer <i>Nanodrop ND-1000</i>	Peqlab
Thermocycler <i>T3</i>	Biometra
Thermomixer <i>5436</i>	Eppendorf
Thermostated hot-block <i>5320</i>	Eppendorf

2.2 Methods

2.2.1 Molecular biological methods

Polymerase chain reaction (PCR)

The polymerase chain reaction (PCR) allows the cyclic enzymatic amplification of defined DNA fragments *in vitro*. Short oligonucleotide-fragments, which anneal to the complementary strands of the DNA template in an inverse orientation, determine the ends of the amplified DNA fragment. In the presence of dNTPs thermostable DNA polymerases extend these forward- and reverse-primers along the denatured single stranded DNA generating a complementary DNA strand.

Standard PCR

Phusion DNA polymerase was used for standard PCR. The man-made chimera is composed of a unique dsDNA-binding domain fused to a *Pyrococcus*-like proofreading polymerase. The 3'→5' proof-reading capacity will excise mismatched 3'-terminal nucleotides from primer-template complexes and incorporate the correct. PCR reactions were set up according to the following standard protocol:

Component	Amount/Volume
Template-DNA	10 ng
Primer fwd (10 μM)	5 μl
Primer rev (10 μM)	5 μl
dNTPs (25 μM per NTP)	0.8 μl
5x Buffer HF or GC	20 μl
DMSO	3 μl
Phusion polymerase (2U/μl)	1 μl
ddH ₂ O	Ad 100 μl

The following PCR program was applied:

Step	Temperature/Time	Cycles
Initial denaturation	98°C; 30 s	1
Denaturation	98°C; 30 s	30
Annealing	45-60°C; 30 s	
Elongation	72°C; 15 s/kb	
Extension	72°C; 10 min	1
Storage	4°C; ∞	1

Correct size of PCR product was validated by agarose gel electrophoresis. For purification of PCR products the QIAquick PCR Purification Kit was used following the protocol of the manufacturer.

Mutagenesis PCR

Pfu DNA polymerase from the marine archaeobacterium *Pyrococcus furiosus* was used for mutagenesis PCR. Pfu DNA polymerase possesses also a 3'→5' proof-reading capacity. PCR reactions were set up according to the following standard protocol:

Component	Amount/Volume
Template-DNA	10 ng
Primer fwd (10 μM)	2.5 μl
Primer rev (10 μM)	2.5 μl
dNTPs (25 μM per NTP)	1 μl
Pfu buffer with MgCl ₂ (10x)	10 μl
Pfu polymerase (2.5 U/μl)	1 μl
ddH ₂ O	Ad 100 μl

The following PCR program was applied:

Step	Temperature/Time	Cycles
Initial denaturation	95°C; 30 s	1
Denaturation	95°C; 10 s	25
Annealing	45-60°C; 30 s	
Elongation	68°C; 4 min/kb	
Extension	68°C; 30 min	1
Storage	4°C; ∞	1

Correct size of PCR product was validated by agarose gel electrophoresis. Subsequently, DNA was digested with DpnI restriction enzyme for at least 3 hours at 37 °C to remove all methylated template DNA (methylation generated during bacterial plasmid DNA amplification). 10 µl newly synthesized mutated plasmid DNA was directly transformed into bacteria for amplification.

Enzymatic manipulation of DNA

Digestion of DNA with restriction endonucleases

For the sequence-specific cleavage of DNA molecules samples were incubated with restriction endonucleases in appropriate reaction conditions. The amount of enzyme and DNA, buffer, temperature and duration of the reaction were adjusted according to the manufacturer's instructions. The digested DNA fragments were subjected to agarose gel electrophoresis for analysis or purification.

Dephosphorylation of linearized vector DNA

Restriction of vector DNA with a single enzyme may lead to subsequent re-ligation. Therefore, 5'-termini of vector DNA were dephosphorylated using calf intestinal phosphatase. The dephosphorylation was incubated for one hour at 37 °C. The linearized, dephosphorylated vectors were subjected to agarose gel electrophoresis for purification.

Ligation of DNA fragments

For the ligation of linearized vectors with DNA-fragments the T4 DNA ligase was used. This enzyme catalyzes the formation of phosphodiester bonds between adjacent 3'-OH and 5'-phosphate ends in dsDNA. The ligation reaction was incubated overnight at 16 °C.

Component	Volume
Digested insert (PCR product)	10 µl
Linearized vector	0.5 µl
T4 DNA ligase	0.5 µl
10 x T4 DNA ligase buffer	2 µl
ddH ₂ O	ad 20 µl

Agarose gel electrophoresis

Double stranded DNA fragments can be separated according to their size on agarose gels. Agarose was added to 1 x TAE-buffer to obtain a final concentration between 0.7 % (w/v) - 2.0 % (w/v). The agarose suspension was boiled in a microwave until it was completely solubilized. Prior to loading DNA samples were mixed with 20 % Orange G loading buffer. Additionally, a DNA molecular weight standard (PCR or 1 kb ladder) was loaded. For visualization of DNA by UV-light the running buffer contained 0.075 % ethidium bromide in 1 x TAE buffer. The gel was run for 0.5-1 h with 120 V. DNA fragments were visualized under UV illumination (312 nm) in a Gel Documentation system (BioRad).

Extraction of DNA from agarose gels

PCR products and linearized vectors for ligation were isolated from agarose gels and purified using the QIAquick Gel extraction kit (Qiagen). Full length vectors were purified using the QIAEX® II Gel extraction kit (Qiagen). The DNA fragment was excised from the agarose gel with a clean, sharp scalpel. The DNA was extracted from the gel slice according to the manufacture's protocol. DNA was eluted by adding 30 to 50 µl sterile H₂O to the center of the membrane followed by centrifugation for 1 min. DNA was stored at -20 °C before further use.

Transformation of competent bacteria

To transform XL-1 Blue competent bacteria with plasmid DNA using the heat shock method, 1 µg of DNA was added to 50 µl of bacteria preparation (thawed on ice), mixed and incubated on ice for 20 min. After a heat shock (42 °C, 2 min), the bacteria were cooled on ice for 5 min.

Then 200 µl of LB++ were added and the bacterial suspension was incubated for 30 min at 37°C with shaking at 800 rpm. Thereafter, 100 µl of the transformation mixture was plated on LB agar plates containing suitable antibiotics. Plates were incubated upside down at 37°C overnight to allow growth of transformants and isolate single colonies.

Cultivation and storage of bacteria

Single colonies were picked from the plates and cultured in small scale (mini 1 ml) or large scale (50 ml) at 37°C on a rotary shaker. Therefore, LB-medium, supplemented with either ampicillin (100 µg/ml) or kanamycin (30 µg/ml), was inoculated with cells of a single colony of transformed bacteria. For the long term strain storage 1-2 ml of a freshly saturated bacterial culture were centrifuged at 3000 g for 5 min. The supernatant was removed and the bacteria were resuspended in ¼ volume of

LB/ampicillin. To generate a glycerol stock $\frac{1}{4}$ volume of 87 % glycerol was added and the cell suspension was mixed. The mixture was stored at -80°C .

Plasmid preparation on analytical scale (Miniprep)

Bacteria were harvested by centrifugation (30 sec, 14,000 rpm). The bacteria pellet was resuspended in 200 μl Flexi I (5 min, shaking). After lysis by addition of an equal amount of Flexi II and incubation for 5 min, the preparation was neutralized with 200 μl Flexi III, and chilled on ice for 5 min. The precipitate was removed by centrifugation for 10 min at 14000 rpm and the supernatant was transferred to a new reaction tube, which contained 400 μl of isopropanol. The precipitated DNA was pelleted by centrifugation (14,000 rpm, 4°C , 10 min), dried at room temperature and solubilized in 50 μl of H_2O . To validate ligation of the correct insert, a control digest of 1 μg DNA was carried out using the appropriate restriction enzymes and subjected to agarose gel electrophoresis.

Plasmid preparation on preparative scale (Midiprep)

Large scale plasmid preparations were carried out using the Nucleobond PC 100 kit or the Nucleobond Xtra Midi kit (Macherey-Nagel) as described by the manufacturer's protocol. DNA concentrations were determined using the Nanodrop 1000 and DNAs were stored at -20°C . Plasmid DNA sequencing was carried out by GATC biotech. Requested concentrations are 30-100 $\text{ng}/\mu\text{l}$ plasmid DNA and 10 $\text{pmol}/\mu\text{l}$ sequencing primer, both in 20 μl volume. Software of DNAMAN 6.0 and Chromas 1.45 was applied to analyze acquired sequences.

RNA isolation and reverse transcription (RT) PCR

RNA from mammalian cells was isolated using the RNeasy Mini Kit (QIAGEN) according to the manufacturer's instructions. RNA concentration was determined on a Nanodrop 1000 (Peglab), and RNAs were stored at -86 °C. Purified RNA was treated with DNaseI (Fermentas) for 45 min at 37 °C according to the supplier's protocol, to remove contamination with genomic DNA. Reverse transcription reactions were set up using Transcriptor Reverse Transcriptase (Roche) and Oligo-dT primers (Invitrogen). For RT PCR the following mix was prepared:

Component	Amount/Volume
RNA	1 µg
Oligo-dT (100 ng/µl)	0.5 µl
ddH ₂ O	ad 7.1 µl

The mix was heated to 65°C for 10 min and subsequently chilled on ice for 5 min before adding:

Component	Amount/Volume
RT-Buffer	2 µl
SUPERase-In	0.25 µl
dNTP mix (25 µM per NTP)	0.4 µl

The final RT reaction was heated for 30 min to 55°C, followed by 85°C for 5 min. The cDNA was stored at -20°C. For DNA-visualization, agarose gel electrophoresis was carried out. For quantitative analyses of a certain gene, qRT-PCR was undertaken.

Quantitative real-time RT-PCR

For quantitative analyses of cellular mRNA levels after transfection or infection, the total RNA was isolated 24 h p.t./p.i. and reverse transcribed to single strand cDNA. Samples were diluted 1:5 and as reference a standard curve was generated by a 10-fold dilution series of one cDNA sample (5 dilutions 1:1, 1:10, 1:100, 1:1,000, 1:10,000). The dilutions were set to relative values for quantification of the samples. A master mix was prepared containing specific primers and SYBR Green, a cyanine dye which preferentially binds to newly transcribed dsDNA. To normalize the results, the same samples were subjected to qRT-PCR with primers for a (steady) housekeeping gene. The standards, the cDNA 1:5, and a no template sample (negative control) were distributed to LightCycler capillaries and placed into a rotor.

For qRT-PCR a 20 μ l PCR-mix was prepared:

Component	Amount/Volume
cDNA	1 μ l
Primer 1	1 μ l
Primer 2	1 μ l
SYBR Green Master Mix	10 μ l
ddH ₂ O	ad 20 μ l

The qRT-PCR-program was comprised of the following steps:

Temperature	Time	Cycles
95°C	15 s	1
94°C	15 s	55
Annealing T	20 s	
72°C	10 s	

The melting curve was generated using following conditions:

Temperature	Time
95°C	10 s
40°C	20 s
to 95°C	0.1 °C/s
40°C	30 s

The LightCycler software 4.0 was used to obtain a relative quantification, and values of single samples were calculated from the standard curve. Finally, target gene mRNA values were normalized against GAPDH. All qRT-PCR assays were carried out in duplicates (standard deviations depicted as error bars). For Western blot analysis, additional wells were transfected with the same mixture used for transfection of cells later subjected to real-time PCR analysis. These cells were lysed directly in SDS sample buffer.

2.2.2 Cell biological methods

Cell culture

Cells were grown in cell culture flasks (T25, T75, T175) with Dulbecco's Modified Eagle Medium (DMEM) supplemented with 10 % (v/v) Fetal Calf Serum (FCS), 2 mM L-Glutamine, 40 U/ml penicillin and 40 µg/ml streptomycin. All media and supplementary products were purchased from Gibco. In the case of 293-3-46 cells and Vero-hSLAM cells 2 mg/ml G418 (Calbiochem) was added to the medium on alternate passages. All used cell lines were cultured at 37 °C in an atmosphere with a relative humidity of 90 % and a CO₂ content of 5 %. Twice a week, cells were suspended by trypsinization and split in ratio 1/6 to 1/10 into fresh cell culture flasks.

Thawing and freezing of eukaryotic cells

Cells were harvested and resuspended in freezing medium containing 92 % (v/v) DMEM 3+ and 8 % (v/v) DMSO. 1 ml cell suspension was transferred into a cryo-tube and immediately stored at -80 °C (liquid nitrogen (-160 °C) for long term storage). Cells were thawed rapidly at 37 °C and immediately transferred into 10 ml culture medium to dilute the DMSO. Afterwards cells were centrifuged, resuspended with fresh culture medium and transferred to a tissue culture dish.

Transfection

One day prior transfection cells were seeded such that they would be at 50 - 60 % confluence at the time of transfection. Cells were transfected with appropriate transfection reagents. For transfection of less than two plasmids, polyethyleneimine (PEI) solution (1 mg/ml) was used. PEI was pre-incubated in DMEM w/o additives for 5 min, subsequently mixed with the DNA (2.5 µl PEI/µg DNA) for 20 min and added to the cells. For transfection of more than two plasmids, *Lipofectamine™2000* (2.5 µl Lipofectamine/µg DNA) was used. It was pre-incubated with DMEM w/o additives for 5 min. Plasmids DNA was diluted in DMEM w/o additives and combined with diluted Lipofectamine/DMEM mix. Following incubation of 20 min, the solution was added to the cells. For virus rescue, 293-3-46 cells were transfected with calcium phosphate using the *ProFection®* Mammalian Transfection System according to the manufacture's protocol.

2.2.3 Biochemical and protein biochemical methods

SDS polyacrylamide gel electrophoresis (SDS-PAGE)

For analysis of endogenous protein expression or protein overexpression after transfection or infection, cells were lysed with an appropriate amount of SDS-containing protein lysis buffer. Subsequently, lysates were boiled (5 min, 95 °C) to denature the proteins. SDS surrounds the protein with a negative charge and the β -mercaptoethanol prevents the reformation of disulfide bonds. The analytical separation of proteins was accomplished by discontinuous SDS-PAGE. Migration of the SDS-protein complexes through polyacrylamide gels in an electric field largely depends on their molecular mass. For electrophoresis 10 % polyacrylamide separating gels and 4 % polyacrylamide stacking gels were prepared. Proteins were electrophoretically separated at a constant voltage of 40 V overnight. To estimate apparent molecular weights of analyzed proteins an appropriate molecular weight marker was loaded next to the denatured proteins onto the gels. Jagow anode and cathode buffer were used as running buffers (see appendix for gels and buffers). Subsequent to SDS-PAGE, the polyacrylamide gel was subjected to Western Blotting.

Western blot analysis and immunodetection

For immunoblot analysis, proteins separated by SDS-PAGE were electrophoretically transferred onto a PVDF membrane using a semi-dry blotting device (PeqLab). Therefore the stacking gel was removed and the separating gel was rinsed by submerging it briefly in semi dry buffer for 10 min. PVDF membranes were activated in 100% methanol, and rinsed in semi dry buffer. The gel was then placed face-to-face with the membrane, sandwiched by Whatman paper (all soaked in semi-dry buffer) and electroblotted for 2 h at 400 mA/gel. After electroblotting the transferred proteins are bound to the membrane providing access for the detection by specific antibodies. To avoid unspecific binding the membrane was incubated in blocking solution (5 %

(w/v) non-fat dried milk in PBS at room temperature for 1 h or at 4 °C overnight on a shaker. The membrane was briefly washed three times with PBS-T. For specific detection of proteins the membrane was incubated with primary antibody solution for at least 1 h on a shaker. Alternatively, the membrane was incubated at 4°C overnight. After washing three times with PBS-T the membrane was incubated with an HRP-conjugated α -immunoglobulin secondary antibody for 2 h on a shaker. Finally, the membrane was washed three times with PBS-T for 10 min. For developing the Western-Blot, the detection kit ECL reagent (PerkinElmer Life Sciences) was used according to the manufacturer's protocol. Membranes were directly subjected to Vilber Lourmat Fusion FX7 to visualize protein bands due to Chemiluminescence.

Immunoprecipitation (IP)

In order to identify protein interaction partners, Co-IP was applied. HEK-293T cells were seeded in a 6 cm dish and transfected with cDNAs coding for potential interaction partners. One day after transfection the cells were detached from the dish by 1 ml PBS + 5 mM EDTA. The cell suspension was centrifuged (5 min, 4 °C, 2,500 rpm) and the pellet was lysed (1 h, 4 °C) with 500 μ l Co-IP buffer containing a protease inhibitor. Afterwards the lysates were cleared (10 min, 4 °C, 14,000 rpm) and transferred to a new tube. 50 μ l of the supernatant was mixed with 50 μ l protein lysis buffer as a control (input) for controlling the amount of total protein expression (10 %). For precipitation of proteins the remaining supernatant (90 %) was incubated with a specific matrix (Flag, HA, or Sepharose A).

Incubation with Flag-matrix and precipitation

The remaining 450 μ l of the cleared lysates were incubated with 100 μ l anti-Flag® M2-Agarose at 4°C on a rotator overnight. This matrix is composed of agarose beads that are covalently linked to anti-Flag-antibody, thus capturing Flag-tagged proteins. In case the Flag-tagged protein interacts with another protein in the cell lysate, the whole complex stays captured to the matrix. The matrix was washed three times with 500 μ l Co-IP buffer (10 min, 4 °C and subsequent centrifugation 2 min, 4 °C, 14,000 rpm) to remove unspecifically adsorbed proteins and subsequently heated in 100 μ l protein

lysis buffer at 95°C for 5 min. Purified proteins were detected by SDS-PAGE and Western blotting.

Incubation with Sepharose A-matrix and precipitation

Besides using the Flag-matrix it is possible to precipitate proteins with Protein A-Sepharose. Protein A, which is covalently conjugated to sepharose, specifically binds to the Ig-part of antibodies. It was used for the immunoprecipitation of Ig-tagged proteins. For preparation of Sepharose A, it was washed twice with buffer A (1.5 g Sepharose A/50 ml buffer) (30 min, 4 °C and centrifugation 2 min, 4 °C, 2,000 rpm) on a roller mixer. After a further centrifugation step, buffer A was removed and the beads incubated with 50 ml of buffer B (30 min, 4 °C). Afterwards, beads were centrifuged (2 min, 4 °C, 3,500 rpm), reconstituted in 7.5 ml buffer B and aliquots of 1 ml stored at 4 °C. Prior usage, the beads were washed three times with 500 µl Co-IP buffer. For precipitation of proteins, the cleared cell lysates (90 %) were incubated with 100 µl SepharoseA-matrix (o/n, 4 °C) and washed three times with 500 µl Co-IP buffer (10 min, 4 °C and subsequent centrifugation 2 min, 4 °C, 14,000 rpm). 100 µl protein lysis buffer was added to the matrix. Purified proteins were detected by SDS-PAGE and Western blotting.

Incubation with HA matrix and precipitation

The cleared cell lysates containing proteins with an HA-tag were purified using 50 µl of an anti-HA affinity matrix, which consists of a rat monoclonal antibody against the HA-tag coupled to agarose beads. After overnight incubation the beads were washed as described before and subsequently 100µl protein lysis buffer were added to remove the proteins from the beads. Afterwards, the lysis buffer was subjected to SDS-PAGE and Western Blotting.

Immunofluorescence microscopy

HEp2 cells were seeded on coverslips in 24-wells. After 24 h cells were transfected with 500 ng of plasmids using Lipofectamine 2000 transfection reagent, incubated for additional 24 h and then treated with 10 ng/ml TNF α . Cells were fixed after 30 min in 3% paraformaldehyde for 20 min at room temperature and were permeabilized in

0.5% Triton X-100 in phosphate-buffered saline (PBS). After blocking with 2,5% milk in 0,1% Triton X-100/PBS, fixed cells were incubated with primary antibodies, α -p65 (rabbit; sc-109; Santa Cruz) diluted 1:50 and α -flag (mouse; Sigma) diluted 1:200 in 0,1% Triton X-100/PBS for 1 h at 4°C, followed by incubation with fluorescence-labeled secondary antibodies (goat α -rabbit Alexa Fluor 488 and α -mouse tetramethylrhodamine, both from Molecular Probes) at a dilution of 1:200 in 0,1% Triton X-100/PBS for 1 h at 4°C. Nuclear chromatin was stained by adding TO-PRO-3-iodide (Molecular Probes, 1:1000) to the secondary antibodies. Confocal laser scanning microscopy was performed with a Zeiss LSM510 Meta laser system using a Zeiss Axiovert 200 microscope. Excitation of Alexa Fluor 488, tetramethylrhodamine, and TO-PRO-3-iodide occurred at wavelengths of 488 nm, 543 nm, and 633 nm, respectively.

Luciferase assay

To examine NF- κ B activity, the dual luciferase reporter system was applied. Therefore HEK-293T cells were seeded into 24-well plates one day prior to transfection. A plasmid for NF- κ B-dependent firefly luciferase p55A2-luc (100 ng), a vector for CMV promoter controlled *Renilla* luciferase pRL-CMV (10 ng) and the indicated amounts of expression vectors were transfected using Lipofectamine 2000 transfection reagent (Invitrogen). The total amount of DNA was kept constant by supplementation with pCR3. In case of stimulation cells were treated with 10ng/ml TNF α . Cells were harvested in 200 μ l passive lysis buffer (Promega) at the indicated time points and luciferase activities were determined from 20 μ l of the lysates using Dual Luciferase® Reporter Assay System (Promega) and the Berthold Lumat LB 9501 luminometer according to the manufacturer's instruction. Firefly luciferase activities were normalized to *Renilla* luciferase activities, and mean values of mock-treated cells were set to 1. The mean and the standard deviation were calculated out of two measurements. For Western blotting, reporter assay lysates were mixed 1:1 with protein lysis buffer.

2.2.4 Virological methods

Generation of recombinant MV from cDNA (virus rescue)

In order to reconstitute infectious virus from cloned cDNA, 293-3-46 cells were detached with Versene/Trypsin-EDTA (5:1) and seeded in 6-well plates. 10 µg of the plasmid coding for the full length MV antigenome together with the helper plasmid pEMC-MV L (20 ng) were transfected using the CaPO₄ *ProFection*[®] Mammalian Transfection System from Promega according to the manufacturer's instructions. After incubation for 6 h under standard conditions the transfected cells were washed twice with DMEM 3+ and grown in 2 ml DMEM 3+ at 37 °C over night. On the next morning the cells were heat shocked for 3 h at 42 °C. Afterwards the cells were incubated under standard conditions for 24 h. In the meantime Vero-hSLAM cells were seeded in 100 mm dishes. On the next day transfected 293-3-46 cells were taken up together with the medium, dropped onto the Vero-hSLAM cells and incubated at 37 °C until syncytia are formed. Each syncytium is picked under sterile conditions, transferred to Vero-hSLAM cells seeded on a 6-well plate and incubated at 32 °C. As soon as the all cells are infected the 6-well plate is frozen at -20 °C. After thawing, the cell debris was removed by low speed centrifugation (1800 rpm, 4 °C, 10 min) and the supernatants were aliquoted and frozen to -80 °C. Afterwards supernatants of positive rescues were titrated and used for stock production.

Virus titration

For virus titration, Vero cells were seeded into 96-well plates. Virus stock was thawed and a 10-fold dilution series was prepared (7 x 450 µl DMEM + 50 µl virus/virus dilution). 2 hours after seeding of the cells they were infected with 100 µl of the virus dilution (in duplicates). 48 hours p.i., cells were fixed with acetone 80 % and stained with an antibody coupled to FITC against the MV N protein. Foci were counted from each well using a fluorescence microscope, and foci forming units per ml (ffu/ml) were calculated from these results.

Generation of virus stocks

For virus stock production, 5×10^6 Vero cells were infected in suspension with an MOI 0.01. Cells were resuspended every 10 min. 1 h p.i., infected cells were seeded in T75 flask, grown at 32 °C and 72 h post infection (p.i.) flasks were frozen at -20 °C. After thawing, cell debris was removed by low speed centrifugation (1,800 rpm, 4 °C, 5 min) and aliquots of the cleared supernatant were stored at -80 °C. To determine the infectious titers of the virus stocks, supernatants were titrated.

Virus growth curve

To analyze growth kinetics of distinct viruses, growth curves were prepared. Therefore, Vero or A549 cells were infected in suspension at an MOI 0.01. Every 10 min the infected cells were resuspended. 1 h p.i., infected cells were washed once with DMEM 3+ and seeded into 6-well plates (1 well/virus/timepoint). 6 h p.i. the first 6-well plate was frozen. At 24 h, 48 h, 72 h, and 96 h p.i., further 6-well plates were frozen. Afterward, 6-well plates are thawed again, centrifuged at 1800 rpm for 10 min at 4 °C to remove cell debris and supernatants were titrated to determine the infectious titers at the given time points.

3 Results

3.1 Measles virus P gene products suppress NF- κ B activation upon TNFR stimulation

Proteins expressed from the P gene of MV (P, V, and C) were shown to counteract multiple host innate immune pathways, including IRF3/7 and JAK/STAT signal transduction, whereas interference of the proteins with NF- κ B signaling is only poorly investigated. Therefore, I wanted to determine whether they also influence NF- κ B activity.

The canonical NF- κ B signaling pathway can be activated by various stimuli including tumor necrosis factor α (TNF α), a cytokine regulating immune functions as well as inflammatory responses (Ghosh and Karin, 2002).

In a first step, the effect of MV P gene derived proteins on NF- κ B activation in response to TNF α stimulation was investigated. To analyze NF- κ B activity I used an NF- κ B-dependent dual luciferase assay based on two independent vectors. The plasmid for NF- κ B-dependent expression (p55A2-luc) contains a *firefly* luciferase reporter gene under control of a trimeric repeat of the NF- κ B-binding motif (PRDII) in the context of the IFN β -promoter (Yoneyama et al., 1996). The plasmid pRL-CMV is composed of a *renilla* gene driven by a CMV promoter and used for normalization of transfection efficiency.

The reporter plasmids were cotransfected in HEK-293T cells together with increasing amounts of expression vectors for MV P, V or C of the Schwarz strain. The start codon of the C protein was changed by site directed silent mutagenesis to prevent expression of MV C, in case of all P or V expressing plasmids, as described previously (Pfaller and Conzelmann, 2008). The P protein of rabies virus (RV-P), which suppresses activation of IRF-3 and STAT1/STAT2 nuclear import but has no influence on NF- κ B signaling, was used as a negative control (Brzózka et al., 2005; Brzózka et al., 2006). Cells were

stimulated with 10 ng/ml TNF α 18 h post transfection and 6 h prior to cell lysis and NF- κ B dependent luciferase activity was determined.

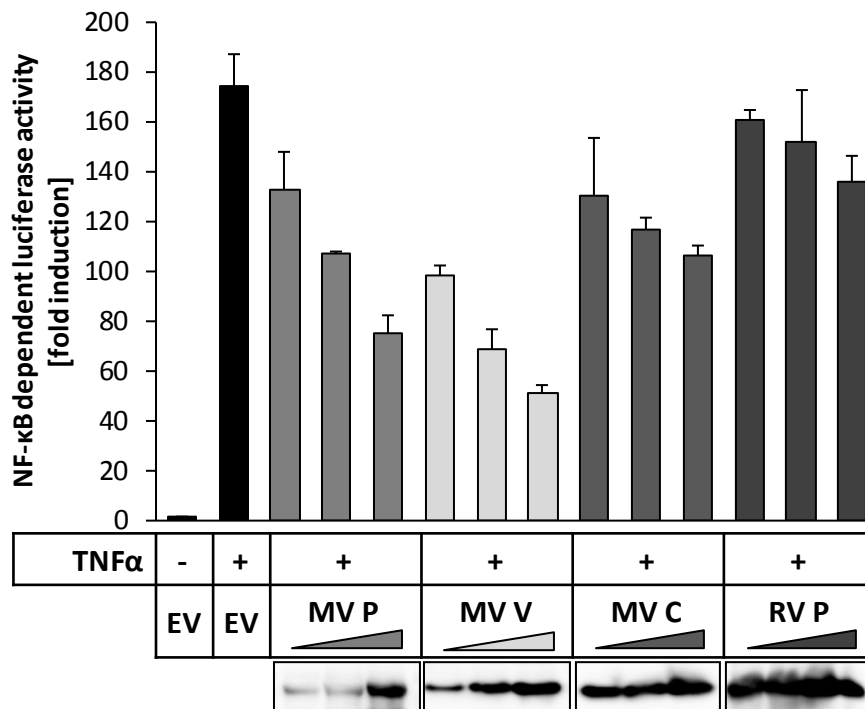


Figure 3-1 Measles virus P gene products suppress NF- κ B activation upon TNFR stimulation

Increasing amounts (200 ng, 400 ng, 600 ng) of expression plasmids encoding for MV P, V, C, RV P or empty vector (EV) were transfected into HEK-293T cells with the NF- κ B dependent reporter plasmid p55A2-luc and pRL-CMV for normalization. After 18 h cells were stimulated with 10 ng/ml recombinant human TNF α . NF- κ B driven luciferase activity was determined 6 h post stimulation by a dual luciferase assay. The bars represent the means and the error bars the standard deviation of two independent experiments. Depicted is a representative experiment out of four repeats. Western Blot of cell lysates were probed with α -MV P/V, α -MV C or α -RV P antibodies by Western Blotting to determine the expression levels. Adapted from (Schuhmann et al., 2011).

All three P gene products MV P, V and C had a considerable and dose-dependent inhibitory effect on TNF α -mediated NF- κ B activation (Fig. 3-1). The V protein showed the strongest suppression, while the inhibitory capacity of MV P and C was less prominent. In contrast, RV P exhibited no NF- κ B suppressive potential.

These results indicate that MV P, V and C interfere with TNF α mediated NF- κ B activation, but to a different extent.

3.2 NF- κ B signaling via PRRs can be suppressed by MV P gene products

Triggering of PRRs, like RLRs or TLRs also lead to activation of NF- κ B. To test the ability of MV P gene products to interfere with RIG-I mediated NF- κ B activation the C-terminal deletion mutant Δ RIG-I (aa 1-284) that was shown to constitutively activate NF- κ B (Yoneyama et al., 2004) was used. Dual luciferase reporter gene assays were performed in HEK-293T cells expressing Δ RIG-I as well as increasing amounts of MV P, V, C or RV P as control. Expression of the Δ RIG-I mutant alone led to more than 40 fold induction of NF- κ B activity (Fig. 3-2A).

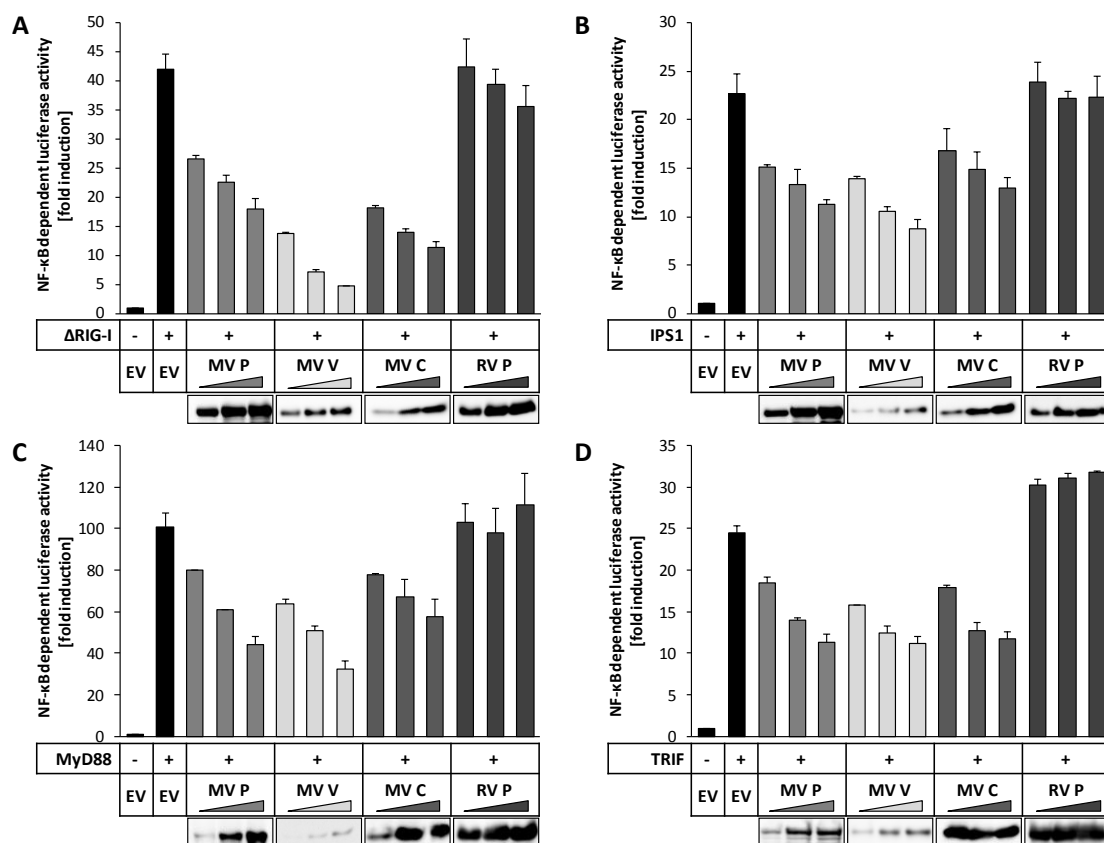


Figure 3-2 NF- κ B signaling via PRRs can be suppressed by MV P gene products

Increasing amounts (200 ng, 400 ng, 600 ng) of vectors encoding for the indicated MV proteins were transfected into HEK-293T cells with either 200 ng of expression plasmids for Δ RIG-I (A), IPS-1(B), MyD88 (C), or TRIF (D) and the NF- κ B dependent reporter system (100 ng p55A2/ 10 ng pRL-CMV). After 24 h cells were lysed and NF- κ B activity was determined by a dual luciferase assay. The depicted values are means of two independent experiments and their standard deviation is displayed by error bars. Depicted are representative experiments out of three repeats. Lower panel: Expression of the viral proteins was assessed by Western blotting. Adapted from (Schuhmann et al., 2011).

In the presence of MV V at the highest dose, activity was suppressed to nearly basal level. MV P had a less pronounced inhibitory effect even though it was expressed at much higher levels, as indicated by Western blotting using an antibody recognizing both MV P and V (Fig 3.2A, bottom panel). The MV C protein had intermediate suppressive capacity, while RV P had no significant influence on NF- κ B activation.

Signaling of the PRRs RIG-I and MDA5 is transmitted via the adaptor molecule IPS-1, while signal transduction of TLRs involves the adaptors MyD88 (TLR1, -2, -4, -5, -6, -7, -8, -9) or TRIF (TLR3) (Kawai and Akira, 2009). To address the question whether MV P, V, and C are able to generally counteract NF- κ B activation by RLRs and TLRs dual luciferase reporter gene assays were performed using overexpression of IPS-1 (Fig. 3-2B), MyD88 (Fig. 3-2C), or TRIF (Fig. 3-2D) for stimulation of NF- κ B activity. Analogous with the previous experiments all MV P gene derived proteins were able to suppress the adaptor induced NF- κ B activation, whereas expression of RV P had no effect (Fig. 3-2A). The level of reduction of NF- κ B activity achieved by MV P and V appeared to be similar in these experiments; however, Western blotting revealed lower expression levels of MV V confirming the previous finding that the V protein is the most potent inhibitor of canonical NF- κ B activity among the MV P gene products.

3.3 MV V inhibits NF- κ B signaling downstream of the IKK complex

The previous experiments revealed that the MV P gene products suppress multiple pathways that lead to activation of the canonical NF- κ B signaling cascade, including TNFR-, RLR- and TLR-signaling. All these canonical NF- κ B signaling pathways converge on the IKK complex that is composed of the kinases IKK α , IKK β and IKK γ (NEMO). In order to test whether the inhibition by MV P, V or C occurs at or downstream of these kinases, NF- κ B-dependent luciferase expression was activated by overexpressing IKK α , IKK β and IKK γ in HEK-293T cells. As positive control, the Ig-tagged NEMO-binding domain (NBD) was used (Ig-NBD). The NBD peptide binds to IKK γ and inhibits the

formation of the IKK complex which is essential for canonical NF- κ B activation (May et al., 2000). Expression of Ig-NBD resulted in a dose dependent inhibition of IKK complex-induced activity, while the Ig-tag alone as well as RV P did not interfere with the NF- κ B activation (Fig. 3-3A). The presence of MV V led to a dose dependent and effective reduction of the IKK complex-induced NF- κ B activation comparable to the inhibition achieved by expression of Ig-NBD. Expression of MV P and MV C had less pronounced effects on NF- κ B activation by the IKK complex.

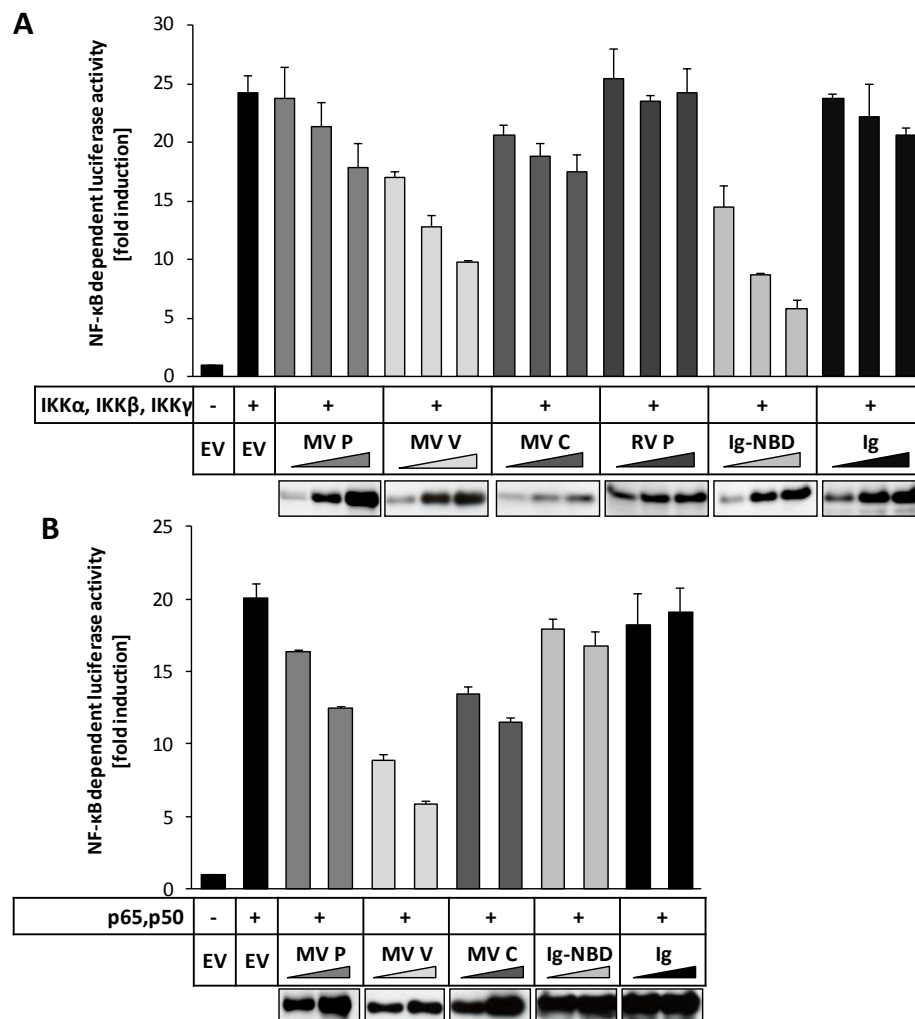


Figure 3-3 MV V inhibits NF- κ B signaling downstream of the IKK complex

(A) HEK-293T cells were transfected with expression plasmids encoding for IKK α , IKK β and IKK γ (100 ng each) together with increasing amounts (200 ng, 400 ng, 600 ng) of vectors coding for the indicated proteins or empty vector and the NF- κ B dependent reporter system (100 ng p55A2/ 10 ng pRL-CMV). After 12 h the cells were lysed and the luciferase activity was measured by dual luciferase assay. The bars represent the means and the error bars the standard deviation of two independent experiments. A representative experiment out of three repeats is shown. (B) Plasmids encoding for p65 and p50 (150 ng each) and increasing amounts (300 ng, 600 ng) of vectors encoding the indicated proteins were transfected into HEK-293T cells with the dual luciferase reporter system. Cells were lysed 12 h after transfection followed by determination of normalized NF- κ B dependent luciferase activity. The depicted values are means of two independent experiments and their standard deviation is displayed by error bars. Shown is a representative experiment out of three repeats. Adapted from (Schuhmann et al., 2011).

To further spot the step where MV V inhibits canonical NF- κ B activation, we induced NF- κ B dependent luciferase activity by coexpression of the NF- κ B subunits p65 and p50 which assemble to the main heterodimer of NF- κ B. Expression of MV V reduced the NF- κ B activity induced by p65/p50 significantly and dose-dependently, whereas MV P and C showed only minor inhibitory potential (Fig. 3-3B). As expected, presence of Ig-NBD had no effect on p65/p50 mediated NF- κ B activity, as this inhibitor acts upstream of the transcription factors. These experiments indicate that the V protein of MV inhibits canonical NF- κ B signaling downstream of the IKK complex.

3.4 MV V specifically binds the NF- κ B subunit p65

The NF- κ B heterodimer p65/p50 is bound to its inhibitor I κ B α in unstimulated cells. In order to elucidate the molecular mechanism of MV P gene products to suppress canonical NF- κ B activation, we assessed the potential of the viral proteins to interact with NF- κ B complex members p65, p50 and I κ B α in co-immunoprecipitation (CoIP) experiments. Extracts from HEK-293T cells coexpressing Ig-tagged MV P, V, or C proteins and p65 from transfected plasmids were purified by protein A-conjugated sepharose beads. To exclude unspecific binding of p65 to the Ig-tag or the beads the plasmid expressing the Ig-tag alone was coexpressed with p65 as control. Precipitates were subjected to SDS-PAGE and analyzed by Western blotting using antibodies against p65 or human IgG. Immunoprecipitation of the Ig-tagged proteins was efficient (Fig. 3-4A; lower right panel). In fact, the NF- κ B subunit p65 was specifically co-precipitated with Ig-MV V, whereas no interaction of p65 with the Ig-tagged P or C constructs was detectable (Fig. 3-4A; upper right panel).

In further experiments, binding of p50 (NF- κ B1) to flag-tagged MV proteins was analyzed. Flag-p65 was included as positive control. Cell extracts were purified with α -flag M2 affinity gel, precipitates were subjected to SDS-PAGE and analyzed by immunoblotting using antibodies specific for p50 and the flag epitope. While flag-p65 efficiently co-precipitated p50, no interactions of the p50 NF- κ B subunit with any of the flag-MV proteins could be detected (Fig. 3-4B).

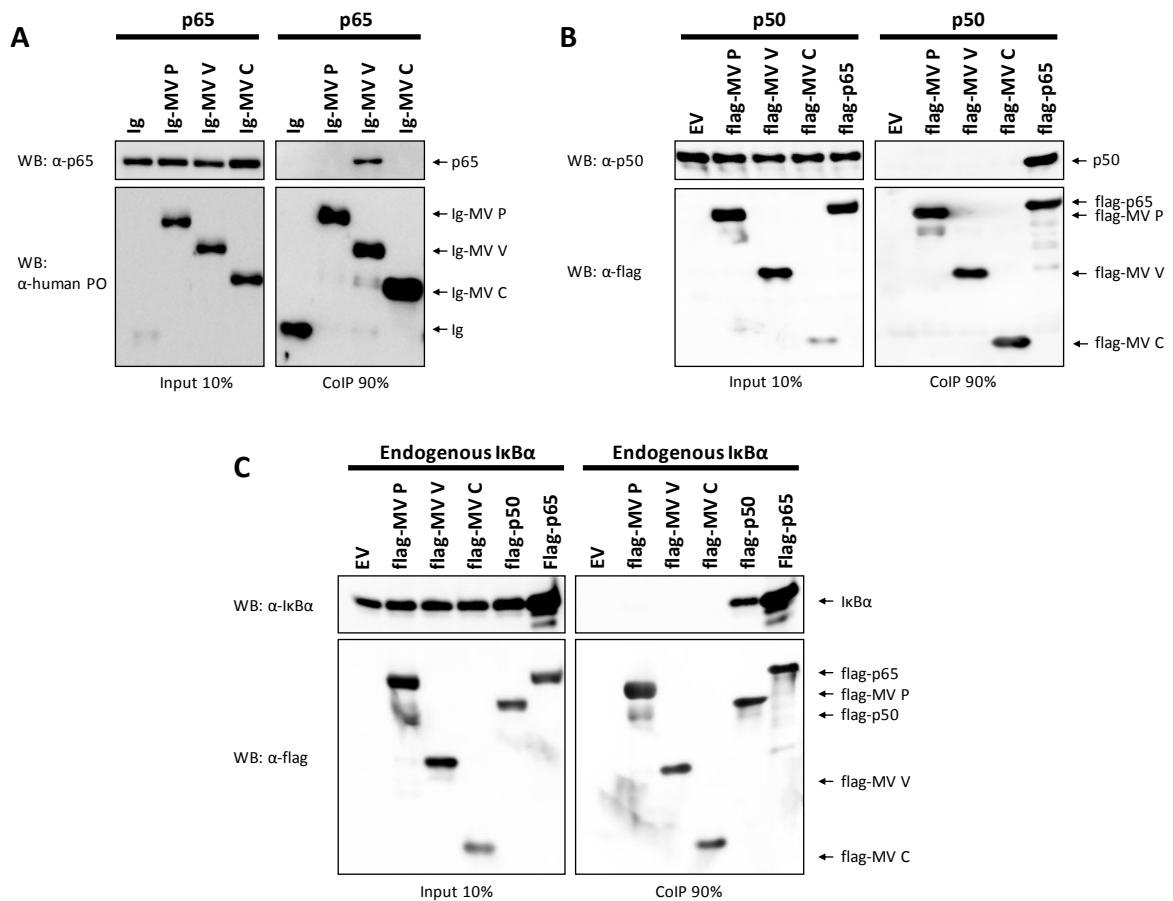


Figure 3-4 MV V specifically binds the NF- κ B subunit p65

(A) HEK-293T cells were used to express p65 in combination with the indicated Ig-tagged proteins or the Ig-tag (Ig) itself (3 μ g each). After 24 h cells were lysed under native conditions and Ig-tagged proteins were pulled down using protein A conjugated sepharose beads. Binding of p65 to measles proteins was visualized by Western blotting. Depicted is a representative experiment out of four repeats. (B) p50 was coexpressed in HEK-293T cells with the indicated flag proteins or empty vector (EV) (3 μ g each). Cells were lysed 24 h post transfection and flag-tagged measles proteins were immunoprecipitated using anti-flag M2 affinity gel. Interactions of p50 and flag-proteins were analyzed by Western blotting. A representative experiment out of three is shown. (C) HEK-293T cells were cotransfected with vectors encoding the indicated flag-tagged constructs or empty vector (EV). CoIP assay was performed as described above and the proteins were stained with the indicated antibodies. A representative experiment out of three is shown. Adapted from (Schuhmann et al., 2011).

To test whether any of the MV P gene products can bind to I κ B α , flag tagged MV P, V, and C were expressed in HEK-293T cells. Flag-p65 and flag-p50 were included as positive controls. Cell extracts were purified with α -flag M2 affinity gel and precipitates were analyzed by Western blotting using antibodies against the flag epitope or I κ B α . None of the MV P gene products were able to co-purify endogenous I κ B α , whereas flag-p65 as well as flag-p50 showed efficient pull down of I κ B α (Fig. 3-4C).

Taken together these results indicate that only MV V, but not MV P and C, binds to the NF- κ B subunit p65. I κ B α and p50, which are associated to p65 in non-stimulated cells, were found not to interact with any of the P gene products.

3.5 RHD of p65 is sufficient for interaction with MV V

All NF- κ B subunits comprise an N-terminal RHD, which is responsible for dimerization, DNA-binding, and nuclear import. To determine if MV V binds to the RHD of p65, a fragment of p65 spanning from aa 1-309 (p65 RHD) was constructed and Co-IP experiments with flag-MV P, V, C were performed in HEK-293T cells. α -flag M2 affinity gel was used to purify the extracts. Immunoblotting of the precipitates with an antibody specific for the N-terminus of p65 revealed that the p65 RHD was efficiently pulled down by flag-MV V (Fig. 3-5A).

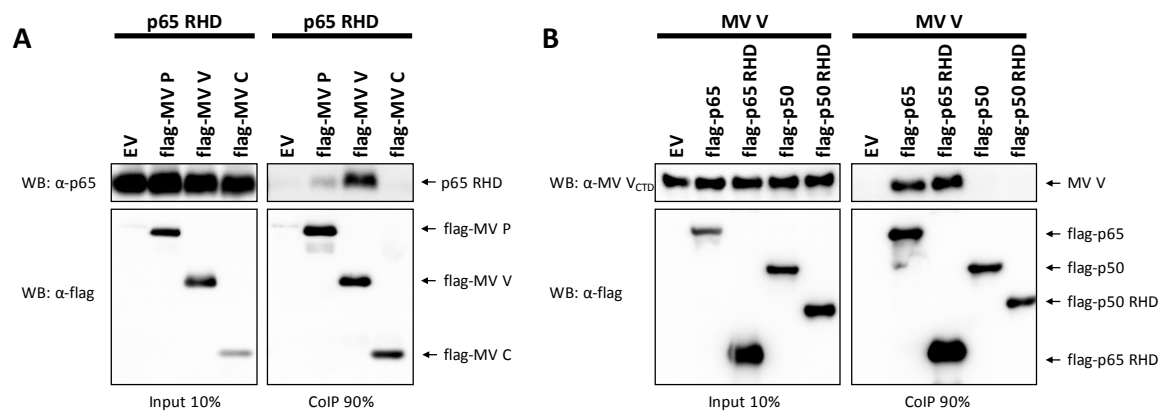


Figure 3-5 RHD of p65 is sufficient for interaction with MV V

(A) HEK-293T cells were cotransfected with vectors encoding for the indicated flag-tagged constructs or empty vector (EV) and the RHD of p65 (aa 1-309). CoIP assays were performed as described above and RHD-p65 was stained using α -p65 (Cell Signaling; 3035). A representative experiment out of three is shown. (B) MV V was coexpressed with the indicated flag tagged proteins or empty vector (EV) (3 μ g each) in HEK-293T cells. CoIP experiments were performed as described above and MV V was stained using α -MV V_{CTD}. Depicted is a representative experiment out of three repeats. Adapted from (Schuhmann et al., 2011).

Notably, RHD p65 also showed some affinity to MV P, though considerably weaker than to MV V. A weak affinity of the MV P protein to bind p65 was also observed occasionally in pull down experiments with flag tagged p65 and authentic, untagged MV proteins (data not shown). Taken together, we observed that MV V binds with a strong affinity to the RHD of p65, while a weak interaction of MV P with the RHD of p65 was suggested. To further verify the specificity of MV V to the RHD of p65 interaction of flag-tagged p65, RHD p65, p50 and RHD p50 to MV V were assessed within one experiment. Therefore, I constructed the RHD of p50 spanning from aa 1-

366 and the other constructs with a flag tag. CoIP experiments of the flag tagged proteins with authentic, untagged MV V confirmed specific binding of V to flag-p65 and flag-RHD p65, while no interaction of V and flag-p50 or flag-RHD p50 could be detected (Fig. 3-5B). These findings confirm the specificity of MV V to the RHD of p65.

3.6 Binding of MV V to p65 is mediated via both N- and C-terminal domains of the RHD of p65

The RHD of p65 can be further divided into the N-terminal domain (NTD) responsible for DNA binding and the C-terminal domain (CTD) that mediates dimerization, nuclear translocation and I κ B binding (Zheng et al., 2011). Figure 3-6A shows the PDB structure 1IKN of the mouse p65/p50/I κ B α complex (Huxford et al., 1998). The structure was displayed and colored using the PyMOL software (version 0.99rc6). The NTD of p65 is displayed in red and the CTD in blue. Associated with the CTD is p50 (light green) and I κ B α (yellow).

To define the interaction site of p65 with MV V more precisely, the flag-tagged NTD (aa1-180) and CTD (aa181-309) fragments of p65 were constructed (Fig. 3-6A). p65-RHD-flag (aa1-309) was used as positive control. CoIP experiments were performed expressing the flag-tagged p65 fragments and MV V in HEK-293T cells. MV V coprecipitated in small amounts with flag-p65-NTD and with a higher extent with a p65-CTD-flag (Fig. 3-6B). The amount of MV V copurified with the entire p65 RHD-flag was even higher. However, coexpression of flag-p65-NTD and p65-CTD-flag resulted in an increased level of co-purified MV V even though the amounts of transfected plasmids encoding for the two p65 fragments were adjusted to the transfected amount of single plasmids. These findings suggest that MV V binds to the NTD as well as to the CTD of p65-RHD and that this binding is stabilized when both domains are coexpressed.

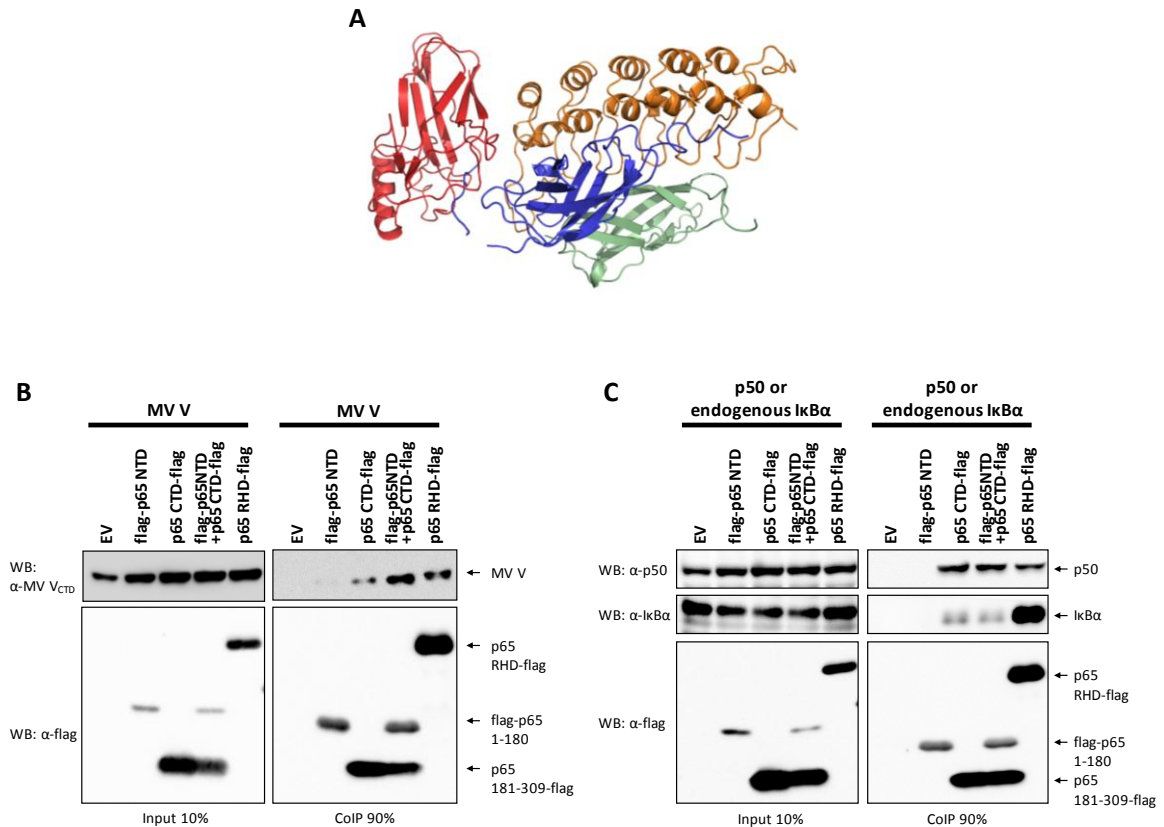


Figure 3-6 Binding of MV V to p65 is mediated via both the N- and the C-terminal domain of the RHD of p65

(A) Crystal structure of mouse p65 in complex with mouse p50 and human IκBα (1IKN.pdb) visualized and colored using PyMOL software. The NTD of the RHD of p65 (residues 19-180) is depicted in red, the CTD (residues 181-304) in blue. The yellow structure resembles the ankyrin repeats of IκBα (residues 67-302) and p50 (residues 245-363) is shown in light green. HEK-293T cells were used to coexpress MV V (B) or p50 (C) and flag-p65-NTD (aa1-180), p65-CTD-flag (aa 181-309) or p65 RHD-flag (aa1-309). CoIP assays were performed using anti-flag M2 affinity gel. The purified proteins were stained with the indicated antibodies. A representative experiment out of three is shown.

To ensure that the CTD of p65 is functional when expressed separately we had a look on its ability to bind to p50 and IκBα using CoIP experiments. Therefore the flag-tagged p65 fragments were coexpressed with p50 in HEK-293T cells. Immunoprecipitation of the flag-tagged constructs and subsequent immunoblotting revealed that p50 coprecipitated with comparable affinity with p65-CTD-flag alone and with coexpressed flag-p65-NTD/p65-CTD-flag, as well as with the complete p65-RHD-flag (Fig. 3-6C right, upper panel). However, binding efficiency of IκBα to p65-CTD-flag and coexpressed flag-p65-NTD/p65-CTD-flag was reduced compared to p65-RHD-flag (Fig. 3-6C right, middle panel). This indicates that p65-CTD-flag is functional in terms of p50 but not of IκBα binding. Nevertheless, the finding that MV V interacts with both domains of p65-RHD is yet valid, since coexpression of both domains enhances the binding affinity of MV V.

3.7 Binding of MV V to p65 does not compete with binding of p50 or IκBα to p65

As MV V was shown to bind to p65, but not to p50 or IκBα this raises the question if the interaction of V and p65 affects the composition of the NF-κB complex (p65/p50/IκBα). To investigate this issue I performed Co-IP experiments with flag-p65, p50, IκBα and MV V. Flag-p65 was immunoprecipitated using α-flag M2 affinity gel and co-purification of p50 or endogenous IκBα was assessed in the presence or the absence of MV V. Flag-p65 was able to pull down equivalent levels of p50 (Fig. 3-7; first right panel) and IκBα (Fig. 3-7; second right panel) matter if MV V was present or not. The level of co-purified MV V was also equal irrespective whether p50 was expressed or not (Fig. 3-7; third right panel). This indicates that binding of p50, IκBα and MV V to p65 are independent of each other and that binding of MV V to p65 does not influence the composition of the NF-κB complex.

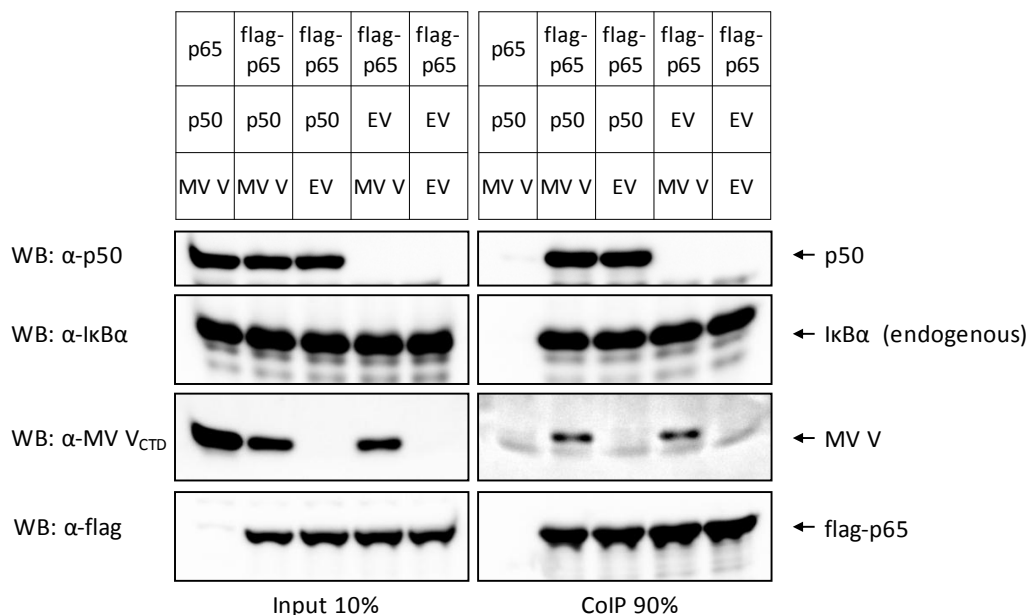


Figure 3-7 Binding of MV V to p65 does not compete with binding of p50 or IκBα to p65

HEK-293T cells were used to express flag-p65 in combination with p50 and V or only with one of those together with empty vector EV (2 μg each). After 24 h cells were lysed under native conditions and flag-tagged proteins were pulled down using anti-flag M2 affinity gel. Binding of p50 or IκBα to flag-p65 in the presence of MV V was visualized by Western blotting using the indicated antibodies. Depicted is a representative experiment out of three repeats.

3.8 MV V prevents nuclear translocation of p65

The MV V protein was shown to exhibit a cytoplasmic distribution (Wardrop and Briedis, 1991). Together with the finding that it interacts with the RHD of p65, which comprises the NLS of p65, the question rises whether binding of V to p65 might interfere with trafficking of this NF- κ B subunit. In order to address this hypothesis, HEp2 cells were transfected with a flag-MV V encoding plasmid, or empty vector to perform immunofluorescence (IF) experiments (done by Christian Pfaller). The cells were stimulated with 10ng/ml TNF α 30 min prior to fixation, followed by immunostaining of p65 and flag-tagged MV V. The subcellular distribution of the proteins was assessed using a laser scanning confocal microscope.

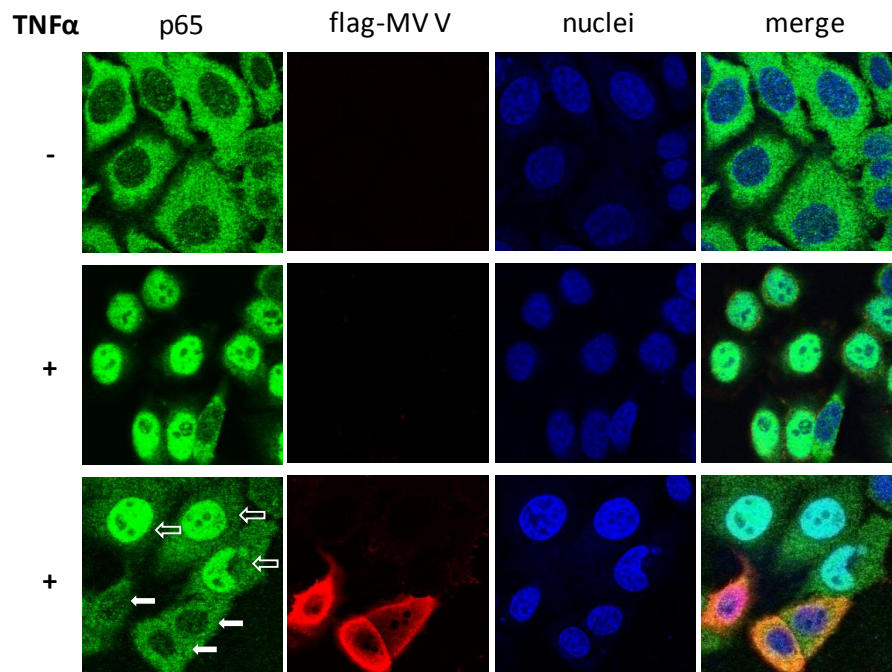


Figure 3-8 MV V prevents nuclear translocation of p65

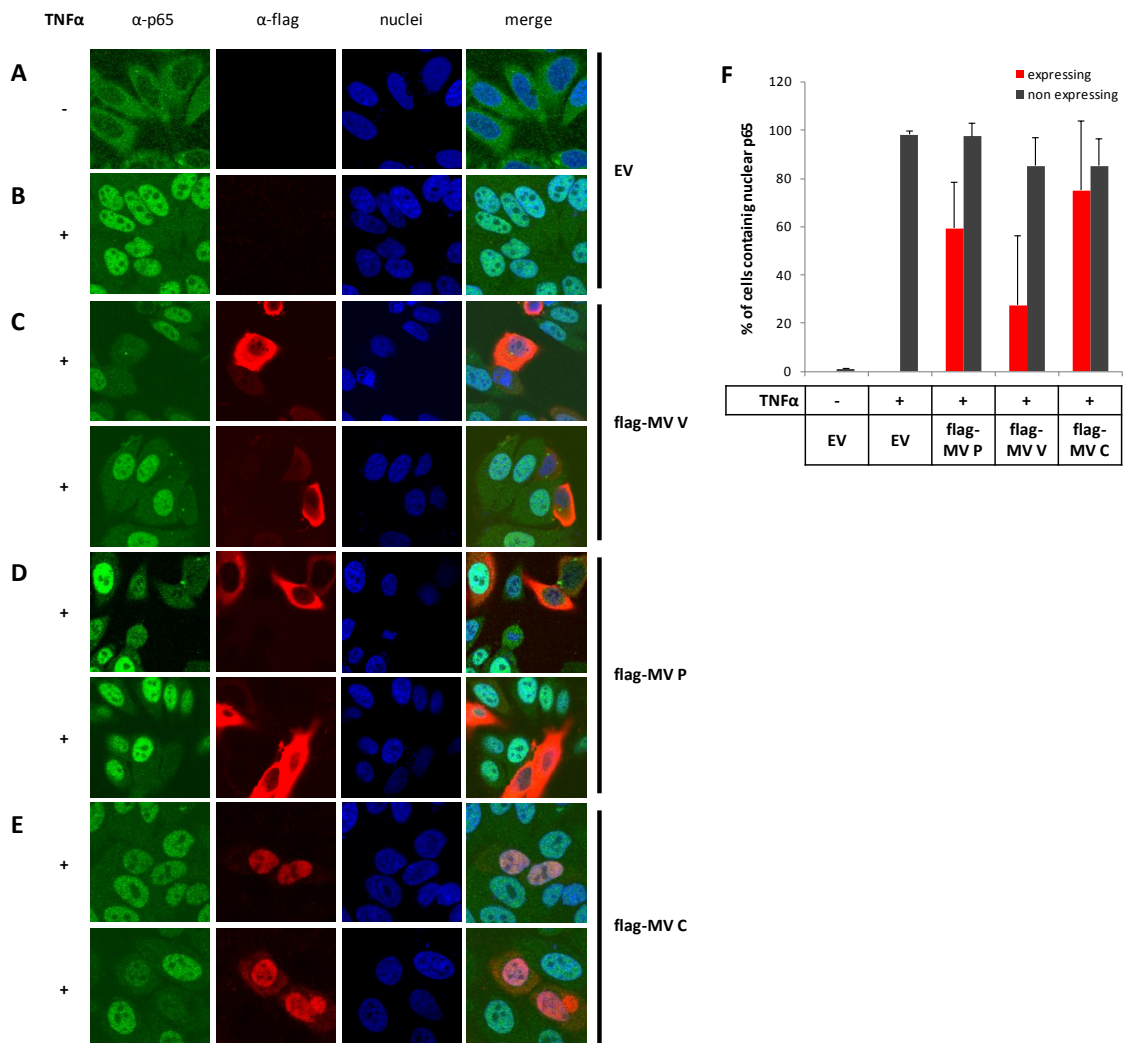
HEp2 cells were transfected with a vector for flag-MV V or empty vector (EV) (500 ng each). 24 h post transfection cells were either treated with 10 ng/ml TNF α for 30 min (+) or left untreated (-). Subsequently, cells were fixed and stained using rabbit α -p65, mouse anti-Flag-M2 primary antibodies, and anti-rabbit Alexa 488 or α -mouse tetramethylrhodamine secondary antibodies, respectively. Images were acquired by confocal laser scanning microscopy and show representative sections. Green: p65 (stained with specific antibody); red: flag-MV V (stained with α -FLAG[®] M2); blue: ToPro3 nuclear staining; open arrow: not flag-MV V expressing cell; closed arrow: flag-MV V expressing cell. Depicted is a representative experiment out of three repeats. Adapted from (Schuhmann et al., 2011).

In unstimulated cells transfected with empty vector, p65 is located predominantly in the cytoplasm (Fig. 3-8; upper panel), however TNF α treatment resulted in almost complete translocation of p65 from the cytoplasm to the nucleus (Fig. 3-8; middle panel). In contrast, accumulation of p65 in the nucleus upon TNF α stimulation in cells expressing flag-MV V was severely impaired (Fig. 3-8; lower panel; closed arrows), while cells failing to express detectable flag-MV V showed a normal nuclear accumulation of p65 (Fig. 3-8; lower panel; open arrows). This demonstrates that the presence of MV V in cells prevents the nuclear accumulation of the NF- κ B-subunit p65 and thereby precludes its transcriptional activity.

3.9 Nuclear translocation of p65 upon TNF α treatment in the presence of MV P and C

Even though MV P and C do not bind to p65 they inhibit canonical NF- κ B activation. To test if they somehow interfere with the nuclear translocation of p65, IF studies with flag-tagged MV P gene products were accomplished. Therefore HEP2 cells were transfected with flag-MV V as positive control or flag-MV P, C, or empty vector. 30 min prior to fixation the cells were treated with TNF α and the proteins were immunostained with antibodies against p65 or the flag-epitope. The NF- κ B subunit p65 is located in the cytoplasm in unstimulated cells (Fig. 3-9A), but translocates to the nucleus upon TNF α treatment (Fig. 3-9B) in cells transfected with empty vector. In cells expressing flag-tagged MV V the TNF α -stimulated nuclear translocation of p65 was blocked, and p65 was retained in the cytoplasm (Fig. 3-9C) as observed before (Fig. 3-8). Flag MV P expressing cells showed p65 in the nucleus as well as in the cytoplasm suggesting a potential inhibition of p65 nuclear accumulation (Fig. 3-9D). In contrast to MV P and V, MV C is located in the nucleus and cells expressing flag-MV C showed no retention of p65 in the cytoplasm (Fig. 3-9E). To determine nuclear translocation of p65 more precisely, the nuclear localization of p65 was quantified (Fig. 3-9F). It was discriminated between cells expressing the appropriate MV protein (red bars) and those that failed to express (gray bars). The quantification revealed that nuclear localization of p65 upon TNF α treatment was only seen in 25% of flag-MV V

expressing cells, while 60% of cells expressing flag-MV P and nearly 80% of flag-MV C expressing cells showed p65 staining within the nucleus (Fig. 3-9F). In cells that failed to express MV proteins at least 80% show nuclear localization of p65 upon TNF α treatment. These findings suggest that MV P and V inhibit NF- κ B activity upstream of the nuclear translocation of p65, whereas MV C probably acts in the nucleus. The difference in the degree of inhibition of MV P and V to inhibit p65 translocation was also reflected in the previous NF- κ B-dependent reporter gene assays.



3.10 MV V does not directly bind to the NLS of p65 or interfere with importin α 5 binding to p65

The nuclear import of p65 is mediated via members of the importin α family, namely importin α 3, 4, and 5 (Fagerlund et al., 2005; Fagerlund et al., 2008). To further clarify the underlying mechanism of MV V mediated inhibition of p65 nuclear translocation, the question whether MV V targets the NLS of p65 was assessed, and furthermore it was tested if MV V interferes with binding of importin α to p65.

First of all the binding of p65 to importin α 3, 4, and 5 should be confirmed with our conditions. Therefore the HA-tagged importin α isoforms were expressed from transfected plasmids with flag-tagged p65 in HEK-293T cells. Extracts were purified using α -flag M2 affinity gel and precipitates were subjected to SDS-PAGE and analyzed by immunoblotting using antibodies specific for the HA- and the flag-epitope. As expected, all importin α subunits were copurified with flag-p65, however, importin α 5 showed the strongest affinity (Fig. 3-10A).

In order to check if MV V binds directly to the nuclear translocation signal (NLS) of p65 two mutants of p65 were constructed. A deletion mutant (p65 1-300) lacking the NLS that is located at amino acid position 301 to 304, as well as a mutant with a mutated NLS (p65 NLS-) according to Fagerlund et al. (301AAA) (Fagerlund et al., 2005). Binding of flag-MV V to the mutants was assessed by CoIP experiments. As positive control full length p65 was included as well as the REL homology domain of p65 (p65 RHD), which comprises the NLS and spans aa 1 to 309. Immunoprecipitated flag-MV V displayed interaction with all p65 constructs even those lacking a functional NLS indicating that the binding of MV V to p65 is not directed to its NLS (Fig. 3-10B).

Although MV V binds not directly to the NLS of p65, but to the RHD it might that MV V competes with importin α 5 for binding to p65. To test for competition in binding, the association of flag-p65 and HA-importin α 5 was challenged by the presence of MV V and vice versa in CoIP experiments against the flag-tag. Irrespective of the presence of MV V, HA-importin α 5 was bound to flag-p65. Furthermore, MV V co-precipitated with

flag-p65 to the same extent whether HA-importin α 5 was present or absent (Fig. 3-10C). This suggests that the interactions of MV V and importin α 5 with p65 are not competitive.

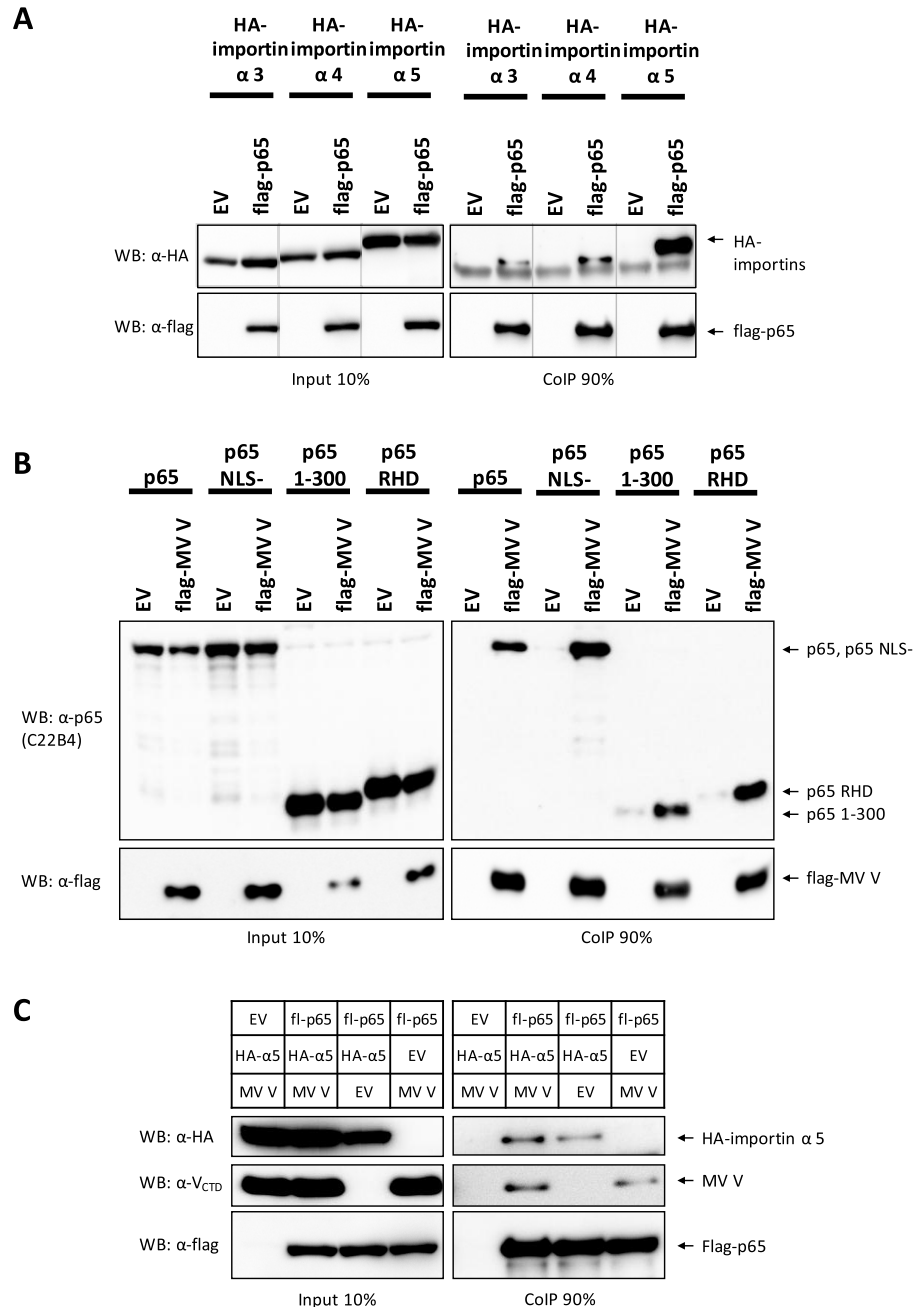


Figure 3-10 MV V does not directly bind to the NLS of p65 or interfere with importin α 5 binding to p65

(A) CoIP experiments were performed in HEK-293T cells expressing flag-p65 and HA-importin α 3, 4 or 5. Flag-p65 was pulled down by anti-flag M2 affinity gel, and precipitates were analyzed for the presence of HA constructs by Western blot. Staining was performed using α -flag and α -HA antibodies. A representative experiment out of two repeats is shown. (B) HEK-293T cells were cotransfected with vectors encoding for flag-MV V or empty vector (EV) and p65, p65 NLS-, p65 1-300 or p65 RHD (3 μ g each). CoIP assay was performed as described above. To visualize the p65 constructs an antibody directed against the N-terminal domain of p65 was used. A representative experiment out of three is shown. (C) HEK-293T cells were used to express flag-p65 in combination with HA-importin α 5 and MV V or only with one of those together with empty vector EV (2 μ g each). CoIPs were carried out as depicted above using anti-flag M2 affinity gel. Binding of both proteins to flag-p65 was visualized by Western blotting using α -MV V_{CTD} and α -HA antibodies. Depicted is a representative experiment out of three repeats.

3.11 The CTD of MV V is required and sufficient for p65 binding and suppression of p65/p50-mediated NF- κ B activity

MV P and V have identical amino-terminal domains (PV_{NTD}), but distinct carboxy-terminal domains (P_{CTD}; V_{CTD}). Since only MV V binds to p65, one could reason that p65 binding is mediated via the V-specific CTD. To verify this, HEK-293T cells were transfected with expression plasmids coding for the individual protein domains fused to an Ig-tag (Ig-MV PV_{NTD}, P_{CTD}, V_{CTD}), or the full length proteins, together with p65. CoIP experiments were performed applying Protein A-Sepharose against the lysates to precipitate the Ig-tagged constructs.

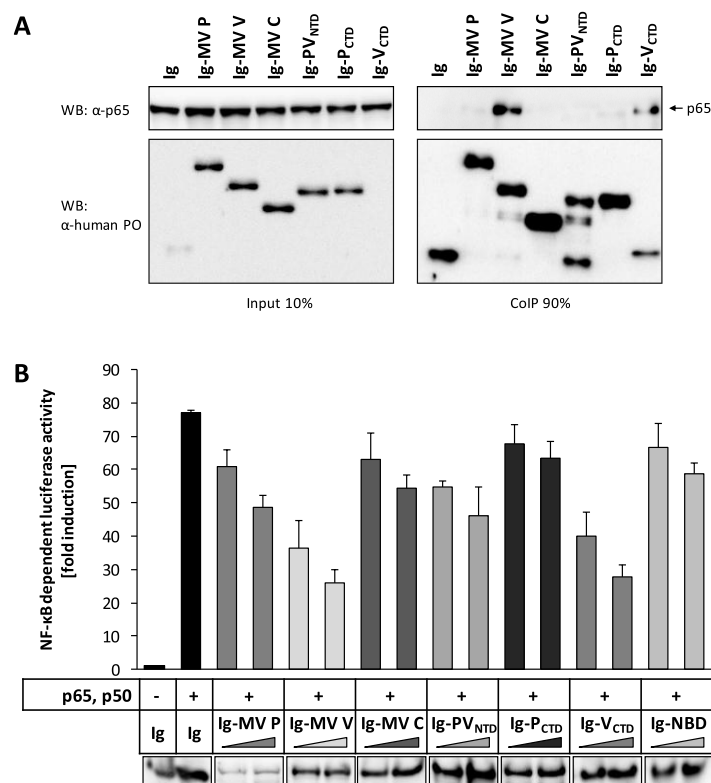


Figure 3-11 The CTD of MV V is sufficient for p65 binding and suppression of p65/p50-mediated NF- κ B activity

(A) HEK-293T cells were cotransfected with vectors encoding for the indicated Ig-tagged constructs or the Ig tag itself (Ig) and p65. CoIP assay was performed as described above. A representative experiment out of four is shown. (B) Increasing amounts (300 ng, 600 ng) of the indicated Ig-tagged constructs were coexpressed in HEK-293T cells together with p65, p50 (150 ng each) and the NF- κ B reporter system (100 ng p55A2/ 10 ng pRL-CMV). 12 h post transfection cells were lysed and NF- κ B activity was determined by a dual luciferase assay. The bars represent the means and the error bars the standard deviation of two independent experiments. Depicted is a representative experiment out of three repeats. Lower panel: Expression levels were determined by Western blotting. Adapted from (Schuhmann et al., 2011).

Indeed, Ig-MV V_{CTD} was sufficient for co-precipitation of p65 with a binding affinity comparable to that of full length Ig-MV V, while the other constructs did not reveal interaction with the NF- κ B subunit (Fig. 3-11A). To clarify whether binding of the small V_{CTD} is also sufficient for inhibition of NF- κ B transcriptional activity, p65 and p50 were overexpressed in HEK-293T cells along with the Ig-tagged constructs and the reporter system. A similar and dose-dependent reduction of NF- κ B-dependent luciferase expression confirmed that binding of V_{CTD} is sufficient for inhibition (Fig. 3-11B). In contrast, expression of the C-terminal portion of the P protein had no considerable effect on p65/p50 mediated luciferase activity. In summary, the C-terminal domain of the V Protein is sufficient for p65 binding and inhibition of p65/p50 mediated NF- κ B activity.

3.12 Mutational analysis of MV V

The CTD of MV V is a 68 aa long cysteine-rich domain (Fig. 3-12A, green marked). Seven cysteine residues form together with a histidine two zinc fingers that are named loop 1 and 2 (Fig. 3-12B) (Liston and Briedis, 1994). Homology modeling of the MV V_{CTD} was accomplished using the crystal structure of PIV5 V (2B5L.pdb (Li et al., 2006)) (done by Johannes Söding, Gene Center). The resulting structure illustrates both zinc fingers that were colored using the PyMOL software. Loop 1 is displayed in orange, loop 2 in blue (Fig. 3-12C).

In addition to binding to p65, the CTD of the V protein was shown to interact with a set of molecules important for the innate immune response, among them MDA5, STAT2 and IRF7 (Goodbourn and Randall, 2009). In order to discriminate the different binding sites and functions located within the V_{CTD} a subset of MV V mutants were generated and tested. It was already published that aa 233R and 235E are crucial for MDA5 binding (Ramachandran and Horvath, 2010) and it was shown in our lab that a MV V mutant (MV V_{dIRF7}) that has four amino acid exchanges to alanine in the loop2 region (259AAAA) failed to bind to IRF7 anymore (Pfaller, 2009). The MDA5 deficient mutants MV V_{dMDA5(1)} (R233A) and MV V_{dMDA5(2)} (E235A) were assessed together with MV V_{dIRF7} and MV V for p65, IRF7 and MDA5 binding in CoIP experiments (Fig. 3-12D).

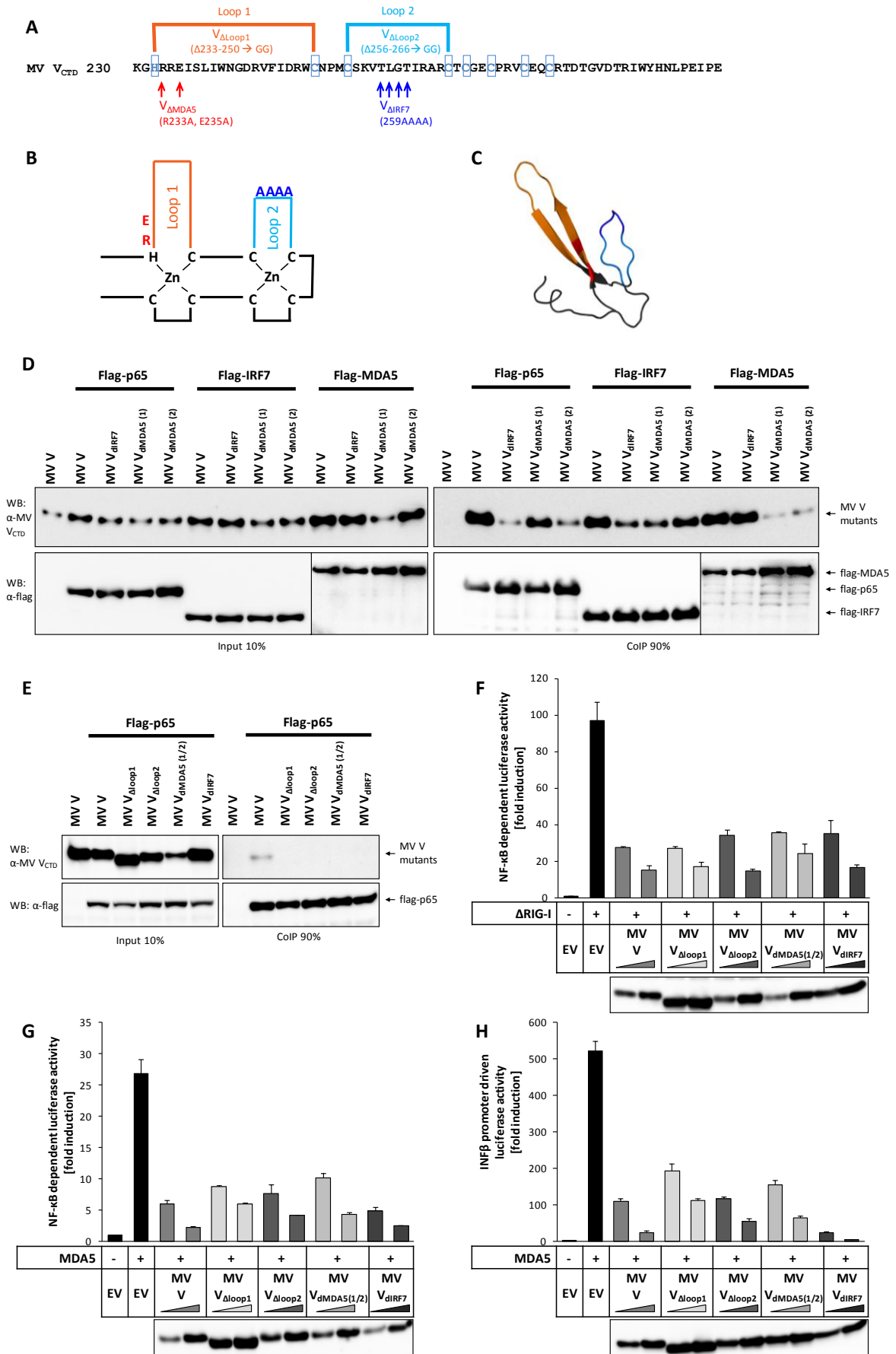


Figure 3-12 Mutational analysis of MV V

Previous page

(A) Amino acid sequence of the cyctein rich- C-terminal region of MV V (aa230- 299). The histidine and all cycteins residues are highlited by a blue box. (B) These residues coordinate two zinc ions building two zinc fingers. (C) Homology modeling of MVCTD was carried out with the crystal strucutre of PIV5 V as template and displayed with the PyMOL software. Loop1 is colored red, loop2 blue. Different MV V mutants were generated. The inserted mutations are displayed (A+B). (D + E) CoIP experiments with flag-p65, flag-IRF7, or flag-MDA5 and MV V mutants were performed as described above. Purified proteins were visualized with α -flag and α -MV VCTD antibodies. NF- κ B dependent luciferase assays were performed as described above with Δ RIG-I (F) or MDA5 (G) as stimulus and different MV V mutants. (H) IFN β promoter activity was measured in dual luciferase assays transfecting HEK-293T cells with p125-luc (100 ng) and pRL-CMV (10 ng) together with plasmids encoding for MDA5 and MV V mutants. IFN β -promoter driven luciferase activity was determined 24h post transfection. The depicted values are means of two independent experiments and their standard deviation is displayed by error bars. Depicted is a representative experiment out of two repeats.

Both MDA5 deficient mutants showed a reduced binding to flag-MDA5 while the binding affinity of the IRF7 deficient mutant to flag-MDA5 was similar to the affinity of parental MV V. The IRF7 deficient mutant as well as MV V_{dMDA5(1)} exhibited reduced binding affinity to flag-IRF7, whereas binding of MV V_{dMDA5(2)} was comparable to binding of MV V to flag-IRF7. In the CoIP assays with flag-p65, MV V_{dIRF7}, and MV V_{dMDA5(2)} showed reduced binding to the NF- κ B subunit compared to MV V. However, none of the mutants completely failed to interact with the signaling molecules. To sum up, the binding sites of different signaling molecules within the MV V_{CTD} cannot be clearly discriminated from each other. While for MDA5 binding only residues in loop1 seem to be relevant, binding to p65 and IRF7 is affected by mutations within loop 1 and 2, suggesting that binding of p65 and IRF7 to MV V_{CTD} involves two independent sites located at loop 1 and 2.

To search for mutants that completely lost their binding affinity to p65 three more mutants were generated. Therefore, either loop 1 (MV V _{Δ loop1}) or loop 2 (MV V _{Δ loop2}) was substituted to two glycine residues (Fig. 3-12A). In addition, a mutant (MV V_{dMDA5(1/2)}) was cloned were both aa relevant for MDA5 binding were substituted to alanine (R233A, E235A). CoIP experiments with flag-p65 and the mutants displayed nearly no binding of all mutants to the NF- κ B subunit (Fig. 3-12E), however, the CoIP efficiency was much lower than in Fig. 3-12D. Together with the results from the repeat experiments I would assume that the binding affinity of all mutants to p65 is

reduced but not completely lost, as already seen in Fig. 3-12D with exception of MV $V_{\Delta\text{MDA5}(1)}$. Next, it was examined whether the reduced binding affinity to p65 of the mutants is also reflected in an extenuated capacity to inhibit NF- κ B signaling. Therefore, NF- κ B-dependent dual luciferase assays were performed using Δ RIG-I as stimulus and the different mutants (MV $V_{\Delta\text{loop}1}$; MV $V_{\Delta\text{loop}2}$; MV $V_{\Delta\text{MDA5}(1/2)}$; MV $V_{\Delta\text{IRF}7}$) as inhibitor. Parental MV V was used as a reference. All mutants displayed an inhibitory capacity similar to that of MV V (Fig. 3-12F). In addition, inhibition of MDA5-dependent activation of either NF- κ B (Fig. 3-12G) or IFN β promoter (Fig. 3-12H) was tested in further reporter gene assays. To measure IFN β promoter activity, a plasmid encoding for firefly luciferase under the control of the IFN β promoter (p125-luc) was applied instead of the NF- κ B reporter plasmid (Yoneyama et al., 1996). The capacities of the mutants to suppress NF- κ B activation (Fig. 3-12G) or IFN β -promoter activation (Fig. 3-12H) were quite similar. Solely, MV $V_{\Delta\text{IRF}7}$ inhibited IFN β promoter activation more potent. However, these findings revealed that reduced binding to p65 was not sufficient to abrogate efficient inhibition of NF- κ B activation. Thus, no mutants that are defective in the blockade of NF- κ B signaling could be identified so far. Possibly, combinations of mutants involving the identified aa at loop 1 (R233A,E235A) and 2 (259AAAA) would be necessary to lose MV V mediated inhibition of NF- κ B activity.

3.13 The V protein of the measles wild type isolate D5 inhibits NF- κ B activity and binds to p65

In the previous experiments I used MV proteins derived from the Schwarz strain (genotype A), a life attenuated vaccine obtained by multiple passaging on chicken embryo fibroblasts (Schwarz, 1962). To check if vaccine and wt measles V proteins differ in their ability to interfere with NF- κ B activity, a wt strain obtained from the Robert Koch Institute in Berlin (genotype D5 – MVi/Berlin.DEU/04.08[D5]) was used to generate an expression plasmid coding for the V protein of wt MV. Sequencing and subsequent sequence alignment with the Schwarz V revealed that there are only 13 aa substitutions within the PV_{NTD} and no mutation was found in the C-terminal domain (done by Christian Pfaller) (Fig. 3-13A). NF- κ B-dependent luciferase assays in HEK-293T

cells illustrated that Δ RIG-I as well as p65/p50-mediated NF- κ B activation was suppressed by both V proteins to the same degree (Fig. 3-13B and C). Furthermore, it was shown that binding to the NF- κ B subunit p65 is also conserved between the V proteins of both virus strains using CoIP experiments (Fig. 3-13D). These results indicate that the capacity to suppress NF- κ B activity and the ability to bind to p65 of wt and Schwarz-derived V proteins are equal.

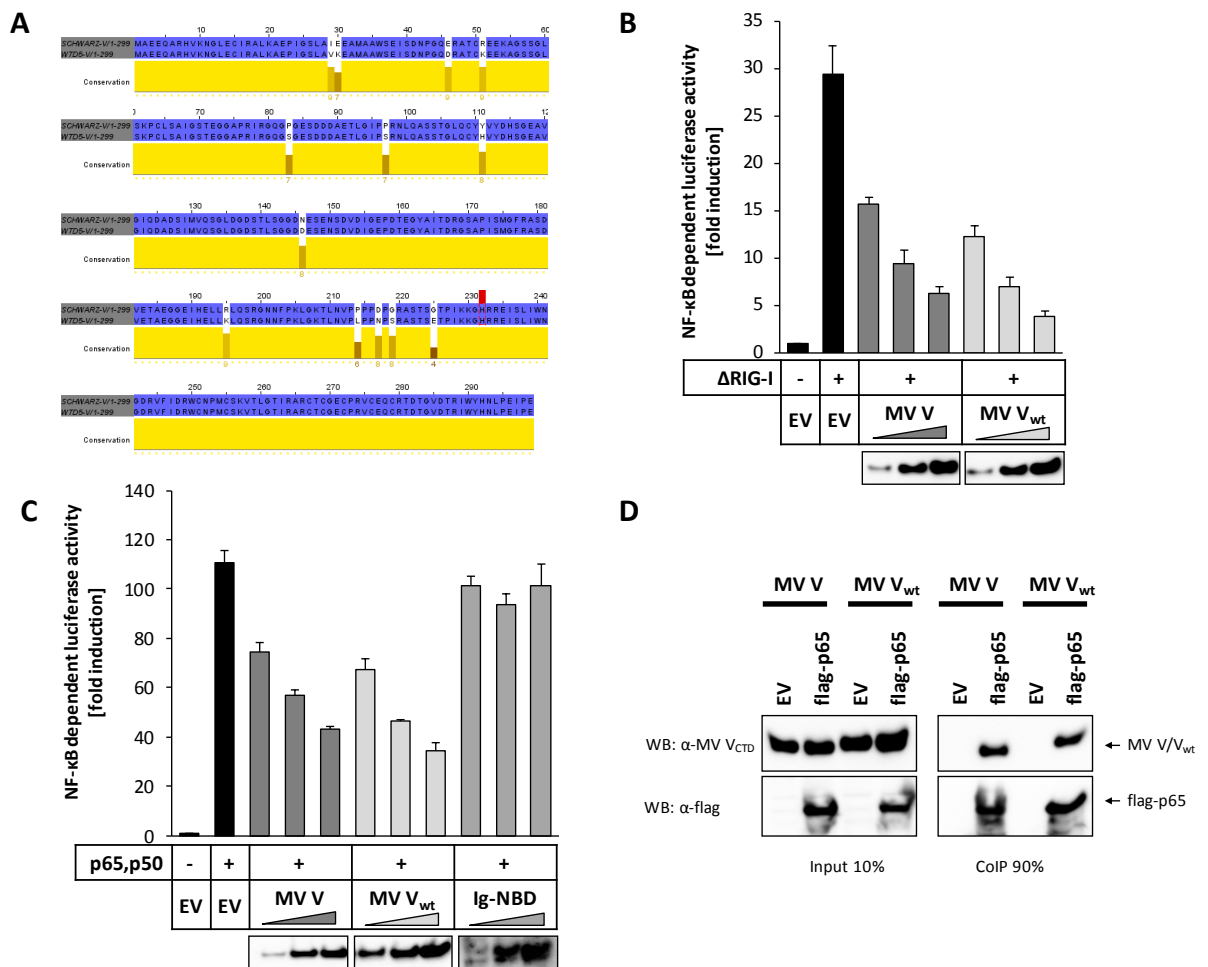


Figure 3-13 The V protein of the measles wild type isolate D5 inhibits NF- κ B activity and binds to p65

(A) Sequence alignment of the amino acid sequence of V proteins of the Schwarz strain and the wild type isolate D5. The sequence alignment was generated using *Clustal W2* and *Jalview*. NF- κ B-dependent luciferase assays in HEK-293T cells were performed using Δ RIG-I (B) or p65/p50 (C) as stimulus and increasing amounts of V proteins of the Schwarz strain (MV V) or the wild type D5 isolate (MV V_{wt}) were coexpressed. (D) HEK-293T cells were cotransfected with vectors encoding flag tagged p65 or an empty vector (EV) and the V protein of the Schwarz strain or the D5 wild type isolate. Flag-tagged proteins were pulled down using Flag M2 Matrix. The purified proteins were stained on Western blots with α -MV V_{CTD} and α -flag antibodies.

3.14 CDV V and NiV V act like MV V and suppress classical NF- κ B activity

Since the C-terminal domains of the V proteins of the *Paramyxovirinae* subfamily members show significant conservation it was tested if the NF- κ B inhibiting potential of the MV V protein is also conserved among paramyxoviruses. Therefore, I generated expression plasmids for flag-tagged paramyxovirus V proteins. We employed the V protein of the canine distemper virus (CDV), another member of the *Morbillivirus* genus, the V protein of the Nipah virus (NiV) of the *Henipavirus* genus and the V protein of the parainfluenza virus type 5 (PIV5) that belongs to the *Rubulavirus* genus (Fig. 3-14A; framed). To illustrate the conservation of the V_{CTD} an amino acid sequence alignment of V proteins of MV (AF266291.1), CDV (AF259549.1), NiV (AF212302.2) and PIV5 (AF052755.1) was performed with the help of ClustalW2 and Jalview software. (Fig. 3-14B).

The capacity of V proteins of CDV, NiV and PIV5 to interfere with NF- κ B activation was compared to the NF- κ B inhibiting potential of MV V using NF- κ B-dependent luciferase assays. NF- κ B was activated by applying different stimuli. Activation of the RIG-I pathway was achieved by overexpression of Δ RIG-I (Fig. 3-14C). Cells expressing only Δ RIG-I showed high induction of the NF- κ B dependent luciferase activity, whereas the coexpression of the V proteins of MV, NiV and CDV decreased NF- κ B activation in a dose dependent manner. The inhibitory potential of these V proteins appeared to be similar. In contrast to that, coexpression of PIV5 V had no effect on RIG-I mediated NF- κ B activation. However, referring to the Western blot of the viral proteins, it becomes obvious that the V protein of PIV5 was much lower expressed than the V proteins of MV, CDV and NiV. Activation of the TLR pathway was stimulated by overexpression of MyD88 (Fig. 3-14B). Consistently, the V proteins of MV, NiV and CDV suppressed NF- κ B activity with a similar potency, while PIV5 V did not show any inhibitory effect. The Western blot illustrates again that PIV5 V was hardly expressed, whereas the V proteins of MV, NiV and CDV showed similar expression levels.

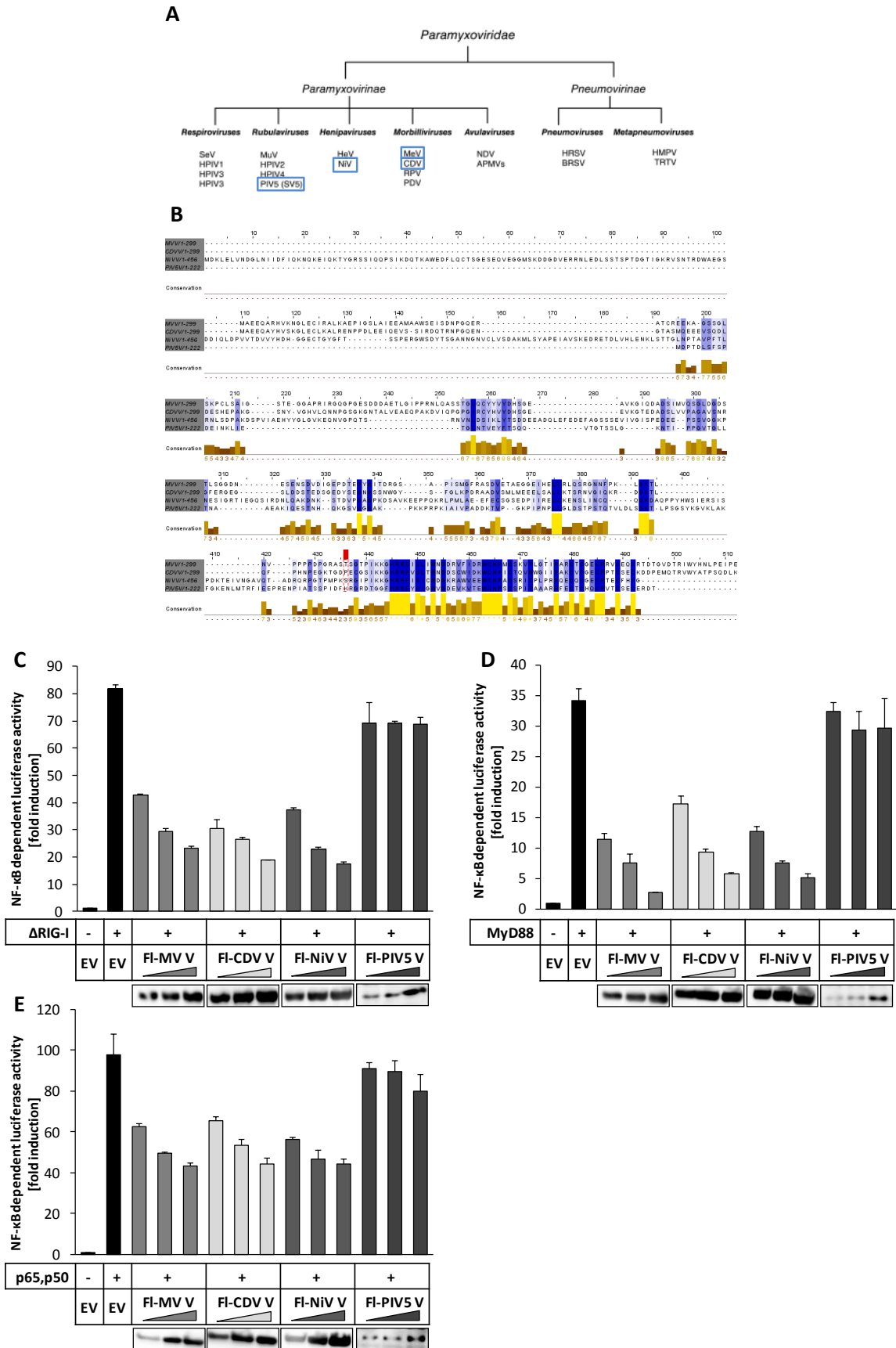


Figure 3-14 CDV V and NiV V act like MV V and suppress classical NF-κB activity

Previous page

(A) The Paramyxoviridae family is divided into two subfamilies. The Paramyxovirinae subfamily comprises five genera: Respiroviruses, Rubulaviruses, Henipaviruses, Morbilliviruses and Avulaviruses, while the Pneumovirinae subfamily consists of two genera, namely the Pneumoviruses and the Metapneumoviruses. Abbreviations: Sendai virus (SeV), human parainfluenza viruses (HPIV), bovine parainfluenza virus 3 (BPIV3), mumps virus (MuV), simian virus 5 (SV5), hendra virus (HeV), nipah virus (NiV), measles virus (MeV), canine distemper virus (CDV), rinderpest virus (RPV), phocine distemper virus (PDV), newcastle disease virus (NDV), avian paramyxoviruses (APMV), human respiratory syncytial virus (HRSV), bovine respiratory syncytial virus (BRSV), human metapneumovirus (HMPV) and turkey rhinotracheitis virus (TRTV). Adapted from (Goodbourn and Randall, 2009). (B) Sequence alignment of different Paramyxovirinae V proteins: MV V: V protein of the Schwarz strain of measles virus; CDV V: V protein of canine distemper virus; NiV V: V protein of Nipah virus; PIV5 V: V protein of parainfluenza virus 5; The sequence alignment was generated using Clustal W2 and Jalview. Increasing amounts (200 ng, 400 ng, 600 ng) of vectors encoding the V proteins of MV, CDV, NiV and PIV5 were cotransfected into HEK-293T cells with 200 ng of an expression plasmid for Δ RIG-I (C), MyD88 (D), or 100 ng of each p50 and p65 (E) and the NF- κ B-dependent reporter system (100 ng p55A2, 10 ng pRL-CMV). After 24 h, cells were lysed and NF- κ B activity was determined by a dual-luciferase assay. Values given are averages and standard-deviations of results from two independent experiments. Expression of the viral proteins was assessed by Western blotting using an α -flag antibody.

To test whether the V proteins of NiV, CDV and PIV5 can block NF- κ B activation downstream of the IKK complex as it was demonstrated for MV V, the NF- κ B dependent luciferase assay was applied using overexpression of the p50/p65 dimer as stimulus. To exclude upstream activation of NF- κ B, Ig-NBD was included as a negative control again. V proteins of MV, NiV and CDV inhibited NF- κ B activity, while PIV5 V did not (Fig. 3-14C). However, PIV5 V was again only weakly expressed, in contrast to the other viral proteins. Upstream activation could be excluded, since Ig-NBD did not inhibit p50/p65 dependent NF- κ B activity.

Taken together, these findings revealed that the inhibitory potential of the V proteins of CDV and NiV is similar to that of MV V.

3.15 The Rel homology domain of p65 is also bound by CDV V and NiV V

To test if the different paramyxovirus V proteins can also bind the NF- κ B subunit p65, Co-IP experiments were performed. Therefore, HEK-293T cells were used to coexpress flag-tagged V proteins together with p65. The flag-tagged proteins and their interaction partners were purified from the cell lysate using Flag-M2 Matrix and subjected to immunoblotting. p65 was copurified with MV V, CDV V, and NiV V but not with PIV5 V (Fig. 3-15A). Notably, the expression levels of flag-PIV5 V was again lower.

Since it was shown that MV V specifically binds to the rel homology domain of p65, the other V proteins were assessed for their binding affinity to this domain. V proteins of CDV and NiV clearly associated with the RHD of p65 whereas PIV5 V showed no interaction (Fig. 3-15B). These findings indicate that not only the NF- κ B inhibitory potential of the V proteins of MV, CDV, and NiV is conserved but also their binding affinity to the RHD of p65 and that PIV5 V does not bind to p65 and therefore cannot interfere with NF- κ B activation.

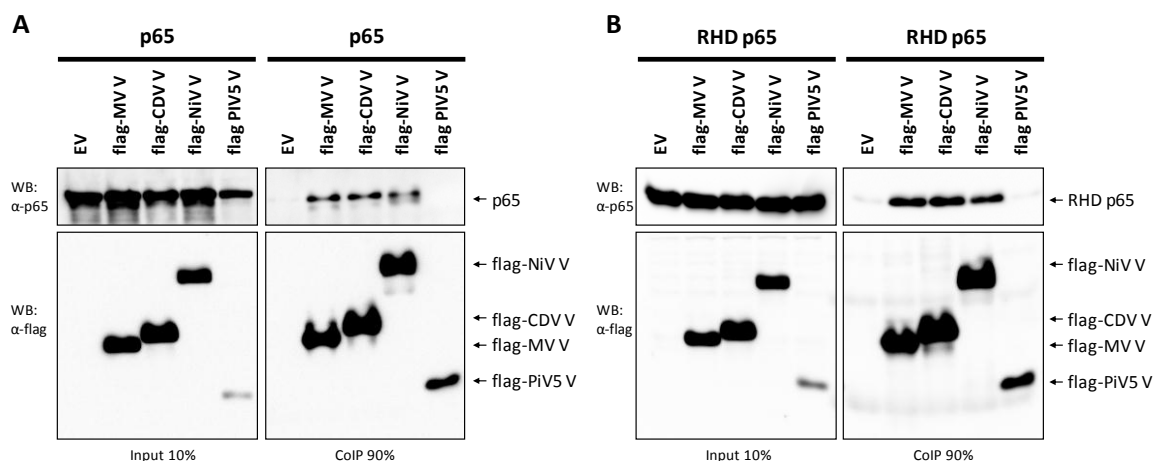


Figure 3-15 The Rel homology domain of p65 is also bound by CDV V and NiV V

HEK-293T cells were cotransfected with vectors encoding the indicated flag tagged constructs or an empty vector (EV) and full length p65 (A) or RHD-p65 (B). Flag-tagged proteins were pulled down using Flag M2 Matrix. The purified proteins were stained with α -p65 and α -flag antibodies on Western blots.

3.16 Binding of P gene products to other NF- κ B subunits

Besides p65 and p50, the main subunits of the classical NF- κ B signaling cascade, additional dimers composed of other NF- κ B subunits exist. RelB and p100/p52 are the key players of the alternative NF- κ B pathway, which is involved in adaptive immune responses (Bonizzi and Karin, 2004). The NF- κ B subunit c-Rel plays an important role in controlling B-cell proliferation, survival, and oncogenesis (Gilmore et al., 2004). Since MV infection *in vivo* can result in immunosuppression of the host that also involves the adaptive immune system (Griffin, 2010), it was checked if any of the MV P gene products can interfere with these NF- κ B subunits. CoIP experiments with flag-tagged MV P, V, and C together with RelB, c-Rel, p100 and p52 were accomplished. Like p65, RelB exhibited binding affinity exclusively to flag-MV V (Fig. 3-16A). Notably, an additional 55 kDa band was seen with the α -RelB antibody directed to the C-terminus of RelB if MV V was present. Weak binding of c-Rel was observed to both flag-MV P and V (Fig. 3-16B). For p100, the precursor of p52, no interaction with any of the P gene products was observed (Fig. 3-16C), whereas the processed p52 associated with both flag-MV P and V, however, with weaker affinity to flag-MV V (Fig. 3-16D). To further validate these findings CoIP experiments were performed the other way around using flag-tagged NF- κ B subunits for co-precipitation of untagged MV proteins. Here, flag-p65 and -p50 were included as positive and negative controls and references. The experiments copurifying MV P revealed only binding to flag-p52. The weak association of c-Rel with flag-MV P was not confirmed (Fig. 3-16E). A very weak band of MV P was observed with flag-p65 as already described in chapter 3.5. CoIP assays with the flag-tagged NF- κ B subunits and MV V prove the binding of MV V to p65 and p52, however, binding of V to flag-RelB and flag-c-Rel was not observed (Fig. 3-16F). But notably, coexpression of MV V and RelB resulted in very low expression levels of V (Fig. 3-16F) and this was also seen for MV P (Fig. 3-16E).

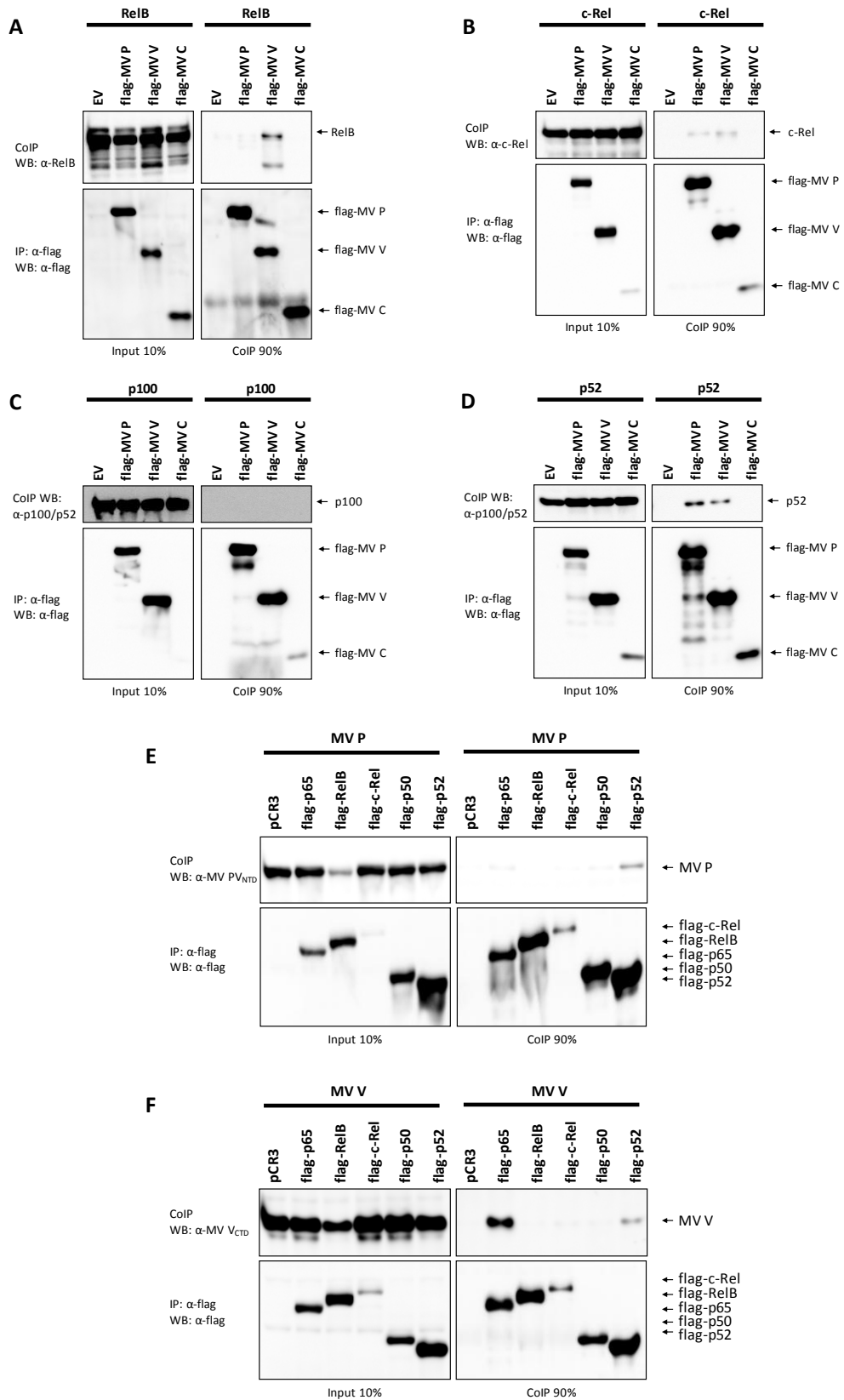


Figure 3-16 Binding of P gene products to other NF- κ B subunits

Lysates of HEK-293T cells expressing flag-tagged MV P, V, or C and RelB (A), c-Rel (B), p100 (C) or p52 (D) were purified with anti-flag M2 affinity gel. Purified proteins were visualized by Western Blotting using antibodies specific for the overexpressed NF- κ B subunits or the flag epitope. CoIPs with flag-tagged p65, RelB, c-Rel, p50 or p52 and MV P (E) or MV V (F) were stained with α -PVNTD or α -VCTD and the α -flag antibody.

Thus binding of RelB and MV V could not be confirmed but is still conceivable. The binding capacity of MV V to p65 was much more prominent than to p52, indicating that the main binding partner among the NF- κ B subunits of MV V is p65. Furthermore, these results indicate that there is an interaction of MV P and V with the alternative NF- κ B subunit p52. Binding of flag-MV V to RelB, and probably a processed form of RelB, suggests also an interaction of V and RelB in cells.

3.17 Inhibition of the alternative NF- κ B pathway

In order to examine if binding of MV P and V to p52 and the supposed binding of MV V to RelB result in inhibition of the alternative NF- κ B signaling pathway, NF- κ B-dependent luciferase assays were implemented. The alternative pathway was stimulated by overexpressing NIK, a kinase involved in the alternative signaling cascade. Cells overexpressing NIK without any viral protein showed high induction of NF- κ B-dependent luciferase activity. However, the presence of MV P, V, and C caused a similar inhibition pattern as seen for the classical pathway (Fig. 3-17A). Since it is known that stimulation of the alternative signaling is not exclusive but also leads to activation of the classical NF- κ B subunits, the observed suppression pattern might result from inhibition of p65 activity. To exclude activation of p65, alternative NF- κ B activation was induced expressing directly the alternative subunits. RelB/p52-mediated induction was not very prominent (less than 10-fold), but this was also seen in other studies. Solely MV V coexpression exhibited a very slight suppressive effect on RelB/p52 mediated-NF- κ B activation (Fig. 3-17B). Last, the effect of MV P, V, and C on c-Rel mediated NF- κ B activation was investigated. Again, NF- κ B activation was quite poor and there was no inhibitory capacity displayed by any of the MV P gene products (Fig. 3-17C). These results suggest that the assumed binding to RelB and c-Rel or the binding to p52 of MV P and V do not result in substantial suppression of NF- κ B activation mediated by these subunits. However, it still remains to be investigated if there is any suppressive effect of the viral gene products upstream of RelB, p52 and c-Rel.

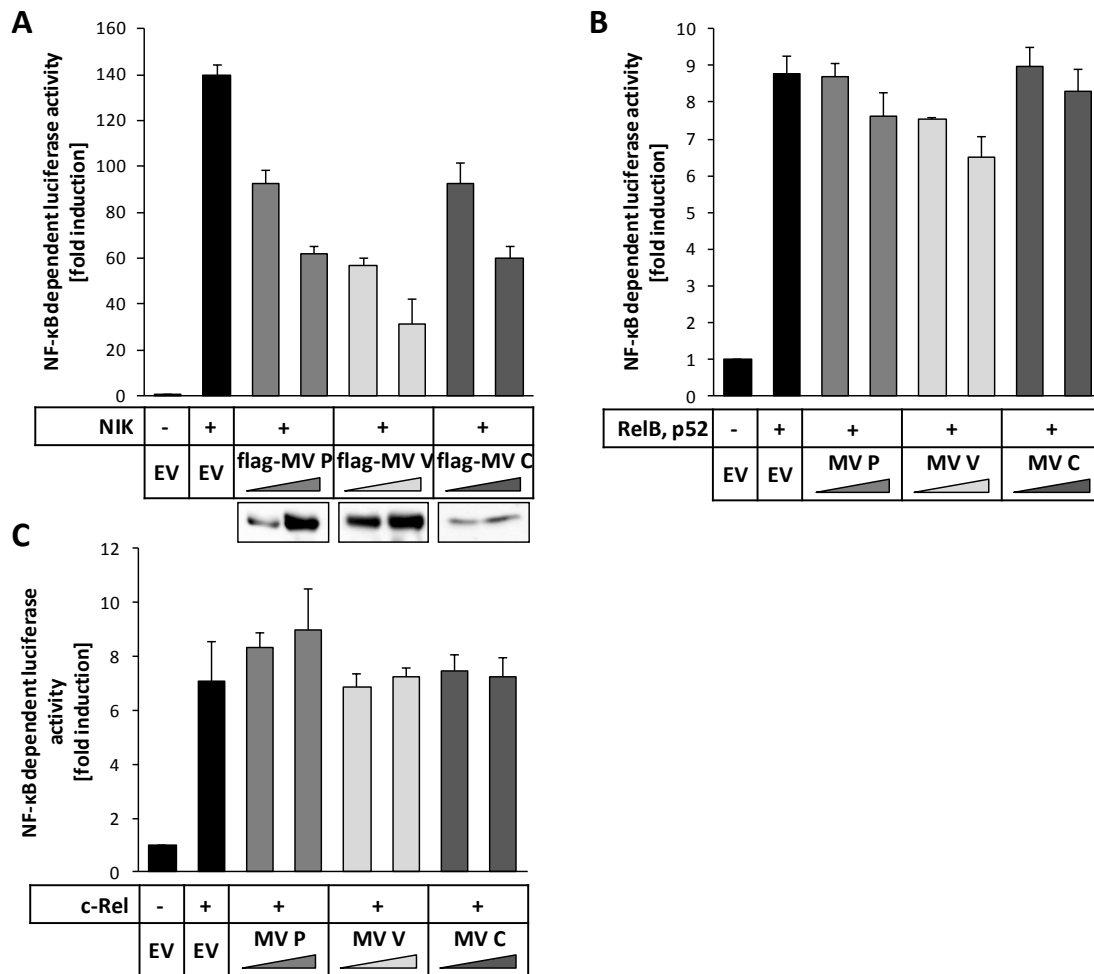


Figure 3-17 Inhibition of the alternative NF- κ B pathway

NF- κ B dependent luciferase activity was measured in HEK-293T cells transfected with 200 ng of plasmids encoding for NIK (A), RelB/p52 (B) or crel (C), increasing amounts (200 ng, 400 ng, 600 ng) of vectors for MV P, V, or C and the NF- κ B-dependent reporter system. The bars represent the means and the error bars the standard deviation of two independent experiments. Depicted is a representative experiment out of three repeats. Expression of the viral proteins was assessed by Western blotting using either α -flag (A) or α -PVNTD, α -VCTD, or α -MV C (B+C) antibodies.

3.18 Generation and characterization of recombinant viruses MV-vac2, MV-MCS, MV-VKO, MV-VKO+V

To investigate the biochemical results obtained so far in the viral context, recombinant measles viruses were rescued. Therefore, different full-length constructs of the MV genome were cloned (Fig. 3-18A). The sequence of the Schwarz MV anti-genome from the pB(+)MVvac2 plasmid (del Valle et al., 2007) was cloned into the backbone of the rescue plasmid pBS-HHrz/Hdrz(sc) which was shown to significantly improve virus rescue efficiency (Ghanem et al., 2012). Virus rescued from this plasmid is referred to

as MV-vac2. To enable insertion of an additional gene, a plasmid where a multiple cloning site (MCS) flanked by the 5'-UTR and the 3'-UTR of the P gene was inserted between the P and the M gene was constructed (done by Christian Pfaller). The corresponding virus is named MV-MCS. For a virus deficient in V protein expression (MV-VKO) a point mutation within the V editing site was inserted in the MV-MCS full length plasmid to destroy V mRNA production (Radecke and Billeter, 1997; Schneider et al., 1997). The introduced point mutation is silent for the P and C protein. The V ORF with mutated editing site was inserted into the MCS of the MV-VKO full length plasmid such that the expression of the V protein is restored in the recombinant virus MV-VKO+V.

To characterize the recombinant viruses on protein level A549 cells were infected at an MOI of 1 for 24 or 48h or mock-treated with supernatant of Vero cells lysed by freeze-thaw. Lysates of the infected cells were subjected to SDS-PAGE followed by Western blotting using α -MV N, α -MV P_{NTD}, α -MV V_{CTD}, α -MV C and α -actin antibodies. All viruses expressed comparable ratios of the MV N, P, and C proteins. In case of infection with MV VKO no expression of the V protein was detected illustrating that knock out (KO) of V was successful (Fig. 3-18B).

The recombinant viruses were further characterized with respect to their growth kinetics on IFN incompetent Vero cells and IFN competent A549 cells. Therefore, Vero or A549 cells were infected at an MOI 0.01. Infectious titers were determined 6 h, 24 h, 48 h, 72 h, and 96 h p.i. The viruses showed similar growth kinetics on Vero cells (Fig. 3-18C) as well as on A549 cells (Fig. 3-18D). Surprisingly, even the KO of the V protein did not influence the growth of the virus on IFN competent cells.

To sum up, the MV-VKO virus appears to be indistinguishable from the other viruses in regards of growth and protein expression in Vero and A549 cells.

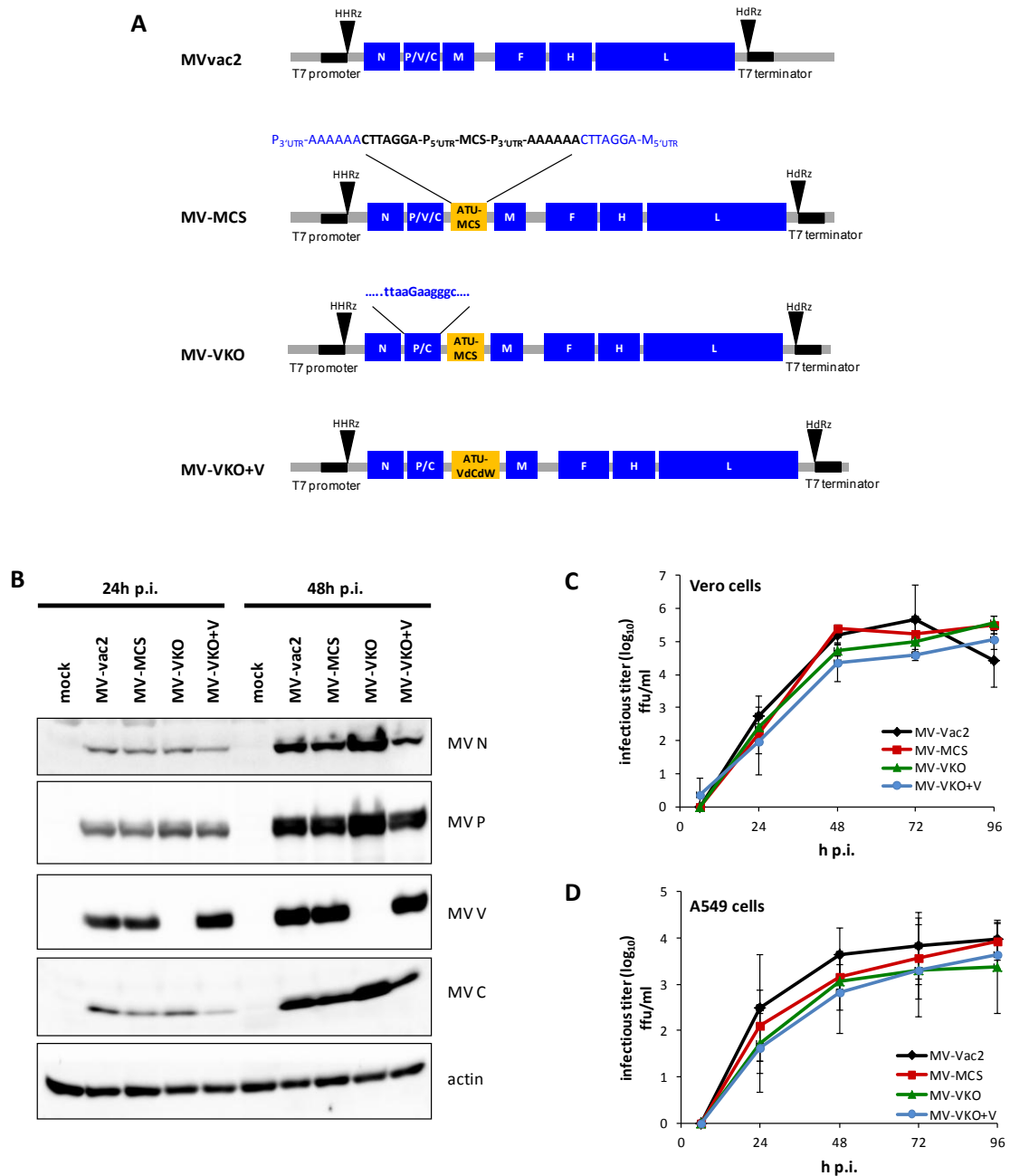


Figure 3-18 Generation and characterisation of recombinant viruses MV-vac2, MV-MCS, MV-VKO, MV-VKO+V

(A) Overview of the full length plasmid used to generate the recombinant viruses MV-vac2, MV-MCS, MV-VKO and MV-VKO+V. The Schwarz measles virus antigenome is cloned in the pBluescript vector (pBS(+)) containing a T7 promoter and a T7 terminator and flanked by ribozyme sequences. The hammerhead ribozyme (HHRz) and Hepatitis delta virus antigenomic ribozyme (Hdrz) were used to enable 5' or 3' processing, respectively. (B) A549 cells were infected (MOI=1) with the indicated viruses and lysed 24h or 48h p.i.. Western blot analysis was carried out and α -MV N (abcam/millipore), α -MV P_{NTD}, α -MV P_{CTD}, α -MV C (FEA/10/1) and α -actin were used to detect expression of the indicated proteins. A representative experiment out of four is shown. (C) Vero cells were infected (MOI=0.01) with the indicated viruses, 1h p.i. the cells were washed and frozen at 6h, 24h, 48h, 72h and 96h p.i.. Virus titers were determined by titration on Vero cells. Shown is the average and standard deviation of two independent experiments. (D) A549 cells were infected at an MOI of 0.01, 1h p.i. cells were washed and frozen at the indicated time points. Titration of the viral titers was carried out on Vero cells. The average and standard deviation of three independent experiments is shown.

3.19 NF- κ B activation upon infection with MV-MCS, MV-VKO, MV-VKO+V

The recombinant viruses were used to determine if the inhibitory effects proven for the MV V protein are also found in the viral context. Thus, HEK-293T cells were transfected with the dual NF- κ B-reporter system, infected 6h p.t. with MV-MCS, MV-VKO, MV-VKO+V at an MOI of 1 or mock-treated with supernatant of frozen Vero cells and lysed 24h later. MV-VKO was expected to induce NF- κ B activity more prominent than MV-MCS and MV-VKO+V, since one of the NF- κ B inhibitors is knocked out in MV-VKO. Surprisingly, analysis of NF- κ B dependent luciferase activity displayed that MV-MCS infection activated NF- κ B slightly (3 fold), infection with MV-VKO resulted in only 6 fold induction of NF- κ B activity whereas MV-VKO+V infected cells showed 15 fold induction (Fig. 3-19A). Furthermore, Western blotting revealed that infection with MV-VKO was slightly enhanced. Using quantitative real-time RT-PCR as an additional readout, mRNA levels of different NF- κ B dependent genes were analyzed upon infection. A549 cells were infected with the indicated viruses at an MOI of 1 or mock-treated, RNA was isolated 24h p.i. and reverse transcribed into cDNA. Quantitative PCR was accomplished using IL-6, RANTES, IFN β , or MV N primers. Levels of IL-6 mRNA were about 600 fold induced in MV-MCS and MV-VKO infected cells, while infection with MV-VKO+V resulted in even 1200 fold induction (Fig. 3-19B). A similar expression pattern was found with RANTES mRNA levels. Induction by MV-MCS and MV-VKO was comparable (around 2000 fold) whereas MV-VKO+V induced twice as much (Fig. 3-19C). In contrast, IFN β mRNA levels were equivalent for all viruses (Fig. 3-19D). Levels of MV N mRNA were checked as infection control and two fold increased levels for MV-VKO+V revealed that infection with this virus was higher (Fig. 3-19E). This is also reflected in the Western blot control (Fig. 3-19F). Increased infection rate with MV-VKO+V might explain the increased levels of IL-6 and RANTES with this virus. In sum, these experiments do not reveal a major impact of the presence of V on NF- κ B activation in HEK-293T and A549 cells 24h post infection.

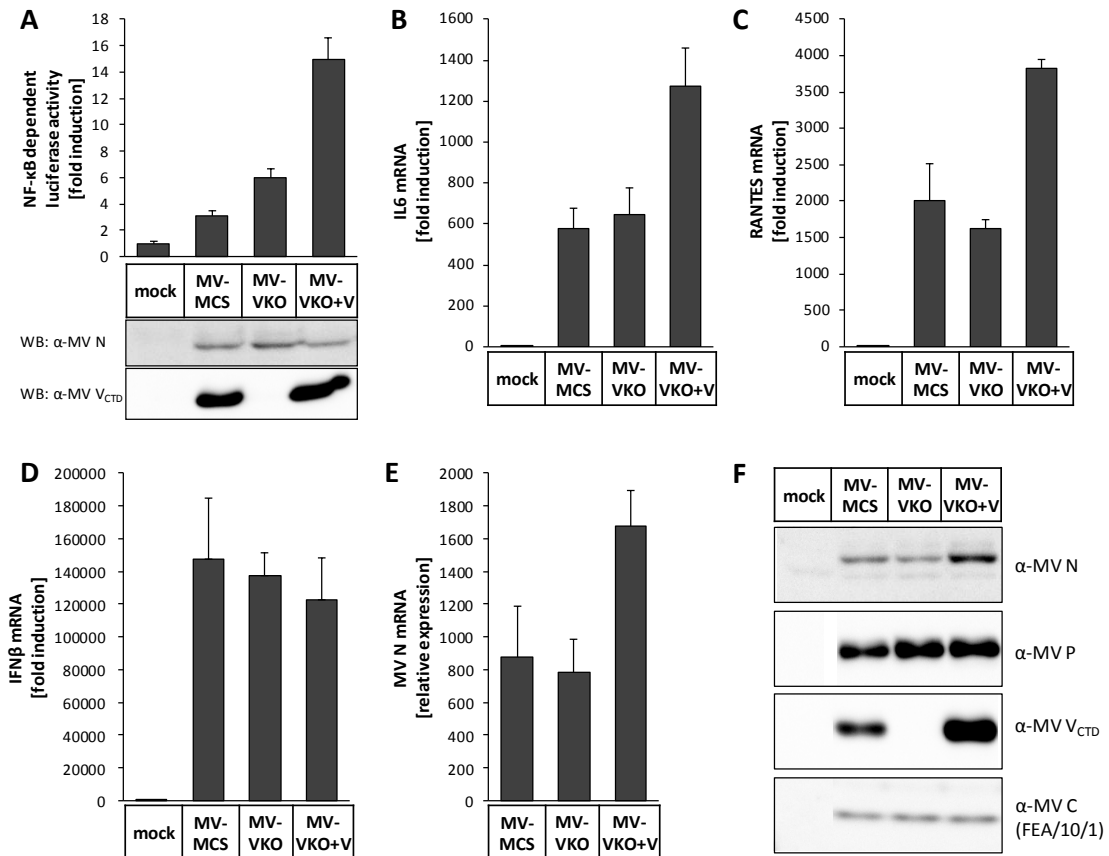


Figure 3-19 NF-κB activation upon infection with MV-MCS, MV-VKO, MV-VKO+V

(A) NF-κB activity was determined on HEK-293T cells transfected with the NF-κB reporter system (p55A2/pRL-CMV) by dual luciferase assays. 6h post transfection cells were infected with the indicated viruses at an MOI of 1 and lysed 24h later to determine luciferase activities. Values shown are average and standard deviations of two independent experiments. Expression of viral proteins was assessed by Western blotting. (B-F) Real-time RT-PCRs for NF-κB-dependent genes in HEK-293T cells infected with the indicated viruses at an MOI of 1. 24h p.i. cells were lysed and subjected to real-time RT-PCR using primer specific for IL-6 (B), RANTES (C), IFNβ (D), or MV N (E) as infection control. Values given are average and standard deviation of two independent experiments. Shown are representative experiments out of two repeats. To control infection on the protein level A549 cells were infected in parallel and lysates were subjected to Western blotting. Protein levels were visualized using antibodies specific for MV N, P, V, or C.

4 Discussion

NF- κ B is a ubiquitously expressed transcription factor that mediates a wide variety of cellular responses, ranging from proliferation, differentiation, and cell survival to cytokine production and other proinflammatory processes thereby regulating innate as well as adaptive immune responses. The primary result of NF- κ B activation by triggering of PRRs during innate immune responses is the expression of chemokines and pro-inflammatory cytokines, such as IL-6 or TNF α . The role of NF- κ B for IFN β expression is highly discussed. Early studies on the activation of the IFN- β promoter, which contains NF- κ B, AP1, and IRF binding sites, implicated NF- κ B as a key mediator of virus-induced IFN- β expression (Lenardo et al., 1989; Thanos and Maniatis, 1995). However, infection of NF- κ B knockout mouse embryonic fibroblasts (MEFs) with Sendai virus initially suggested the lack of an essential role for NF- κ B in virus induced IFN- β expression (Wang et al., 2007), but the same group then showed that NF- κ B is crucial during the early phase of virus infection (Wang et al., 2010). The important role of NF- κ B during infections in general is emphasized by reports showing that mice lacking different NF- κ B family members become more susceptible to various viral, bacterial, and parasitic infections (Rahman and McFadden, 2011). However, all these studies were conducted in mice, and therefore the role of NF- κ B in human IFN-expression needs to be evaluated.

In this study, it was shown that P gene products of the immunosuppressive measles virus, including the essential P protein, and the 'accessory' proteins V and C, interfere with activation of NF- κ B in human epithelial cells. MV P, V, and C, which are established MV virulence factors, were found to individually suppress NF- κ B-dependent reporter gene expression in response to activation of TNF receptor, RLRs, or TLRs. While the V protein exhibited the most potent inhibitory capacity, MV P and C proteins suppressed NF- κ B activation more moderately. As indicated by reporter gene assays involving overexpression of the IKK complex, which phosphorylates I κ B α to

liberate NF- κ B, V protein targets a downstream step in the signaling cascade. CoIP experiments revealed that V specifically binds to the RHD of the NF- κ B subunit p65 but not of p50, which constitute the main dimers involved in the classical NF- κ B signaling. As observed by confocal microscopy, the presence of MV V abolished nuclear accumulation of p65 upon TNF α stimulation. Notably, the short C-terminal domain of the V protein that is also involved in binding STAT2, IRF7, and MDA5, was sufficient for interaction with p65 and for preventing reporter gene activity (Schuhmann et al., 2011). This highlights V_{CTD} as a cellular hub for innate immune signaling molecules. Mutational analysis of the V protein revealed that p65, IRF7, and MDA5 recognize common binding sites at the C-terminal domain of V. Besides binding of MV V to the classical NF- κ B subunit p65, CoIP experiments indicated MV V binding to the alternative NF- κ B subunits RelB and p52. Notably, MV P, which does not bind to the classical subunits, was found to bind to p52 as well. These findings reveal NF- κ B as a key target of MV and stress the importance of the V protein as the major viral immune-modulatory factor.

4.1 Inhibition of NF- κ B by MV P and C

Overexpression of the MV P and C protein resulted in suppression of classical NF- κ B activation upon different stimuli, like TNF α , Δ RIG-I, IPS-1, MyD88, and TRIF (Fig. 3-1 and 3.2) in reporter gene assays. Immunofluorescence experiments with flag-tagged P revealed that MV P interferes with nuclear accumulation of the NF- κ B subunit p65 to some extent. 40% of cells expressing flag-MV P showed no nuclear p65 upon TNF α stimulation (Fig. 3-9) even though P was not found to interact with p65 in CoIP experiments (Fig. 3-4). This partial inhibition of nuclear translocation correlates well with the partial inhibition of NF- κ B activation seen in the reporter gene assays. Taken together and in view of the fact that the P protein itself is located in the cytoplasm, an inhibitory mechanism upstream of p65 translocation is indicated. In monocytes but not in epithelial cells, MV P was previously shown to directly activate the expression of the ubiquitin-modifying enzyme A20, a potent inhibitor of the classical NF- κ B pathway (Yokota et al., 2008). MV P was reported to indirectly interact with a negative

regulatory motif in the A20 gene promoter and thereby the suppression of A20 expression is released. It was already revealed before that MV P has transactivating properties due to the acid-rich PV_{NTD} (Chen et al., 2003), however, how P reaches the nucleus is not known. Importantly, upregulation of the NF- κ B inhibitor A20 was not observed in HEK-293T cells with any of the MV proteins (data not shown), excluding the possibility of a contribution of this recently described mechanism (Yokota et al., 2008). Besides the potential of P to inhibit the classical NF- κ B signaling pathway, P might have the capacity to suppress the alternative pathway as well. MV P was able to interact with p52 (Fig. 3-16) and to inhibit NF- κ B-dependent reporter gene expression mediated by NIK, a kinase involved in the alternative NF- κ B pathway (Fig. 3-17A). However, stimulation of NF- κ B by RelB/p52 was apparently not impeded by P (Fig 3-17B). Thus, further investigations must be implemented to clarify if P interferes with alternative NF- κ B signaling.

In contrast to the P protein, MV C, which was shown to shuttle between the nucleus and the cytoplasm (Nishie et al., 2007), is mainly located in the nucleus in the steady state and does not interfere with nuclear translocation of p65 (Fig. 3-9). These findings suggest that MV C protein suppresses classical NF- κ B activation within the nucleus by a so far unknown mechanism in analogy to the nuclear blockage of IFN β induction (Sparrer et al., 2012). Notably, infection with a MV engineered to prevent expression of the C protein efficiently activates NF- κ B in comparison to infection with the parental MV (McAllister et al., 2010). This indicates that the C protein plays a pivotal role to inhibit NF- κ B activation during MV infection even though the direct capacity to suppress NF- κ B in my *in vitro* studies was only moderate.

4.2 Inhibitory mechanism of MV V

In all conducted reporter gene assays, the NF- κ B inhibitory capacity of the V protein was the most pronounced irrespective of the stimulus (Fig. 3-2, 3-2, 3-3). Specifically, in cells stimulated by overexpression of Δ RIG-I the inhibitory capacity of MV V appeared to be particularly pronounced (Fig. 3-2A). Interestingly, it was recently found that V binds to LGP2 which builds a complex with RIG-I in the presence of V and this

complex cannot be activated by RIG-I ligands (Childs et al., 2012). However, the inhibitory effect of LGP2 is operating at the level of RIG-I activation and is dependent on the helicase domain of RIG-I. Since I stimulated only with the CARD domains of RIG-I, the strong inhibition of NF- κ B activity cannot be explained by the interplay of V and RLRs. Therefore, I suggest that binding of MV V to the downstream transcription factor p65 is the major mechanism for suppression of RLR-mediated NF- κ B activation.

MV V was the only P gene product that substantially interacted with the NF- κ B subunit p65 as revealed with CoIP studies (Fig. 3-4) as well as with IF images which suggested co-localization of MV V and p65 (Fig. 3-8). The V protein of an MV wild type isolate (genotype D5) bear some point mutations in its PV_{NTD}, which is the common domain of P and V, while the sequence of the unique V_{CTD}, which is responsible for p65 binding, is completely conserved in the wild-type isolate and the Schwarz strain. Consistent with this fact, binding of wild-type V to p65 and similar levels of inhibition of NF- κ B-dependent reporter gene activity were observed (Fig. 3-13).

Binding of MV V to p65 might interfere with posttranslational modifications (PTMs) of p65, which are not essential for NF- κ B activation, but regulate the transcriptional efficiency of p65 by affecting the localization, stability and ability of p65 to interact with DNA and transcriptional cofactors (Huang et al., 2010). Numerous regulatory PTMs of p65 have been reported so far, such as phosphorylation, acetylation, and ubiquitination. Phosphorylation of serine (S) 276 within the RHD of p65 by protein kinase A (PKA) promotes the interaction of p65 with the transcriptional coactivators CREB-binding protein (CBP) and p300 (Zhong et al., 1998). This enhances the activation of a subset of NF- κ B target genes (Dong et al., 2008). Western Blot analysis of the phosphorylation state of p65 at S276 using an antibody for P-p65 S276 revealed no difference in the absence or presence of MV V (data not shown). However, there are concerns regarding the specificity of commercially available α -P-S276-p65 antibodies, since they were found to react with other PKA-regulated proteins, but do not detect S276-phosphorylation of p65 via Western Blotting (Spooren et al., 2010). Besides this phosphorylation within the RHD, a variety of phosphorylation sites within the TAD have been demonstrated (Hayden and Ghosh, 2012). Since MV V was shown to interact with the RHD of p65 (Fig. 3-5), these phosphorylation events will probably not

contribute to the inhibition seen in the presence of the V protein. Interestingly, ubiquitination of p65 was associated with the regulation of p65 localization (Maine et al., 2007). Ubiquitination seems to favor p65 localization in the cytoplasm, however MV V binding to p65 did not mediate ubiquitination of p65 as analyzed by Western blotting using an antibody against ubiquitin (data not shown).

Another consequence of MV V binding to p65 could be the disruption of the NF- κ B/I κ B α complex. However, I could demonstrate that binding of V does not prevent I κ B α or p50 binding to p65 (Fig. 3-7). This is also supported by the finding that MV V binds to both NTD and CTD of p65 RHD in contrast to I κ B α and p50, which bind only to the CTD of p65 RHD (Fig. 3-6). Since MV V retains p65 in the cytoplasm upon TNF α treatment (Fig. 3-8, 3-9), I assumed that binding of V to p65 leads to the inhibition of p65 translocation. Upon stimulation, p65 is imported into the nucleus by a subset of importin α isoforms, namely importin α 3, 4, and 5 (Fagerlund et al., 2005; Fagerlund et al., 2008). I found that p65 interacts most efficiently with the importin α 5 subunit (Fig. 3-10A). In unstimulated cells, I κ B α shields the NLS thereby preventing binding of the importin subunits (Hinz et al., 2012). Upon stimulation, I κ B α is degraded in presence and absence of V (data not shown) and importin α molecules can recognize the liberated NLS of p65, bind to p65 and associate with importin β to form a trimeric complex. Subsequently, importin β mediates docking of the complex to the cytoplasmic side of the nuclear pore complex (NCP) leading to translocation of the complex through the NCP (Funasaka and Wong, 2011).

Here I found that the inhibition of the translocation is not due to direct binding of V to the NLS of p65 (Fig. 3-10B). Furthermore, it could be excluded that the V protein competed with importin α 5 binding to p65 (Fig. 3-10C). However, weak binding of MV V to importin α 5 was observed in some experiments (data not shown), which might indicate that the retention of p65 in the cytoplasm in the presence of V might be due to interference of MV V with the import machinery. Since STAT1 and STAT2 are also cargos of importin α 5 (Fagerlund et al., 2002) and their nuclear translocation is inhibited by MV V as well (Palosaari et al., 2003), this common hub of signaling molecules might be a general target for MV V. However, preliminary data (not shown) suggest that nuclear translocation of heterogeneous nuclear ribonucleoprotein

complex C1/C2 (hnRNP C1/C2), an additional importin α 5 cargo (Shabman et al., 2011), was not inhibited in the presence of V contradicting the idea of a general inhibition of importin α 5 mediated nuclear import. Furthermore, the inhibition of STAT1 translocation by V is probably rather due to inhibition of JAK1 mediated phosphorylation (Caignard et al., 2007) than to interference of V with importin α 5.

The idea that MV V interferes with the import machinery in general is in turn supported by a study using mass spectrometry to identify interaction partners of the V protein, which identified different components of the nuclear pore such as nuclear pore complex protein 93 (NUP93) and NUP205 as well as importin α 1, importin β to interact with MV V (Komarova et al., 2011). Although the study could confirm well known interaction partners of the V protein such as STAT1 and STAT2, other interaction partners like LGP2, IKK α , IRF7, or JAK1 as well as p65 were not found in the mass spectrometry dataset. Nevertheless, possible interactions with proteins of the import machinery should be further investigated. NUP93 and NUP205 are part of the nucleoporin complex and required for correct nuclear pore assembly (Grandi et al., 1997). Although NUP93 and NUP205 are not involved in the transfer of the cargo/importin complex through the NCP (Shah et al., 1998), interaction of MV V with both proteins, which are localized to central channel of the pore and the nuclear basket, might eventually block the channel. However, this would result in a general blockage of nuclear import, which is not observed upon expression of MV V. On the contrary, the blockage of the nuclear import by V is even very specific. So, it might rather be the importins, which are interesting targets for V mediated specific nuclear import inhibition. Although V could not compete with binding of importin α 5 to its cargo p65 (Fig. 3-10C), it might interfere with downstream events of the import machinery, like importin β binding.

4.3 MV V binds a variety of cellular proteins but with specificity

Besides binding to p65, MV V was shown to interact with a variety of cellular proteins. Interestingly, these interactions seem to be very specific, since MV V binds only to selected members of a protein family. Here, it was revealed that the V protein interacts with the NF- κ B subunits p65 and p52, but not with p50 or p100, the precursor of p52 (Fig. 3-4 and 3-16). Especially, p52 and p50 are highly conserved, which highlights the high specificity of V to interact with defined molecules. Since it was shown that p50 homodimers, which are lacking the TAD to mediate gene transcription, repress a subset of IFN-inducible genes (Cheng et al., 2011), it might be a strategy of the virus to refrain from targeting the inhibitory p50 dimer.

It is also known that MV V binds to the RLRs MDA5 and LGP2, but not to the closely related RIG-I (Childs et al., 2012; Childs et al., 2007). Furthermore, MV V interacts with IKK α , but not with IKK β or IKKi (Pfaller and Conzelmann, 2008). Besides its dual role in the canonical as well as alternative NF- κ B signaling pathway, IKK α is also involved in the activation of IRF7 through TLR7/8/9. *In vitro* kinase assays showed that the IKK α -dependent phosphorylation of IRF7 was diminished in the presence of MV V, whereas the phosphorylation of the NF- κ B inhibitor I κ B α by IKK α was not altered (Pfaller and Conzelmann, 2008). Thus, binding of MV V to IKK α suppresses IRF7 activation but does not affect activation of NF- κ B. This displays another layer of specificity of MV V mediated modulation of the immune system. In the same study it was revealed that the transcription factor IRF7 is bound by MV V. However, no interaction with IRF3 could be detected in their study. This is consistent with the finding that the V proteins of PIV5 and related rubulaviruses, but not MV V, targets the IRF3 rather than the IRF7 signaling pathway, by binding to IKKi, which prevents IRF3 activation and RLR-dependent IFN β induction (Lu et al., 2008). In contradiction with this findings, it was recently suggested that V proteins of different paramyxoviruses, including MV V, inhibit IRF3 signaling by binding to IRF3 (Irie et al., 2012). However, this binding could not be verified in my experiments (data not shown), speaking for the specificity for the V protein to IRF7 as found before (Lu et al., 2008; Pfaller and Conzelmann, 2008).

All these interactions with V are mediated via its unique C-terminal domain, which turns out to be a hub for specific binding of numerous cellular proteins. This includes not only targets of the innate immunity but also proteins related to proliferation and cell death, like p53 family member p73, which down regulates expression of the proapoptotic target gene PUMA and might therefore function as a viral antiapoptotic factor (Cruz et al., 2006).

Taken together, all these specific interactions of MV V with cellular proteins might contribute to the fine regulation and modulation of the immune system by MV, emphasizing the important role of the V protein for MV-mediated immune escape.

4.4 Interactions of V with cellular molecules are often conserved among paramyxoviruses

Most of the interactions of MV V with the cellular proteins are conserved among V proteins of other paramyxoviruses such as the interactions with MDA5, IKK α , and IRF7 (Andrejeva et al., 2004; Kitagawa et al., 2011). Indeed, an interaction of p65 with the V proteins of CDV and NiV was found here (Fig. 3-15). However, no interaction was detected with PIV5 V, which might be either the consequence of the low expression levels of PIV5 V in all reporter gene assays, or PIV5 V fails to interact with p65 due to its nuclear localization within the cell (Precious et al., 1995). Interestingly, the V protein of PIV5 was reported to suppress NF- κ B activation only upon triggering with synthetic dsRNA or upon viral infection, whereas inhibition of LPS- or TNF α -dependent NF- κ B activity was not observed (Lin et al., 2007; Poole et al., 2002). This is in accordance with my NF- κ B reporter gene experiments where expression of PIV5 V was ineffective in preventing NF- κ B activity induced by Δ RIG-I, MyD88, or p65/p50 (Fig. 3-14). Thus, it is likely that NF- κ B inhibition and p65 binding is not generally conserved among members of the *Paramyxoviridae* family, but that the immune-modulatory strategies of MV to inhibit NF- κ B activation are applied by a selected subset of paramyxoviruses, as proven for the highly related CDV and the more distinct NiV.

This emphasizes the broad usage of the revealed NF- κ B inhibitory mechanism and therefore it helps to understand the complex and multifaceted mechanisms, which are applied by paramyxoviruses to circumvent innate immune responses.

4.5 p65 shares binding sites at the C-terminal domain of V with MDA5 and IRF7

Intriguingly, numerous interactions of V with cellular proteins, such as MDA5, LGP2, STAT2, or IRF7 are mediated via the 68 aa long C-terminal domain of V. And it was also MV V_{CTD}, which was shown to mediated interaction with p65 (Fig. 3-11).

Since MV V interferes with different steps of the signaling cascades it is important to reveal the aa of motifs which are responsible for each interaction in order to be able to discriminate the resulting effects. Responsible aa for MV V binding to MDA5 were already identified in two independent studies (Ramachandran and Horvath, 2010; Takaki et al., 2011). Ramachandran and Horvath identified two aa (233R and 235E) as important for MDA5 interaction and interference by site-directed mutagenesis. In contrast, Takaki et al. recognized 272C to be critical for interaction with MDA5 due to sequence alignment of different MV strains. However, mutation of 272C or of any other cysteine might destroy the zinc finger structure of V_{CTD} and affect other interactions as well. Therefore, the 233 and 235 mutations, located within the first loop, are probably more promising for dissecting V protein functions. The aa 246F and 248D, which are important to mediate the interactions with STAT2 are also found within the first loop (Ramachandran et al., 2008). Residues mediating binding to IRF7 were identified to be localized within the second loop. A stretch of four amino acids (aa 259-262) seems to be important for IRF7 binding and substitution of these residues against alanine resulted in decreased binding to the transcription factor (Pfaller, 2009).

It could be revealed here, that aa responsible for MDA5 binding as well as for IRF7 binding are also important for p65 binding (Fig. 3-12D). Specifically, mutants either lacking loop 1 or 2 were compromised to interact with p65 to the full range (Fig. 3-12E), however could still interfere to some degree with NF- κ B or IFN promoter

activity (Fig. 3-12F-H). This indicates that, in case of p65 binding, both regions loop 1 and 2 are involved in the interaction and that one of them might be enough for inhibition. Since binding of V to p65 was reduced rather than completely lost, the reduced binding is obviously sufficient for inhibition. It seems that both IRF7 and MDA5 binding domains overlap with the p65 binding site to MV V (Fig. 3-12D). For that reason, it might be possible that MV V rather binds a common hypothetical adaptor protein of the cellular interaction partners. Thus, the interaction at least of some cellular proteins with MV V might be indirect. So far, a direct binding of MV V was only shown for STAT1, JAK1, and MDA5 using a yeast two-hybrid approach (Caignard et al., 2007). However, if binding of all cellular proteins is direct, the different interaction partners of V might compete for their common binding sites, which might be another layer of regulation applied by the V protein.

4.6 Relevance of the P gene products for the alternative pathway

In contrast to the classical NF- κ B signaling pathway, which plays a major role in innate immune processes, the alternative pathway is rather thought to be involved in the regulation of the adaptive immune system. For example, mice deficient in p52 present defects in humoral responses and splenic microarchitecture (Franzoso et al., 1998). RelB deficient mice have a lack of bone marrow-derived DCs (Lo et al., 1992) and decreased T cell responses upon vaccinia virus infections, which leads to impaired clearance of the virus (Freyschmidt et al., 2007). Furthermore, it was shown that RelB-deficient mice are more susceptible for influenza A virus infection (Castiglioni et al., 2008). This highlights the important function of the alternative NF- κ B pathway during viral infections.

Here, I could show that both MV P and V interact with the alternative NF- κ B subunit p52, but not with its precursor p100 (Fig. 3-16). This indicates that in the full-length protein the binding sites for MV V or P are shielded by the inhibitory C-terminus of

p100, which gets degraded upon stimulation of the alternative pathway. This specific binding might be an additional mechanism applied by MV to counteract immune responses. An interaction of MV V and RelB, however, was indicated in a certain setting of experiments only. When V was coexpressed with untagged RelB, an additional 55 kDa band was always co-precipitated with flag-MV V using an antibody directed against the C-terminus of RelB for visualization. This might be due to an N-terminal cut of RelB, as it is seen upon 12-O-tetradecanoylphorbol-13-acetate/ionomycin treatment of EL-4 T-cells, where RelB was shown to be N-terminally processed followed by degradation of RelB (Marienfeld et al., 2001). The N-terminal processing is also supported by the finding that the additional band was not observed when MV V was coexpressed with an N-terminal flag-tagged RelB. It might be possible that RelB processing is supported by the V protein. Besides binding to the alternative NF- κ B subunits, the capacity of the P gene products to suppress NIK-mediated NF- κ B signaling was also demonstrated (Fig. 3-17). Triggering of the alternative pathway also activates the classical NF- κ B subunits. Although V interactions with the alternative subunits RelB and p52 suggest points of interference, it cannot be excluded that the inhibitory effect on NIK-mediated NF- κ B activity observed in reporter gene assays is primarily due to inhibition of the classical pathway. The finding that RelB/p52-mediated NF- κ B activation cannot be inhibited by any of the P gene products argues in favor of an only minor role of the P gene products to suppress alternative NF- κ B signaling downstream of the NF- κ B subunits. However, they might target the signaling cascade just upstream of p52 and RelB. For example IKK α targeting of MV V might be involved in modulation of alternative signaling. It was shown that MV V interaction with IKK α does not interfere with phosphorylation of I κ B α *in vitro* (Pfaller and Conzelmann, 2008), argues against an involvement of the interaction of V and IKK α to inhibit classical NF- κ B signaling, but its role in suppression of the alternative pathway should be further analyzed.

4.7 Role of the V protein during MV infection

To characterize the relevance of the V protein in a viral context, suitable cDNAs were constructed and recombinant viruses were rescued including the parental virus with an additional MCS, the VKO virus and the VKO virus with an ORF for the V protein within the MCS. The viruses were shown to grow with similar growth kinetics on Vero as well as on A549 cells (Fig. 3-18C+D). At least for infection of the IFN-competent A549 cells one could expect a growth defect of the virus deficient in V expression, due to the lack of V-mediated IFN-inhibiting activities, such as suppression of IFN-expression as a result of MDA5 or IRF3 binding (Andrejeva et al., 2004; Irie et al., 2012). However, also the finding that the mRNA levels of IFN β upon infection were comparable for all viruses point in a direction that IFN inhibition by MV is sufficient in the viral context even in the absence of V (Fig. 3-19D). Similar results were obtained in a study where macaques were infected with viruses either deficient in V or C expression. Infection of the animals with the viruses revealed that the V protein had no effect on IFN β induction *in vivo*, since no significant difference of IFN β mRNA levels in PBMCs was seen between infection with the VKO or the parental virus, whereas the C deficient virus showed enhanced IFN β induction (Devaux et al., 2008). Furthermore, this study showed that expression of IFN-stimulated genes (ISG), like MxA or OAS (2,5-oligoadenylate synthetase) was also not altered whether the V protein was present or not during infections. This is contradictory to the findings in cultivated cells, where MV V was shown to counteract STAT signaling at multiple steps and subsequently suppress ISG expression (Caignard et al., 2007; Ohno et al., 2004; Palosaari et al., 2003; Ramachandran et al., 2008). These findings may indicate that effects seen by studies overexpressing the V protein are only conditionally transferable to the situation of a viral infection. The effects of the V protein might be compensated by the P or the C protein, since they have been shown to have similar functions. For example, the C protein was shown to inhibit IFN induction as well (Sparrer et al., 2012) and inhibition of STAT signaling via STAT1 binding is mediated by the common N-terminal domain of the P and V protein (Devaux et al., 2007). So, a loss of the V protein in the viral context

may lead to a more pronounced role of either the P or the C protein and therefore compensate the effect normally mediated by the V protein.

As far as NF- κ B inhibition is concerned, infection of epithelial cells with the viruses revealed that there were also nearly no effect of the V protein on the induction of the NF- κ B dependent genes IL-6 and RANTES, as both viruses, the VKO virus and the parental one, induced comparable levels of the respective mRNAs (Fig. 3-19B+C). The advanced induction of IL-6 and RANTES mRNA levels due to infection with the VKO+V virus is probably caused by an increased initial infection kinetics, which is reflected by the increased mRNA and protein levels of the MV N protein (Fig. 3-19E+F). The NF- κ B reporter gene assays in HEK-293T cells showed also no difference in NF- κ B activation comparing infections with the V deficient virus to the parental one (Fig. 3-19A). The enhanced induction seen with the rescued VKO virus (VKO+V) is very surprising and cannot be explained by the initial infection rate, as the Western blots show similar levels of the N protein.

In contrast to IFN β and ISG expression, the levels of the NF- κ B dependent genes TNF α and IL6 were increased upon infection of macaques with the VKO virus in comparison to the parental one (Devaux et al., 2008). This strongly suggests that the NF- κ B inhibitory capacity of the V protein is of importance in *in vivo* infections, although I could not detect any effect of V on NF- κ B dependent genes in infections of cultured cell lines. This difference might result from the different cell types which were studied, since I used epithelial cell lines, whereas the *in vivo* study investigated primary PMBCs from infected macaques. Thus, the inhibitory effect of V on NF- κ B activity in the viral context can be either cell type specific or solely observed *in vivo*.

4.8 Future prospects

The biochemical data obtained in this study identify multiple targets within NF- κ B signaling pathways for the MV P gene products. A very prominent inhibition of the classical pathway was seen with the V protein, which binds to the NF- κ B subunit p65 and retains it in the cytoplasm. The exact mechanism how this is achieved should be further investigated and studies on the modulation of the import machinery might be a very promising option. In particular, it would be very interesting to see if MV V interacts with a common hub of different signaling molecules. In addition, *in vitro* binding assays would bring further knowledge into the overall organization of the different inhibitory mechanisms mediated by the small 68 aa long MV V_{CTD}.

Clarification of the inhibitory mechanism of MV P and C would help to understand different aspects of NF- κ B inhibition during MV infections. The compensatory mechanism which might be applied by the C protein in a virus which lacks the V protein could be investigated by generation of a virus defective in V and C expression. The role of MV P within the alternative signaling is of particular interest for clarification of the inhibitory mechanism applied by MV P, since it interacted solely with the alternative NF- κ B subunit p52. However, P deficient virus is not viable, such that these studies would require first identification of relevant P domains by mutagenesis.

The role of the inhibitory capacity of the V protein in the viral context should be further investigated. Thereby it would be very interesting to see whether, infection of cultured cells other than epithelial cells with VKO virus leads to an upregulation of NF- κ B dependent genes. PBMCs are here of special interest, since an effect in these cells was already observed *in vivo*. If the inhibitory effect of the V protein *in vivo* can be further confirmed, it might be worthwhile to check if the oncolytic efficiency, which was extensively utilized for MV (Galanis, 2010), can be enhanced by controlling NF- κ B activity, which was shown to be constitutively active in cancer cells (DiDonato et al., 2012).

5 References

- Andrejeva, J., K.S. Childs, D.F. Young, T.S. Carlos, N. Stock, S. Goodbourn, and R.E. Randall. 2004. The V proteins of paramyxoviruses bind the IFN-inducible RNA helicase, mda-5, and inhibit its activation of the IFN-beta promoter. *Proc Natl Acad Sci U S A*. 101:17264-17269.
- Arimoto, K., H. Takahashi, T. Hishiki, H. Konishi, T. Fujita, and K. Shimotohno. 2007. Negative regulation of the RIG-I signaling by the ubiquitin ligase RNF125. *Proc Natl Acad Sci U S A*. 104:7500-7505.
- Beckford, A.P., R.O. Kaschula, and C. Stephen. 1985. Factors associated with fatal cases of measles. A retrospective autopsy study. *South African medical journal = Suid-Afrikaanse tydskrif vir geneeskunde*. 68:858-863.
- Bellini, W.J., G. Englund, S. Rozenblatt, H. Arnheiter, and C.D. Richardson. 1985. Measles virus P gene codes for two proteins. *J Virol*. 53:908-919.
- Berghall, H., J. Siren, D. Sarkar, I. Julkunen, P.B. Fisher, R. Vainionpaa, and S. Matikainen. 2006. The interferon-inducible RNA helicase, mda-5, is involved in measles virus-induced expression of antiviral cytokines. *Microbes and infection / Institut Pasteur*. 8:2138-2144.
- Bieback, K., E. Lien, I.M. Klagge, E. Avota, J. Schneider-Schaulies, W.P. Duprex, H. Wagner, C.J. Kirschning, V. Ter Meulen, and S. Schneider-Schaulies. 2002. Hemagglutinin protein of wild-type measles virus activates toll-like receptor 2 signaling. *J Virol*. 76:8729-8736.
- Bonizzi, G., and M. Karin. 2004. The two NF- κ B activation pathways and their role in innate and adaptive immunity. *Trends in Immunology*. 25:280-288.
- Brzózka, K., S. Finke, and K.K. Conzelmann. 2005. Identification of the rabies virus alpha/beta interferon antagonist: phosphoprotein P interferes with phosphorylation of interferon regulatory factor 3. *J Virol*. 79:7673-7681.
- Brzózka, K., S. Finke, and K.K. Conzelmann. 2006. Inhibition of interferon signaling by rabies virus phosphoprotein P: activation-dependent binding of STAT1 and STAT2. *J Virol*. 80:2675-2683.
- Bunting, C.H. 1950. The giant-cells of measles. *The Yale journal of biology and medicine*. 22:513-519.
- Caignard, G., M. Guerbois, J.L. Labernardiere, Y. Jacob, L.M. Jones, F. Wild, F. Tangy, and P.O. Vidalain. 2007. Measles virus V protein blocks Jak1-mediated phosphorylation of STAT1 to escape IFN-alpha/beta signaling. *Virology*. 368:351-362.

- Campbell, H., N. Andrews, K.E. Brown, and E. Miller. 2007. Review of the effect of measles vaccination on the epidemiology of SSPE. *International journal of epidemiology*. 36:1334-1348.
- Castiglioni, P., D.S. Hall, E.L. Jacovetty, E. Ingulli, and M. Zanetti. 2008. Protection against Influenza A Virus by Memory CD8 T Cells Requires Reactivation by Bone Marrow-Derived Dendritic Cells. *The Journal of Immunology*. 180:4956-4964.
- Cathomen, T., B. Mrkic, D. Spehner, R. Drillien, R. Naef, J. Pavlovic, A. Aguzzi, M.A. Billeter, and R. Cattaneo. 1998. A matrix-less measles virus is infectious and elicits extensive cell fusion: consequences for propagation in the brain. *EMBO J*. 17:3899-3908.
- Cattaneo, R., K. Kaelin, K. Baczko, and M.A. Billeter. 1989. Measles virus editing provides an additional cysteine-rich protein. *Cell*. 56:759-764.
- Cattaneo, R., G. Rebmann, K. Baczko, V. ter Meulen, and M.A. Billeter. 1987. Altered ratios of measles virus transcripts in diseased human brains. *Virology*. 160:523-526.
- Chen, M., J.C. Cortay, and D. Gerlier. 2003. Measles virus protein interactions in yeast: new findings and caveats. *Virus Research*. 98:123-129.
- Cheng, C.S., K.E. Feldman, J. Lee, S. Verma, D.-B. Huang, K. Huynh, M. Chang, J.V. Ponomarenko, S.-C. Sun, C.A. Benedict, G. Ghosh, and A. Hoffmann. 2011. The Specificity of Innate Immune Responses Is Enforced by Repression of Interferon Response Elements by NF- κ B p50. *Sci. Signal*. 4:ra11-.
- Childs, K., R. Randall, and S. Goodbourn. 2012. Paramyxovirus V Proteins Interact with the RNA Helicase LGP2 To Inhibit RIG-I-Dependent Interferon Induction. *Journal of Virology*. 86:3411-3421.
- Childs, K., N. Stock, C. Ross, J. Andrejeva, L. Hilton, M. Skinner, R. Randall, and S. Goodbourn. 2007. mda-5, but not RIG-I, is a common target for paramyxovirus V proteins. *Virology*. 359:190-200.
- Cruz, C.D., H. Palosaari, J.-P. Parisien, P. Devaux, R. Cattaneo, T. Ouchi, and C.M. Horvath. 2006. Measles Virus V Protein Inhibits p53 Family Member p73. *J. Virol*. 80:5644-5650.
- Cui, S., K. Eisenacher, A. Kirchhofer, K. Brzozka, A. Lammens, K. Lammens, T. Fujita, K.K. Conzelmann, A. Krug, and K.P. Hopfner. 2008. The C-terminal regulatory domain is the RNA 5'-triphosphate sensor of RIG-I. *Mol Cell*. 29:169-179.
- de Swart, R.L., M. Ludlow, L. de Witte, Y. Yanagi, G. van Amerongen, S. McQuaid, S. Yuksel, T.B. Geijtenbeek, W.P. Duprex, and A.D. Osterhaus. 2007. Predominant infection of CD150+ lymphocytes and dendritic cells during measles virus infection of macaques. *PLoS Pathog*. 3:e178.
- del Valle, J.R., P. Devaux, G. Hodge, N.J. Wegner, M.B. McChesney, and R. Cattaneo. 2007. A Vectored Measles Virus Induces Hepatitis B Surface Antigen Antibodies While Protecting Macaques against Measles Virus Challenge. *Journal of Virology*. 81:10597-10605.
- Dev, A., S. Iyer, B. Razani, and G. Cheng. 2011. NF- κ B and Innate Immunity

- In* NF- κ B in Health and Disease. Vol. 349. M. Karin, editor. Springer Berlin Heidelberg. 115-143.
- Devaux, P., G. Hodge, M.B. McChesney, and R. Cattaneo. 2008. Attenuation of V- or C-defective measles viruses: infection control by the inflammatory and interferon responses of rhesus monkeys. *J Virol.* 82:5359-5367.
- Devaux, P., V. von Messling, W. Songsungthong, C. Springfield, and R. Cattaneo. 2007. Tyrosine 110 in the measles virus phosphoprotein is required to block STAT1 phosphorylation. *Virology.* 360:72-83.
- DiDonato, J.A., F. Mercurio, and M. Karin. 2012. NF- κ B and the link between inflammation and cancer. *Immunological Reviews.* 246:379-400.
- Dong, J., E. Jimi, H. Zhong, M.S. Hayden, and S. Ghosh. 2008. Repression of gene expression by unphosphorylated NF- κ B p65 through epigenetic mechanisms. *Genes Dev.* 22:1159-1173.
- Dorig, R.E., A. Marcil, A. Chopra, and C.D. Richardson. 1993. The human CD46 molecule is a receptor for measles virus (Edmonston strain). *Cell.* 75:295-305.
- Fagerlund, R., L. Kinnunen, M. Kohler, I. Julkunen, and K. Melen. 2005. NF- κ B is transported into the nucleus by importin α 3 and importin α 4. *J Biol Chem.* 280:15942-15951.
- Fagerlund, R., K. Melén, X. Cao, and I. Julkunen. 2008. NF- κ B p52, RelB and c-Rel are transported into the nucleus via a subset of importin α molecules. *Cellular Signalling.* 20:1442-1451.
- Fagerlund, R., K. Melén, L. Kinnunen, and I. Julkunen. 2002. Arginine/Lysine-rich Nuclear Localization Signals Mediate Interactions between Dimeric STATs and Importin α 5. *Journal of Biological Chemistry.* 277:30072-30078.
- Ferreira, C.S., M. Frenzke, V.H. Leonard, G.G. Welstead, C.D. Richardson, and R. Cattaneo. 2010. Measles virus infection of alveolar macrophages and dendritic cells precedes spread to lymphatic organs in transgenic mice expressing human signaling lymphocytic activation molecule (SLAM, CD150). *J Virol.* 84:3033-3042.
- Franzoso, G., L. Carlson, L. Poljak, E.W. Shores, S. Epstein, A. Leonardi, A. Grinberg, T. Tran, T. Scharon-Kersten, M. Anver, P. Love, K. Brown, and U. Siebenlist. 1998. Mice deficient in nuclear factor (NF)- κ B/p52 present with defects in humoral responses, germinal center reactions, and splenic microarchitecture. *J Exp Med.* 187:147-159.
- Freyschmidt, E.J., C.B. Mathias, D.H. MacArthur, A. Laouar, M. Narasimhaswamy, F. Weih, and H.C. Oettgen. 2007. Skin inflammation in RelB(-/-) mice leads to defective immunity and impaired clearance of vaccinia virus. *The Journal of allergy and clinical immunology.* 119:671-679.
- Fugier-Vivier, I., C. Servet-Delprat, P. Rivaller, M.C. Rissoan, Y.J. Liu, and C. Roubrouin-Combe. 1997. Measles virus suppresses cell-mediated immunity by interfering with the survival and functions of dendritic and T cells. *J Exp Med.* 186:813-823.

- Funasaka, T., and R.W. Wong. 2011. The role of nuclear pore complex in tumor microenvironment and metastasis. *Cancer metastasis reviews*. 30:239-251.
- Gack, M.U., Y.C. Shin, C.H. Joo, T. Urano, C. Liang, L. Sun, O. Takeuchi, S. Akira, Z. Chen, S. Inoue, and J.U. Jung. 2007. TRIM25 RING-finger E3 ubiquitin ligase is essential for RIG-I-mediated antiviral activity. *Nature*. 446:916-920.
- Galanis, E. 2010. Therapeutic Potential of Oncolytic Measles Virus: Promises and Challenges. *Clin Pharmacol Ther*. 88:620-625.
- Ghanem, A., A. Kern, and K.-K. Conzelmann. 2012. Significantly improved rescue of rabies virus from cDNA plasmids. *European Journal of Cell Biology*. 91:10-16.
- Ghosh, G., V.Y. Wang, D.B. Huang, and A. Fusco. 2012. NF-kappaB regulation: lessons from structures. *Immunol Rev*. 246:36-58.
- Ghosh, S., and M. Karin. 2002. Missing Pieces in the NF-[kappa]B Puzzle. *Cell*. 109:S81-S96.
- Ghosh, S., M.J. May, and E.B. Kopp. 1998. NF-kappa B and Rel proteins: evolutionarily conserved mediators of immune responses. *Annu Rev Immunol*. 16:225-260.
- Giard, D.J., S.A. Aaronson, G.J. Todaro, P. Arnstein, J.H. Kersey, H. Dosik, and W.P. Parks. 1973. In vitro cultivation of human tumors: establishment of cell lines derived from a series of solid tumors. *J Natl Cancer Inst*. 51:1417-1423.
- Gilmore, T.D., D. Kalaitzidis, M.-C. Liang, and D.T. Starczynowski. 2004. The c-Rel transcription factor and B-cell proliferation: a deal with the devil. *Oncogene*. 23:2275-2286.
- Gitlin, L., W. Barchet, S. Gilfillan, M. Cella, B. Beutler, R.A. Flavell, M.S. Diamond, and M. Colonna. 2006. Essential role of mda-5 in type I IFN responses to polyriboinosinic:polyribocytidylic acid and encephalomyocarditis picornavirus. *Proc Natl Acad Sci U S A*. 103:8459-8464.
- Goodbourn, S., and R.E. Randall. 2009. The regulation of type I interferon production by paramyxoviruses. *J Interferon Cytokine Res*. 29:539-547.
- Graham, F.L., J. Smiley, W.C. Russell, and R. Nairn. 1977. Characteristics of a human cell line transformed by DNA from human adenovirus type 5. *J Gen Virol*. 36:59-74.
- Grandi, P., T. Dang, N. Pane, A. Shevchenko, M. Mann, D. Forbes, and E. Hurt. 1997. Nup93, a vertebrate homologue of yeast Nic96p, forms a complex with a novel 205-kDa protein and is required for correct nuclear pore assembly. *Mol Biol Cell*. 8:2017-2038.
- Griffin, D.E. 2010. Measles virus-induced suppression of immune responses. *Immunol Rev*. 236:176-189.
- Griffin, D.E., W.-H. Lin, and C.-H. Pan. 2012. Measles virus, immune control, and persistence. *FEMS Microbiology Reviews*. 36:649-662.
- Griffin, D.E., and B.J. Ward. 1993. Differential CD4 T cell activation in measles. *The Journal of infectious diseases*. 168:275-281.

- Hacker, H., V. Redecke, B. Blagoev, I. Kratchmarova, L.C. Hsu, G.G. Wang, M.P. Kamps, E. Raz, H. Wagner, G. Hacker, M. Mann, and M. Karin. 2006. Specificity in Toll-like receptor signalling through distinct effector functions of TRAF3 and TRAF6. *Nature*. 439:204-207.
- Hall, W.W., and V. Meulen. 1977. Rolyadenylic acid [poly(A)] sequences associated with measles virus intracellular ribonucleic acid (RNA) species. *J Gen Virol*. 35:487-510.
- Hashiguchi, T., M. Kajikawa, N. Maita, M. Takeda, K. Kuroki, K. Sasaki, D. Kohda, Y. Yanagi, and K. Maenaka. 2007. Crystal structure of measles virus hemagglutinin provides insight into effective vaccines. *Proc Natl Acad Sci U S A*. 104:19535-19540.
- Hashimoto, C., K.L. Hudson, and K.V. Anderson. 1988. The Toll gene of *Drosophila*, required for dorsal-ventral embryonic polarity, appears to encode a transmembrane protein. *Cell*. 52:269-279.
- Hausmann, S., J.B. Marq, C. Tapparel, D. Kolakofsky, and D. Garcin. 2008. RIG-I and dsRNA-induced IFN β activation. *PLoS One*. 3:e3965.
- Hayden, M.S., and S. Ghosh. 2012. NF- κ B, the first quarter-century: remarkable progress and outstanding questions. *Genes Dev*. 26:203-234.
- Hayden, M.S., A.P. West, and S. Ghosh. 2006. NF- κ B and the immune response. *Oncogene*. 25:6758-6780.
- Hinz, M., S.C. Arslan, and C. Scheidereit. 2012. It takes two to tango: I κ Bs, the multifunctional partners of NF- κ B. *Immunol Rev*. 246:59-76.
- Honda, K., Y. Ohba, H. Yanai, H. Negishi, T. Mizutani, A. Takaoka, C. Taya, and T. Taniguchi. 2005. Spatiotemporal regulation of MyD88-IRF-7 signalling for robust type-I interferon induction. *Nature*. 434:1035-1040.
- Hornung, V., J. Ellegast, S. Kim, K. Brzozka, A. Jung, H. Kato, H. Poeck, S. Akira, K.K. Conzelmann, M. Schlee, S. Endres, and G. Hartmann. 2006. 5'-Triphosphate RNA is the ligand for RIG-I. *Science*. 314:994-997.
- Huang, B., X.D. Yang, A. Lamb, and L.F. Chen. 2010. Posttranslational modifications of NF- κ B: another layer of regulation for NF- κ B signaling pathway. *Cell Signal*. 22:1282-1290.
- Huxford, T., D.-B. Huang, S. Malek, and G. Ghosh. 1998. The Crystal Structure of the I κ B α /NF- κ B Complex Reveals Mechanisms of NF- κ B Inactivation. *Cell*. 95:759-770.
- Ikegame, S., M. Takeda, S. Ohno, Y. Nakatsu, Y. Nakanishi, and Y. Yanagi. 2010. Both RIG-I and MDA5 RNA Helicases Contribute to the Induction of Alpha/Beta Interferon in Measles Virus-Infected Human Cells. *J. Virol*. 84:372-379.
- Iretton, R.C., and M. Gale, Jr. 2011. RIG-I like receptors in antiviral immunity and therapeutic applications. *Viruses*. 3:906-919.
- Irie, T., K. Kiyotani, T. Igarashi, A. Yoshida, and T. Sakaguchi. 2012. Inhibition of Interferon Regulatory Factor 3 Activation by Paramyxovirus V Protein. *Journal of Virology*. 86:7136-7145.

- Iwasaki, M., M. Takeda, Y. Shirogane, Y. Nakatsu, T. Nakamura, and Y. Yanagi. 2009. The matrix protein of measles virus regulates viral RNA synthesis and assembly by interacting with the nucleocapsid protein. *J Virol.* 83:10374-10383.
- Kato, H., O. Takeuchi, E. Mikamo-Satoh, R. Hirai, T. Kawai, K. Matsushita, A. Hiiragi, T.S. Dermody, T. Fujita, and S. Akira. 2008. Length-dependent recognition of double-stranded ribonucleic acids by retinoic acid-inducible gene-I and melanoma differentiation-associated gene 5. *The Journal of Experimental Medicine.* 205:1601-1610.
- Kato, H., O. Takeuchi, S. Sato, M. Yoneyama, M. Yamamoto, K. Matsui, S. Uematsu, A. Jung, T. Kawai, K.J. Ishii, O. Yamaguchi, K. Otsu, T. Tsujimura, C.S. Koh, C. Reis e Sousa, Y. Matsuura, T. Fujita, and S. Akira. 2006. Differential roles of MDA5 and RIG-I helicases in the recognition of RNA viruses. *Nature.* 441:101-105.
- Kato, S.I., K. Nagata, and K. Takeuchi. 2012. Cell tropism and pathogenesis of measles virus in monkeys. *Frontiers in microbiology.* 3:14.
- Kawai, T., and S. Akira. 2009. The roles of TLRs, RLRs and NLRs in pathogen recognition. *International Immunology.* 21:317-337.
- Kawai, T., K. Takahashi, S. Sato, C. Coban, H. Kumar, H. Kato, K.J. Ishii, O. Takeuchi, and S. Akira. 2005. IPS-1, an adaptor triggering RIG-I- and Mda5-mediated type I interferon induction. *Nat Immunol.* 6:981-988.
- Kawasaki, T., T. Kawai, and S. Akira. 2011. Recognition of nucleic acids by pattern-recognition receptors and its relevance in autoimmunity. *Immunol Rev.* 243:61-73.
- Kitagawa, Y., M. Yamaguchi, M. Zhou, T. Komatsu, M. Nishio, T. Sugiyama, K. Takeuchi, M. Itoh, and B. Gotoh. 2011. A Tryptophan-Rich Motif in the Human Parainfluenza Virus Type 2 V Protein Is Critical for the Blockade of Toll-Like Receptor 7 (TLR7)- and TLR9-Dependent Signaling. *Journal of Virology.* 85:4606-4611.
- Kolakofsky, D., L. Roux, D. Garcin, and R.W. Ruigrok. 2005. Paramyxovirus mRNA editing, the "rule of six" and error catastrophe: a hypothesis. *J Gen Virol.* 86:1869-1877.
- Komarova, A.V., C. Combredet, L. Meyniel-Schicklin, M. Chapelle, G. Caignard, J.M. Camadro, V. Lotteau, P.O. Vidalain, and F. Tangy. 2011. Proteomic analysis of virus-host interactions in an infectious context using recombinant viruses. *Molecular & cellular proteomics : MCP.* 10:M110 007443.
- Kumar, H., T. Kawai, and S. Akira. 2011. Pathogen recognition by the innate immune system. *International reviews of immunology.* 30:16-34.
- Lemaitre, B., E. Nicolas, L. Michaut, J.M. Reichhart, and J.A. Hoffmann. 1996. The dorsoventral regulatory gene cassette *spatzle/Toll/cactus* controls the potent antifungal response in *Drosophila* adults. *Cell.* 86:973-983.
- Lemon, K., R.D. de Vries, A.W. Mesman, S. McQuaid, G. van Amerongen, S. Yuksel, M. Ludlow, L.J. Rennick, T. Kuiken, B.K. Rima, T.B. Geijtenbeek, A.D.

- Osterhaus, W.P. Duprex, and R.L. de Swart. 2011. Early target cells of measles virus after aerosol infection of non-human primates. *PLoS Pathog.* 7:e1001263.
- Lenardo, M.J., C.M. Fan, T. Maniatis, and D. Baltimore. 1989. The involvement of NF-kappa B in beta-interferon gene regulation reveals its role as widely inducible mediator of signal transduction. *Cell.* 57:287-294.
- Leonard, V.H., P.L. Sinn, G. Hodge, T. Miest, P. Devaux, N. Oezguen, W. Braun, P.B. McCray, Jr., M.B. McChesney, and R. Cattaneo. 2008. Measles virus blind to its epithelial cell receptor remains virulent in rhesus monkeys but cannot cross the airway epithelium and is not shed. *J Clin Invest.* 118:2448-2458.
- Li, T., X. Chen, K.C. Garbutt, P. Zhou, and N. Zheng. 2006. Structure of DDB1 in Complex with a Paramyxovirus V Protein: Viral Hijack of a Propeller Cluster in Ubiquitin Ligase. *Cell.* 124:105-117.
- Liao, G., M. Zhang, E.W. Harhaj, and S.C. Sun. 2004. Regulation of the NF-kappaB-inducing kinase by tumor necrosis factor receptor-associated factor 3-induced degradation. *J Biol Chem.* 279:26243-26250.
- Liljeroos, L., J.T. Huiskonen, A. Ora, P. Susi, and S.J. Butcher. 2011. Electron cryotomography of measles virus reveals how matrix protein coats the ribonucleocapsid within intact virions. *Proc Natl Acad Sci U S A.* 108:18085-18090.
- Lin, Y., M. Sun, S.M. Fuentes, C.D. Keim, T. Rothermel, and B. He. 2007. Inhibition of interleukin-6 expression by the V protein of parainfluenza virus 5. *Virology.* 368:262-272.
- Liston, P., and D.J. Briedis. 1994. Measles Virus V Protein Binds Zinc. *Virology.* 198:399-404.
- Liu, F., Y. Xia, A.S. Parker, and I.M. Verma. 2012. IKK biology. *Immunol Rev.* 246:239-253.
- Lo, D., H. Quill, L. Burkly, B. Scott, R.D. Palmiter, and R.L. Brinster. 1992. A recessive defect in lymphocyte or granulocyte function caused by an integrated transgene. *Am J Pathol.* 141:1237-1246.
- Loo, Y.M., J. Fornek, N. Crochet, G. Bajwa, O. Perwitasari, L. Martinez-Sobrido, S. Akira, M.A. Gill, A. Garcia-Sastre, M.G. Katze, and M. Gale, Jr. 2008. Distinct RIG-I and MDA5 signaling by RNA viruses in innate immunity. *J Virol.* 82:335-345.
- Lu, L.L., M. Puri, C.M. Horvath, and G.C. Sen. 2008. Select Paramyxoviral V Proteins Inhibit IRF3 Activation by Acting as Alternative Substrates for Inhibitor of Ikb Kinase ϵ (IKK ϵ)/TBK1. *Journal of Biological Chemistry.* 283:14269-14276.
- Ludlow, M., L.J. Rennick, S. Sarlang, G. Skibinski, S. McQuaid, T. Moore, R.L. de Swart, and W.P. Duprex. 2010. Wild-type measles virus infection of primary epithelial cells occurs via the basolateral surface without syncytium formation or release of infectious virus. *J Gen Virol.* 91:971-979.
- Lund, G.A., D.L. Tyrrell, R.D. Bradley, and D.G. Scraba. 1984. The molecular length of measles virus RNA and the structural organization of measles nucleocapsids. *J Gen Virol.* 65 (Pt 9):1535-1542.

- Maine, G.N., X. Mao, C.M. Komarck, and E. Burstein. 2007. COMMD1 promotes the ubiquitination of NF-kappaB subunits through a cullin-containing ubiquitin ligase. *EMBO J.* 26:436-447.
- Marienfeld, R., F. Berberich-Siebelt, I. Berberich, A. Denk, E. Serfling, and M. Neumann. 2001. Signal-specific and phosphorylation-dependent RelB degradation: a potential mechanism of NF-kappaB control. *Oncogene.* 20:8142-8147.
- May, M.J., F. D'Acquisto, L.A. Madge, J. Glockner, J.S. Pober, and S. Ghosh. 2000. Selective inhibition of NF-kappaB activation by a peptide that blocks the interaction of NEMO with the IkappaB kinase complex. *Science.* 289:1550-1554.
- May, M.J., R.B. Marienfeld, and S. Ghosh. 2002. Characterization of the Ikappa B-kinase NEMO binding domain. *J Biol Chem.* 277:45992-46000.
- McAllister, C.S., A.M. Toth, P. Zhang, P. Devaux, R. Cattaneo, and C.E. Samuel. 2010. Mechanisms of Protein Kinase PKR-Mediated Amplification of Beta Interferon Induction by C Protein-Deficient Measles Virus. *Journal of Virology.* 84:380-386.
- Meylan, E., J. Curran, K. Hofmann, D. Moradpour, M. Binder, R. Bartenschlager, and J. Tschopp. 2005. Cardif is an adaptor protein in the RIG-I antiviral pathway and is targeted by hepatitis C virus. *Nature.* 437:1167-1172.
- Moss, W.J., and D.E. Griffin. 2006. Global measles elimination. *Nat Rev Microbiol.* 4:900-908.
- Moss, W.J., and D.E. Griffin. 2012. Measles. *The Lancet.* 379:153-164.
- Muhlebach, M.D., M. Mateo, P.L. Sinn, S. Prufer, K.M. Uhlig, V.H. Leonard, C.K. Navaratnarajah, M. Frenzke, X.X. Wong, B. Sawatsky, S. Ramachandran, P.B. McCray, Jr., K. Cichutek, V. von Messling, M. Lopez, and R. Cattaneo. 2011. Adherens junction protein nectin-4 is the epithelial receptor for measles virus. *Nature.* 480:530-533.
- Nakai, M., and D.T. Imagawa. 1969. Electron microscopy of measles virus replication. *J Virol.* 3:187-197.
- Naniche, D., G. Varior-Krishnan, F. Cervoni, T.F. Wild, B. Rossi, C. Roubardin-Combe, and D. Gerlier. 1993. Human membrane cofactor protein (CD46) acts as a cellular receptor for measles virus. *J Virol.* 67:6025-6032.
- Nishie, T., K. Nagata, and K. Takeuchi. 2007. The C protein of wild-type measles virus has the ability to shuttle between the nucleus and the cytoplasm. *Microbes and infection / Institut Pasteur.* 9:344-354.
- Noyce, R.S., D.G. Bondre, M.N. Ha, L.T. Lin, G. Sisson, M.S. Tsao, and C.D. Richardson. 2011. Tumor cell marker PVRL4 (nectin 4) is an epithelial cell receptor for measles virus. *PLoS Pathog.* 7:e1002240.
- Oeckinghaus, A., M.S. Hayden, and S. Ghosh. 2011. Crosstalk in NF-kappaB signaling pathways. *Nat Immunol.* 12:695-708.

- Ohno, S., N. Ono, M. Takeda, K. Takeuchi, and Y. Yanagi. 2004. Dissection of measles virus V protein in relation to its ability to block alpha/beta interferon signal transduction. *J Gen Virol.* 85:2991-2999.
- Okada, H., F. Kobune, T.A. Sato, T. Kohama, Y. Takeuchi, T. Abe, N. Takayama, T. Tsuchiya, and M. Tashiro. 2000. Extensive lymphopenia due to apoptosis of uninfected lymphocytes in acute measles patients. *Archives of virology.* 145:905-920.
- Ono, N., H. Tatsuo, Y. Hidaka, T. Aoki, H. Minagawa, and Y. Yanagi. 2001. Measles Viruses on Throat Swabs from Measles Patients Use Signaling Lymphocytic Activation Molecule (CDw150) but Not CD46 as a Cellular Receptor. *Journal of Virology.* 75:4399-4401.
- Oshiumi, H., M. Miyashita, N. Inoue, M. Okabe, M. Matsumoto, and T. Seya. 2010. The Ubiquitin Ligase Riplet Is Essential for RIG-I-Dependent Innate Immune Responses to RNA Virus Infection. *Cell Host Microbe.* 8:496-509.
- Palosaari, H., J.-P. Parisien, J.J. Rodriguez, C.M. Ulane, and C.M. Horvath. 2003. STAT Protein Interference and Suppression of Cytokine Signal Transduction by Measles Virus V Protein. *J. Virol.* 77:7635-7644.
- Pfaller, C.K. 2009. Subversion of Toll-like receptor 7/9 signaling by Measles virus – V holds the key. *PhD thesis.*
- Pfaller, C.K., and K.K. Conzelmann. 2008. Measles virus V protein is a decoy substrate for I κ B kinase alpha and prevents Toll-like receptor 7/9-mediated interferon induction. *J Virol.* 82:12365-12373.
- Pichlmair, A., O. Schulz, C.P. Tan, T.I. Naslund, P. Liljestrom, F. Weber, and C. Reis e Sousa. 2006. RIG-I-mediated antiviral responses to single-stranded RNA bearing 5'-phosphates. *Science.* 314:997-1001.
- Pichlmair, A., O. Schulz, C.P. Tan, J. Rehwinkel, H. Kato, O. Takeuchi, S. Akira, M. Way, G. Schiavo, and C. Reis e Sousa. 2009. Activation of MDA5 requires higher-order RNA structures generated during virus infection. *J Virol.* 83:10761-10769.
- Plempner, R.K., M.A. Brindley, and R.M. Iorio. 2011. Structural and mechanistic studies of measles virus illuminate paramyxovirus entry. *PLoS Pathog.* 7:e1002058.
- Poole, E., B. He, R.A. Lamb, R.E. Randall, and S. Goodbourn. 2002. The V Proteins of Simian Virus 5 and Other Paramyxoviruses Inhibit Induction of Interferon-[beta]. *Virology.* 303:33-46.
- Precious, B., D.F. Young, A. Bermingham, R. Fearn, M. Ryan, and R.E. Randall. 1995. Inducible expression of the P, V, and NP genes of the paramyxovirus simian virus 5 in cell lines and an examination of NP-P and NP-V interactions. *Journal of Virology.* 69:8001-8010.
- Qing, G., Z. Qu, and G. Xiao. 2005. Stabilization of basally translated NF-kappaB-inducing kinase (NIK) protein functions as a molecular switch of processing of NF-kappaB2 p100. *J Biol Chem.* 280:40578-40582.

- Radecke, F., and M.A. Billeter. 1996. The nonstructural C protein is not essential for multiplication of Edmonston B strain measles virus in cultured cells. *Virology*. 217:418-421.
- Radecke, F., and M.A. Billeter. 1997. Reverse Genetics Meets the Nonsegmented Negative-Strand RNA Viruses. *Reviews in Medical Virology*. 7:49-63.
- Radecke, F., P. Spielhofer, H. Schneider, K. Kaelin, M. Huber, C. Dotsch, G. Christiansen, and M.A. Billeter. 1995. Rescue of Measles Viruses from Cloned DNA. *Embo Journal*. 14:5773-5784.
- Rahman, M.M., and G. McFadden. 2011. Modulation of NF-kappaB signalling by microbial pathogens. *Nat Rev Microbiol*. 9:291-306.
- Ramachandran, A., and C.M. Horvath. 2010. Dissociation of Paramyxovirus Interferon Evasion Activities: Universal and Virus-Specific Requirements for Conserved V Protein Amino Acids in MDA5 Interference. *J. Virol*. 84:11152-11163.
- Ramachandran, A., J.P. Parisien, and C.M. Horvath. 2008. STAT2 is a primary target for measles virus V protein-mediated alpha/beta interferon signaling inhibition. *J Virol*. 82:8330-8338.
- Ramakrishnan, P., W. Wang, and D. Wallach. 2004. Receptor-specific signaling for both the alternative and the canonical NF-kappaB activation pathways by NF-kappaB-inducing kinase. *Immunity*. 21:477-489.
- Razani, B., A.D. Reichardt, and G. Cheng. 2011. Non-canonical NF-kappaB signaling activation and regulation: principles and perspectives. *Immunol Rev*. 244:44-54.
- Rima, B.K., and W.P. Duprex. 2011. New concepts in measles virus replication: getting in and out in vivo and modulating the host cell environment. *Virus Res*. 162:47-62.
- Schlender, J., V. Hornung, S. Finke, M. Gunthner-Biller, S. Marozin, K. Brzozka, S. Moghim, S. Endres, G. Hartmann, and K.K. Conzelmann. 2005. Inhibition of toll-like receptor 7- and 9-mediated alpha/beta interferon production in human plasmacytoid dendritic cells by respiratory syncytial virus and measles virus. *J Virol*. 79:5507-5515.
- Schlender, J., J.J. Schnorr, P. Spielhoffer, T. Cathomen, R. Cattaneo, M.A. Billeter, V. ter Meulen, and S. Schneider-Schaulies. 1996. Interaction of measles virus glycoproteins with the surface of uninfected peripheral blood lymphocytes induces immunosuppression in vitro. *Proc Natl Acad Sci U S A*. 93:13194-13199.
- Schneider, H., K. Kaelin, and M.A. Billeter. 1997. Recombinant Measles Viruses Defective for RNA Editing and V Protein Synthesis Are Viable in Cultured Cells. *Virology*. 227:314-322.
- Schuhmann, K.M., C.K. Pfaller, and K.K. Conzelmann. 2011. The measles virus V protein binds to p53 (RelA) to suppress NF-kappaB activity. *J Virol*. 85:3162-3171.
- Schwarz, A.J. 1962. Preliminary tests of a highly attenuated measles vaccine. *Am J Dis Child*. 103:386-389.

- Sen, R., and D. Baltimore. 1986. Multiple nuclear factors interact with the immunoglobulin enhancer sequences. *Cell*. 46:705-716.
- Senftleben, U., Y. Cao, G. Xiao, F.R. Greten, G. Krahn, G. Bonizzi, Y. Chen, Y. Hu, A. Fong, S.C. Sun, and M. Karin. 2001. Activation by IKK α of a second, evolutionary conserved, NF-kappa B signaling pathway. *Science*. 293:1495-1499.
- Seth, R.B., L. Sun, C.K. Ea, and Z.J. Chen. 2005. Identification and characterization of MAVS, a mitochondrial antiviral signaling protein that activates NF-kappaB and IRF 3. *Cell*. 122:669-682.
- Shabman, R.S., E.E. Gulcicek, K.L. Stone, and C.F. Basler. 2011. The Ebola virus VP24 protein prevents hnRNP C1/C2 binding to karyopherin alpha1 and partially alters its nuclear import. *The Journal of infectious diseases*. 204 Suppl 3:S904-910.
- Shaffer, J.A., W.J. Bellini, and P.A. Rota. 2003. The C protein of measles virus inhibits the type I interferon response. *Virology*. 315:389-397.
- Shah, S., S. Tugendreich, and D. Forbes. 1998. Major binding sites for the nuclear import receptor are the internal nucleoporin Nup153 and the adjacent nuclear filament protein Tpr. *The Journal of cell biology*. 141:31-49.
- Sidorenko, S.P., and E.A. Clark. 2003. The dual-function CD150 receptor subfamily: the viral attraction. *Nat Immunol*. 4:19-24.
- Solt, L.A., and M.J. May. 2008. The IkappaB kinase complex: master regulator of NF-kappaB signaling. *Immunologic research*. 42:3-18.
- Sparrer, K.M., C.K. Pfaller, and K.K. Conzelmann. 2012. Measles virus C protein interferes with Beta interferon transcription in the nucleus. *J Virol*. 86:796-805.
- Spooren, A., K. Kolmus, L. Vermeulen, K. Van Wesemael, G. Haegeman, and S. Gerlo. 2010. Hunting for serine 276-phosphorylated p65. *Journal of biomedicine & biotechnology*. 2010:275892.
- Sun, S.C. 2011. Non-canonical NF-kappaB signaling pathway. *Cell Res*. 21:71-85.
- Tahara, M., M. Takeda, Y. Shirogane, T. Hashiguchi, S. Ohno, and Y. Yanagi. 2008. Measles virus infects both polarized epithelial and immune cells by using distinctive receptor-binding sites on its hemagglutinin. *J Virol*. 82:4630-4637.
- Takaki, H., Y. Watanabe, M. Shingai, H. Oshiumi, M. Matsumoto, and T. Seya. 2011. Strain-to-strain difference of V protein of measles virus affects MDA5-mediated IFN- β -inducing potential. *Molecular Immunology*. 48:497-504.
- Takayama, I., H. Sato, A. Watanabe, M. Omi-Furutani, A. Sugai, K. Kanki, M. Yoneda, and C. Kai. 2012. The nucleocapsid protein of measles virus blocks host interferon response. *Virology*. 424:45-55.
- Takeda, K., and S. Akira. 2004. TLR signaling pathways. *Seminars in immunology*. 16:3-9.
- Takeda, M., M. Tahara, T. Hashiguchi, T.A. Sato, F. Jinnouchi, S. Ueki, S. Ohno, and Y. Yanagi. 2007. A human lung carcinoma cell line supports efficient measles

- virus growth and syncytium formation via a SLAM- and CD46-independent mechanism. *J Virol.* 81:12091-12096.
- Takeuchi, O., and S. Akira. 2010. Pattern Recognition Receptors and Inflammation. *Cell.* 140:805-820.
- Tatsuo, H., N. Ono, K. Tanaka, and Y. Yanagi. 2000. SLAM (CDw150) is a cellular receptor for measles virus. *Nature.* 406:893-897.
- Thanos, D., and T. Maniatis. 1995. Virus induction of human IFN beta gene expression requires the assembly of an enhanceosome. *Cell.* 83:1091-1100.
- Toolan, H.W. 1954. Transplantable human neoplasms maintained in cortisone-treated laboratory animals: H.S. No. 1; H.Ep. No. 1; H.Ep. No. 2; H.Ep. No. 3; and H.Emb.Rh. No. 1. *Cancer Res.* 14:660-666.
- Wang, J., S.H. Basagoudanavar, X. Wang, E. Hopewell, R. Albrecht, A. Garcia-Sastre, S. Balachandran, and A.A. Beg. 2010. NF- κ B RelA Subunit Is Crucial for Early IFN- β Expression and Resistance to RNA Virus Replication. *J Immunol.* 185:1720-1729.
- Wang, X., S. Hussain, E.J. Wang, M.O. Li, A. Garcia-Sastre, and A.A. Beg. 2007. Lack of essential role of NF-kappa B p50, RelA, and cRel subunits in virus-induced type 1 IFN expression. *J Immunol.* 178:6770-6776.
- Wardrop, E.A., and D.J. Briedis. 1991. Characterization of V protein in measles virus-infected cells. *Journal of Virology.* 65:3421-3428.
- WHO. 2012. Fact sheet on measles. *WHO fact sheet #286.*
- Xu, L.G., Y.Y. Wang, K.J. Han, L.Y. Li, Z. Zhai, and H.B. Shu. 2005. VISA is an adapter protein required for virus-triggered IFN-beta signaling. *Mol Cell.* 19:727-740.
- Yamamoto, M., K. Takeda, and S. Akira. 2004. TIR domain-containing adaptors define the specificity of TLR signaling. *Mol Immunol.* 40:861-868.
- Yanagi, Y., M. Takeda, S. Ohno, and T. Hashiguchi. 2009. Measles virus receptors. *Curr Top Microbiol Immunol.* 329:13-30.
- Yasumura, Y.K., Y. 1963. Studies on SV40 virus in tissue culture cells. *Nippon Rinsho.* 21:1201-1215.
- Yokota, S., T. Okabayashi, N. Yokosawa, and N. Fujii. 2008. Measles virus P protein suppresses Toll-like receptor signal through up-regulation of ubiquitin-modifying enzyme A20. *FASEB J.* 22:74-83.
- Yoneyama, M., M. Kikuchi, K. Matsumoto, T. Imaizumi, M. Miyagishi, K. Taira, E. Foy, Y.M. Loo, M. Gale, Jr., S. Akira, S. Yonehara, A. Kato, and T. Fujita. 2005. Shared and unique functions of the DExD/H-box helicases RIG-I, MDA5, and LGP2 in antiviral innate immunity. *J Immunol.* 175:2851-2858.
- Yoneyama, M., M. Kikuchi, T. Natsukawa, N. Shinobu, T. Imaizumi, M. Miyagishi, K. Taira, S. Akira, and T. Fujita. 2004. The RNA helicase RIG-I has an essential function in double-stranded RNA-induced innate antiviral responses. *Nat Immunol.* 5:730-737.

- Yoneyama, M., W. Suhara, Y. Fukuhara, M. Sato, K. Ozato, and T. Fujita. 1996. Autocrine amplification of type I interferon gene expression mediated by interferon stimulated gene factor 3 (ISGF3). *J Biochem.* 120:160-169.
- Yoshikawa, Y., K. Mizumoto, and K. Yamanouchi. 1986. Characterization of messenger RNAs of measles virus. *J Gen Virol.* 67 (Pt 12):2807-2812.
- Zarnegar, B., S. Yamazaki, J.Q. He, and G. Cheng. 2008. Control of canonical NF-kappaB activation through the NIK-IKK complex pathway. *Proc Natl Acad Sci U S A.* 105:3503-3508.
- Zheng, C., Q. Yin, and H. Wu. 2011. Structural studies of NF-kappaB signaling. *Cell Res.* 21:183-195.
- Zhong, H., R.E. Voll, and S. Ghosh. 1998. Phosphorylation of NF-kappa B p65 by PKA stimulates transcriptional activity by promoting a novel bivalent interaction with the coactivator CBP/p300. *Mol Cell.* 1:661-671.
- Zhu, J., Y. Ding, F. Gao, T. Wu, C.W. Zhang, P. Tien, Z. Rao, and G.F. Gao. 2003. Crystallization and preliminary X-ray crystallographic analysis of the trimer core from measles virus fusion protein. *Acta crystallographica. Section D, Biological crystallography.* 59:587-590.

6 List of abbreviations

5'-ppp	5'-triphosphate
A	alanine
aa	amino acid
AP-1	activator protein 1
APS	ammonium persulfate
BAFFR	B-cell activating factor receptor
BCR	B-cell receptor
bp	base pair
CARD	terminal caspase activation and recruitment domain
CBP	CREB-binding protein
cDNA	copy DNA
CDV	Canine distemper virus
CIAP	calf intestine alkaline phosphatase

ciAP	cellular inhibitor of apoptosis
CMV	cytomegalovirus
CoIP	co-immunoprecipitation
cRNA	copy (antigenomic) RNA
C-terminus	Carboxy-terminus
DCs	dendritic cells
DI	defective interfering
DMEM	Dulbecco's Modified Eagle Medium
DNA	deoxyribonucleic acid
ds	double-strand
DTT	1,4-dithiothreitol
<i>E. coli</i>	<i>Escherichia coli</i>
EDTA	ethylene-diamin-tetraacetic acid-disodium salt
EMCV	encephalomyocarditis virus
EV	empty vector
F	fusion protein
FADD	Fas-associated death domain
FCS	fetal calf serum
ffu	focus forming units
FITC	fluorescein isothiocyanate
G	guanosine
GFP	green fluorescent protein
H	hemagglutinin protein
HA	hemagglutinin tag
hnRNP c1c2	Heterogeneous nuclear ribonucleoproteins C1/C2
HRP	horseradish peroxidase
IFN	interferon
IFNR	IFN receptor
IKK	I κ B kinase
IL	interleukin
IPS-1	interferon beta promoter stimulator 1
IRAK	interleukin-1 receptor associated kinase
IRF	interferon regulatory factor

ISG	interferon stimulated genes
I κ B	inhibitor of κ B
JAK	Janus kinase
K	lysine
KO	knock out
L	large protein
LB	lysogeny broth
Le	leader
LGP2	laboratory of genetics and physiology 2
LT β R	lymphotoxin- β receptor
M	matrix protein
MAPK	mitogen-activated protein kinase
MCP	membrane cofactor protein
MDA5	melanoma differentiation-associated gene 5
MOI	multiplicity of infection
MV	measles virus
MyD88	myeloid differentiation factor 88
N	nucleocapsid protein
NBD	nemo binding domain
ncp	nuclear pore complex
NEMO	NF- κ B essential modifier
NF- κ B	nuclear factor κ B
NIK	NF- κ B-inducing kinase
NiV	Nipah virus
NLS	nuclear localization signal
N-terminus	Amino-terminus
OAS	2'5'-oligoadenylate synthetase
OD	optical density
P	phosphoprotein
p.i.	post infection
p.t.	post transfection
PAGE	polyacrylamide gel electrophoresis
PAMP	pathogen-associated molecular pattern

PBMCs	peripheral blood mononuclear cells
PBS	Phosphate buffered saline
PCR	polymerase chain reaction
pDCs	plasmacytoid dendritic cells
PEI	polyethyleneimine
PFA	paraformaldehyde
PIV 5	Parainfluenza virus type 5
PO	peroxidase
Poly(I:C)	polyriboinosinic:polyribocytidylic acid
PRR	pattern recognition receptor
PVDF	polyvinylidene fluoride
PVRL4	poliovirus receptor-like protein 4
RD	regulatory domain
RHD	Rel homology domain
RIG-I	retinoic acid-inducible gene I
RIP1	receptor-interacting protein 1
RL	Renilla luciferase
RLR	RIG-like receptor
RNA	ribonucleic acid
RNP	ribonucleoprotein
RT	reverse transcriptase
RV	rabies virus
S	serine
SDS	sodium-dodecyl sulfate
SLAM	Signaling lymphocytic activation molecule
ss	single-strand
SSPE	Subacute sclerosing panencephalitis
STAT	signal transducer and activator of transcription
TAB	TAK1 binding protein
TAD	transactivation domain
TAK	transforming growth factor β
TANK	TRAF family member-associated activator NF- κ B
TBK-1	TANK-binding kinase 1

TCR	T-cell receptor
TEMED	tetramethylenediamine
TIR	Toll/interleukin-1-receptor
TLR	Toll-like receptor
TNF	Tumor necrosis factor
Tr	trailer
TRADD	TNF receptor 1-associated death domain protein
TRAF	TNF-receptor-associated factor
TRIF	TIR domain-containing adapter inducing IFN- β
TRIM	tripartite motif
vRdRp	viral RNA-dependent RNA polymerase
vRNA	viral (genomic) RNA
WB	Western blot
WHO	world health organization
wt	wild-type

7 List of figures

Figure 1-1 Measles virus – the basics	2
Figure 1-2 Measles virus P gene products	3
Figure 1-3 The mammalian NF- κ B family and its inhibitors	9
Figure 1-4 Two different NF- κ B signaling pathways	10
Figure 1-5 Endosomal TLR-signaling.....	14
Figure 1-6 RLR signaling pathways	16
Figure 3-1 Measles virus P gene products suppress NF- κ B activation upon TNFR stimulation	60
Figure 3-2 NF- κ B signaling via PRRs can be suppressed by MV P gene products.....	61
Figure 3-3 MV V inhibits NF- κ B signaling downstream of the IKK complex.....	63
Figure 3-4 MV V specifically binds the NF- κ B subunit p65.....	65

Figure 3-5 RHD of p65 is sufficient for interaction with MV V	66
Figure 3-6 Binding of MV V to p65 is mediated via both the N- and the C-terminal domain of the RHD of p65	68
Figure 3-7 Binding of MV V to p65 does not compete with binding of p50 or I κ B α to p65.....	69
Figure 3-8 MV V prevents nuclear translocation of p65	70
Figure 3-9 Nuclear translocation of p65 upon TNF α treatment in the presence of MV P and C.....	72
Figure 3-10 MV V does not directly bind to the NLS of p65 or interfere with importin α 5 binding to p65	74
Figure 3-11 The CTD of MV V is sufficient for p65 binding and suppression of p65/p50-mediated NF- κ B activity	75
Figure 3-12 Mutational analysis of MV V	77
Figure 3-13 The V protein of the measles wild type isolate D5 inhibits NF- κ B activity and binds to p65.....	80
Figure 3-14 CDV V and NiV V act like MV V and suppress classical NF- κ B activity.....	82
Figure 3-15 The Rel homology domain of p65 is also bound by CDV V and NiV V.....	84
Figure 3-16 Binding of P gene products to other NF- κ B subunits	86
Figure 3-17 Inhibition of the alternative NF- κ B pathway.....	88
Figure 3-18 Generation and characterisation of recombinant viruses MV-vac2, MV-MCS, MV-VKO, MV-VKO+V	90
Figure 3-19 NF- κ B activation upon infection with MV-MCS, MV-VKO, MV-VKO+V	92